

# 國立交通大學

資訊科學與工程研究所

## 博士論文

WiMAX 系統的行動管理機制之改進

Enhancing Mobility Management for WiMAX



研究生：林湧鈞

指導教授：林一平 博士

中華民國九十八年九月

WiMAX 系統的行動管理機制之改進  
Enhancing Mobility Management for WiMAX


研究生：林湧鈞

Student : Yung-Chun Lin

指導教授：林一平 博士

Advisor : Dr. Yi-Bing Lin

國立交通大學  
資訊科學與工程研究所  
博士論文



A Dissertation  
Submitted to Institute of Computer Science and Engineering  
College of Computer Science  
National Chiao Tung University  
in partial Fulfillment of the Requirements  
for the Degree of  
Doctor of Philosophy  
in

Computer Science

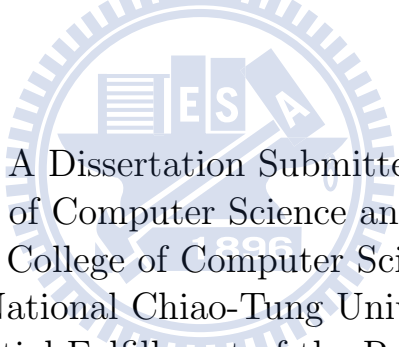
September 2009

Hsinchu, Taiwan, Republic of China

中華民國九十八年九月

# Enhancing Mobility Management for WiMAX

Student: Yung-Chun Lin  
Advisor: Dr. Yi-Bing Lin



A Dissertation Submitted to  
Institute of Computer Science and Engineering  
College of Computer Science  
National Chiao-Tung University  
In Partial Fulfillment of the Requirements  
for the Degree of  
Doctor of Philosophy  
in  
Computer Science

Hsinchu, Taiwan, Republic of China

September, 2009

# WiMAX 系統的行動管理機制之改進

學生：林湧鈞

指導教授：林一平博士

國立交通大學資訊科學與工程研究所

## 摘 要

隨著行動用戶的快速增加，行動寬頻服務已成為人們生活的一部分。全球互通微波存取(WiMAX)系統為新一代的行動網路，能提供大服務範圍、高吞吐量與支援快速移動的無線寬頻服務。為了提供行動服務，WiMAX 的行動管理(包含位置管理功能與交遞管理功能)當為最重要的議題之一。其中，位置管理功能負責追蹤用戶之移動以提供服務，而交遞管理功能負責在用戶的移動中維持服務正常運作。此二項功能對一些較耗資源的電信服務尤為重要，例如影像電話、隨按即說等。本研究即探討 WiMAX 系統的行動管理相關議題。

在行動管理方面，首先我們提出數學模型來評估當位置區域(LA)部分重疊時，對位置更新(LU)機制效能的影響。本研究結果提供了如何選取適當重疊範圍的準則。接著我們研究 WiMAX 的 LU 機制之效能。由於 WiMAX 會為每個行動用戶指定一主傳呼控制中心(APC)來管理與追蹤該用戶，並可在用戶更新位置時即時更換 APC。此研究找出了能依照使用者移動模式，

即時更換 APC 的準則。

在交遞管理方面，為了支援 WiMAX 用戶的高速移動，本研究在考量不同的使用者移動速度後，提出了基於階層式 WiMAX 網路架構的隨需重整(RoD)方法。本研究指出隨需重整方法較不受使用者移動速度影響，且其效能明顯優於其他通道配置方法。

本論文的研究成果提供了一些可供 WiMAX 業者參考使用的機制與準則，以期提升 WiMAX 系統的行動管理機制之效能。

**關鍵字：**行動管理、位置區域、位置更新、階層式 WiMAX 網路、通道配置、通道重整、隨按即說、隨需重整



# Enhancing Mobility Management for WiMAX

Student: Yung-Chun Lin

Advisor: Dr. Yi-Bing Lin

Institute of Computer Science and Engineering

National Chiao Tung University

## ABSTRACT

As mobile subscriber population rapidly grows, mobile access for broadband services becomes an important part of human life. IEEE 802.16e mobile *Worldwide Interoperability for Microwave Access* (WiMAX) provides broadband wireless services with wide service coverage, high data throughput, and high mobility. In WiMAX, *mobility management* (i.e., *location management* and *handoff management*) is one of the most important issues to support mobile services. Location management function tracks the roaming *Mobile Stations* (MSs) for service delivery, and handoff management function maintains service continuity during MS mobility. Such functions are important for mobile telephony services, including *conference/video call* and *Push to Talk over Cellular* (PoC). In this dissertation, we investigate the mobility management issues for WiMAX networks.

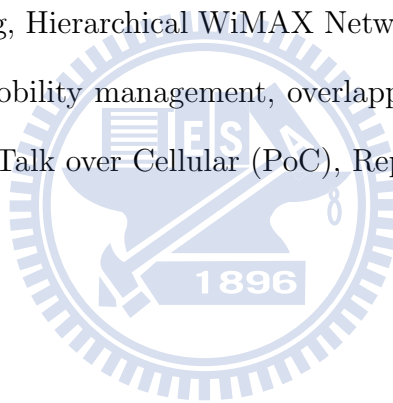
For location management, we first propose an analytic model to study the *Location Update* (LU) performance with overlapping *Location Area* (LA) configuration. Our study indicates how to determine the appropriate overlap among LAs. Then we investigate the performance for WiMAX LU procedure with *Anchor Paging Controller* (APC) relocation. In WiMAX, an APC is assigned to an MS to handle its location tracking and can be dynamically relocated during the LU procedure. By the analytic results, we provide

guidelines to utilize the APC relocation for MSs with various moving behaviors.

For handoff management, to support service continuity for high mobility MSs, we proposed the *Repacking on Demand* (RoD) for the *Hierarchical WiMAX Network* (HWN) by considering the MS moving speeds. Our study quantitatively indicates that RoD is less sensitive to MS speeds and outperforms the other previous proposed schemes significantly.

The research results presented in this dissertation provide some useful mechanisms and guidelines for WiMAX operators to achieve high system performance in their networks.

**Key words:** repacking, Hierarchical WiMAX Network (HWN), Location Area (LA), Location Update (LU), mobility management, overlapping LA, Paging Controller (PC), ping-pong effect, Push to Talk over Cellular (PoC), Repacking on Demand (RoD)



# Acknowledgement

I would like to express my sincere thanks to my advisor, Prof. Yi-Bing Lin. Without his supervision and perspicacious advice, I can not complete this dissertation. Special thanks are due to my committee members: Dr. Chung-Hwa Rao, Prof. Chu-Sing Yang, Prof. Han-Chieh Chao, Prof. Hsi-Lu Chao, Prof. Jean-Lien Chen and Prof. Ming-Feng Chang for their valuable comments and helpful discussions.

I also express my appreciation to all the faculty, staff and colleagues in the Department of Computer Science and Engineering. In particular, I would like to thank Prof. Phone Lin, Dr. Hsien-Ming Tsai, Prof. Ai-Chun Pang, Prof. Shun-Ren Yang, Prof. Pei-Chun Lee, Prof. Sok-Ian Sou, Dr. Lin-Yi Wu, Dr. Shih-Feng Hsu, Dr. Meng-Hsun Tsai, Mr. Chien-Chun Hung-Fu, Ms. Ya-Chin Sung, Ms. Hsin-Yi Lee and the other labmates in the Laboratory 117 for their friendship and support in various ways.

Finally, I am grateful to my dear parents, brother, wife Yu-Chi Chang and lovely son DJ for their encouragement and firm support during these years.



# Contents

Abstract in Chinese	i
Abstract in English	iii
Acknowledgement	v
Contents	vi
List of Figures	ix
List of Tables	xii
Notation	xiii
<b>1 Introduction</b>	<b>1</b>
1.1 Location Management for WiMAX System . . . . .	4
1.2 Repacking for Hierarchical WiMAX Networks . . . . .	6
1.3 Dissertation Organization . . . . .	8
<b>2 Performance for Mobile Network with Overlapping Location Area Con- figuration</b>	<b>10</b>
2.1 Location Area Overlap . . . . .	10
2.2 System Model and LA Selection Policies . . . . .	12
2.3 Analytic Model . . . . .	15



2.3.1	Case 1: $0 \leq K < \frac{N}{2}$ . . . . .	15
2.3.2	Case 2: $\frac{N}{2} \leq K < N$ . . . . .	19
2.4	Performance Evaluation . . . . .	23
2.5	Summary . . . . .	31
<b>3</b>	<b>WiMAX Location Update for Vehicle Applications</b>	<b>33</b>
3.1	WiMAX Location Tracking Mechanism . . . . .	33
3.2	The Location Update Procedure . . . . .	37
3.3	Analytic Analysis . . . . .	39
3.4	Performance Evaluation . . . . .	47
3.5	Summary . . . . .	50
<b>4</b>	<b>Repacking on Demand for the Hierarchical WiMAX Networks</b>	<b>51</b>
4.1	Channel Repacking for the HWNs . . . . .	51
4.2	Speed-sensitive Channel Assignment for HWNs . . . . .	53
4.3	System Model for HWN Channel Assignment . . . . .	62
4.4	Results and Discussions . . . . .	66
4.5	Summary . . . . .	74
<b>5</b>	<b>Conclusions and Future Work</b>	<b>76</b>
5.1	Concluding Remarks . . . . .	76
5.2	Future Work . . . . .	77
<b>A</b>	<b>An OSA Application Server for Mobile Services</b>	<b>79</b>
A.1	Open Service Access (OSA) . . . . .	79
A.2	Application Server Architecture . . . . .	83
A.3	PoC Session Establishment . . . . .	87
A.4	Summary . . . . .	92

**B Simulation Model For Speed-Sensitive RoD-R**

**94**

**Bibliography**

**101**



# List of Figures

1.1	A Simplified Architecture for the Mobile Network . . . . .	2
1.2	WiMAX Experience Buses . . . . .	4
1.3	A Simplified WiMAX Network Architecture . . . . .	5
1.4	Hierarchical WiMAX Network Architecture . . . . .	7
2.1	Ping-pong Effect Reduction with Overlapping LA Configuration . . . . .	11
2.2	One-dimensional Overlapping LA Registration Scheme for $0 \leq K < \frac{N}{2}$ . . .	12
2.3	One-dimensional Overlapping LA Registration Scheme for $\frac{N}{2} \leq K < N$ . .	13
2.4	State Transition Diagram for $K$ -degree Overlapping LA Configuration (the LA Size is $N$ , and $0 \leq K < \frac{N}{2}$ ) . . . . .	15
2.5	Modified State Transition Diagram for $K$ -degree Overlapping LA Config- uration (the LA Size is $N$ , and $0 \leq K < \frac{N}{2}$ ) . . . . .	18
2.6	State Transition Diagram for the Central Policy ( $\frac{N}{2} \leq K < N$ ) . . . . .	20
2.7	State Transition Diagram for the Random Policy ( $\frac{N}{2} \leq K < N$ ) . . . . .	21
2.8	State Transition Diagram for the MinOL Policy ( $\frac{N}{2} \leq K < N$ ) . . . . .	23
2.9	Distances $D$ and $D_1$ in the New LA . . . . .	25
2.10	Effect of $K$ on $E[M]$ for $p = 0.5$ and $N = 15$ . . . . .	27
2.11	Effect of $K$ on $E[M]$ for $p = 0.7$ and $N = 15$ . . . . .	27
2.12	Effect of $K$ on $E[M]$ for $p = 0.9$ and $N = 15$ . . . . .	28
2.13	Effect of $K$ on $E[M]$ for $p = 1.0$ and $N = 15$ . . . . .	28
2.14	Effect of $K$ on $E[M]$ for $p = 0.5$ and $N = 100$ . . . . .	29

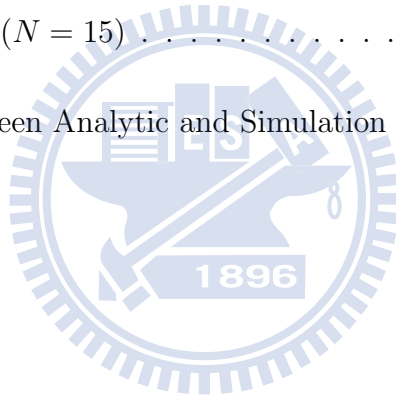
2.15	Effect of $K$ on $E[M]$ for $p = 0.7$ and $N = 100$ . . . . .	29
2.16	Effect of $K$ on $E[M]$ for $p = 0.9$ and $N = 100$ . . . . .	30
2.17	Effect of $K$ on $E[M]$ for $p = 1.0$ and $N = 100$ . . . . .	30
3.1	A Simplified WiMAX Network Architecture . . . . .	34
3.2	Flows of Inter-PC LUs with Signalling Costs . . . . .	38
3.3	Flows of Intra-PC LUs with Signalling Costs . . . . .	41
3.4	The MS Movement State-transition Diagram with Linear Configuration of PGs and PCs . . . . .	41
3.5	$U_R$ and $U_W$ for $V = 1/\gamma^2$ . . . . .	48
3.6	$U_R$ and $U_W$ for $p = 0.8$ and $\eta/\gamma = 24$ . . . . .	50
4.1	Hierarchical WiMAX Network Architecture . . . . .	52
4.2	No Repacking for Slow MSs . . . . .	55
4.3	No Repacking for Fast MSs . . . . .	56
4.4	Channel Repacking Procedures for AR . . . . .	58
4.5	RoD I: RoD for Slow MSs . . . . .	60
4.6	RoD II: RoD for Fast MSs . . . . .	61
4.7	Hierarchical WiMAX Network with Wrapped Mesh Configuration . . . . .	63
4.8	Handoff Types . . . . .	65
4.9	Effects of Macrocell Channel Number $C$ . . . . .	67
4.10	Effects of the Macrocell Channel Number $C$ . . . . .	68
4.11	Effect of the Proportion $\beta$ of Fast MSs on Incomplete Probability $P_{nc}$ . . . . .	71
4.12	Effect of MS Mobility on Incomplete Probability $P_{nc}$ . . . . .	72
4.13	Effect of the Arrival Rate $\lambda$ on Incomplete Probability $P_{nc}$ . . . . .	72
4.14	Effects of the Variance $V_c$ for the Call Holding Times . . . . .	73
4.15	Effects of Variance $V_{m,s}$ for Microcell Residence Times . . . . .	74
A.1	OSA Architecture . . . . .	80

A.2	Application Server Architecture . . . . .	84
A.3	Application Server Architecture for PoC Service . . . . .	85
A.4	Message Flow for PoC Session Establishment . . . . .	88
A.5	Message Flow for PoC Session Termination . . . . .	92
B.1	Simulation Flow Chart for RoD-R . . . . .	96
B.2	Flow Chart of Algorithm A . . . . .	97



# List of Tables

2.1	Analytic and Simulation Results ( $N = 15$ ) . . . . .	24
2.2	The Distance $D$ between the Entrance Cell and the Cental Cell of the New LA ( $N = 15$ ) . . . . .	26
2.3	The Distance $D_1$ ( $N = 15$ ) . . . . .	26
3.1	Comparison between Analytic and Simulation Results ( $k = 39$ ) . . . . .	46



# Notation

The notation used in this dissertation is listed below.

- $\alpha_j$ : the probability that starting from cell  $j$ , the MS leaves the old LA from the right-hand side (Chapter 2)
- $\beta$ : the proportion of fast calls (Chapter 4)
- $c$ : the number of radio channel in the microcell (Chapter 4)
- $C$ : the number of radio channel in the macrocell (Chapter 4)
- $D$ : the distance (the number of cells) between the entrance cell and the central cell of the new LA (Chapter 2)
- $D_1$ : the distance (the number of cells) between the entrance cell and the new LA's right-hand side (left-hand side) boundary cell if the MS enters the new LA from the left-hand side (right-hand side) of the LA (Chapter 2)
- $1/\eta$ : the expected PG residence time (Chapter 3)
- $1/\eta_f$ : the expected microcell residence time of fast MSs (Chapter 4)
- $1/\eta_s$ : the expected microcell residence time of slow MSs (Chapter 4)
- $f(t)$ : the density function of the idle period  $t$  (Chapter 3)
- $f^*(s)$ : the laplace transform of  $f(t)$  (Chapter 3)



- $1/\gamma$ : the expected idle period (Chapter 3)
- $H$ : the expected number of handoffs and repackings during a call (Chapter 4)
- $H_{mm}$ : the expected number of microcell-to-microcell handoffs during a call (Chapter 4)
- $H_{mM}$ : the expected number of microcell-to-macrocell handoffs during a call (Chapter 4)
- $H_{Mm}$ : the expected number of macrocell-to-microcell handoffs during a call (Chapter 4)
- $H_{MM}$ : the expected number of macrocell-to-macrocell handoffs during a call (Chapter 4)
- $H_R$ : the expected number of repackings (including m-to-M and M-to-m repackings) during a call (Chapter 4)
- $K$ : the number of overlapping cells between two neighboring LAs (Chapter 2)
- $\lambda$ : the call arrival rate to a microcell (for both incoming and outgoing calls) (Chapter 4)
- $1/\mu$ : the expected call holding time (Chapter 4)
- $M$ : the number of cell movement before the MS leaves the LA (Chapter 2)
- $N$  (Chapter 2): the number of cells in each LA
- $N$  (Chapter 3): the number of PGs within a PC
- $N_j$ : the number of cell movement, starting from cell  $j$  and before the MS leaves the LA (Chapter 2)
- $N_O$ : the number of the LAs covering the entrance cell (Chapter 2)

- $\pi(k)$ : the expected number of the intra-PC movements within PC 0 during  $k$  PG movements of the MS (Chapter 3)
- $\pi^*(k)$ : the expected number of the intra-PC movements in any PC other than PC 0 during  $k$  PG movements of the MS (Chapter 3)
- $\Pi_I(k)$ : the expected number of the inter-PC movements from PC  $-1$  or PC  $1$  “Into” PC 0 during  $k$  PG movements of the MS (Chapter 3)
- $\Pi_O(k)$ : the expected number of the inter-PC movements “Out” from PC 0 (to PC  $-1$  or PC  $1$ ) during  $k$  PG movements of the MS (Chapter 3)
- $\Pi^*(k)$ : the expected number of the inter-PC movements without visiting PC 0 during  $k$  PG movements of the MS (Chapter 3)
- $p$  (Chapter 2): the routing probability that the MS moves to the right-hand side neighboring cell
- $p$  (Chapter 3): the routing probability that the MS moves to the right-hand side neighboring PG
- $P_b$ : the call blocking probability (Chapter 4)
- $P_f$ : the force-termination probability (Chapter 4)
- $P_{ff}$ : the force-termination probability of fast calls (Chapter 4)
- $P_{i,j}^k$ : the probability that starting from PG  $i$ , the MS visits PG  $j$  after  $k$  PG movements (Chapter 2)
- $P_j^k$ : the probability that from PG 0, the MS visits PG  $j$  after  $k$  PG movements, where  $k \geq 0$  (Chapter 2)
- $P_{nc}$ : the call incomplete probability (Chapter 4)

- $P(k)$ : the probability that the MS makes  $k$  PG movements during the idle period (Chapter 3)
- $q$ : the probability that the MS enters the new LA from a left-hand side LA for case  $0 \leq K < \frac{N}{2}$  (Chapter 2)
- $q_l$ : the probability that in the Random policy, the MS enters the new LA from a left-hand side LA for case  $\frac{N}{2} \leq K < N$  (Chapter 2)
- $q'$ : the probability that in the Central policy, the MS enters the new LA from a left-hand side LA for case  $\frac{N}{2} \leq K < N$  (Chapter 2)
- $q''$ : the probability that in the MinOL policy, the MS enters the new LA from a left-hand side LA for case  $\frac{N}{2} \leq K < N$  (Chapter 2)
- $q_r$ : the probability that in the Random policy, the MS enters the new LA from a right-hand side LA for case  $\frac{N}{2} \leq K < N$  (Chapter 2)
- $u$ : the cost of an intra-PC LU within PC 0 (Chapter 3)
- $u^*$ : the cost of an intra-PC LU in any PC other than PC 0 (Chapter 3)
- $U$ : the expected cost of an LU in the idle mode (Chapter 3)
- $U_I$ : the cost of an inter-PC LU from the neighboring PCs “Into” PC 0 (Chapter 3)
- $U_O$ : the cost of an inter-PC LU “Out” from PC 0 (to any neighboring PC) (Chapter 3)
- $U_R$ : the LU cost (the expected number of messages sent in an LU) for  $S_R$  (Chapter 3)
- $U^*$ : the cost of an inter-PC LU without involving PC 0 (Chapter 3)
- $U_W$ : the LU cost (the expected number of messages sent in an LU) for  $S_W$  (Chapter 3)

- $V$ : the variance for the idle periods (Chapter 3)
- $V_c$ : the variance for call holding times (Chapter 4)
- $V_{m,f}$ : the variance for microcell residence times of fast MSs (Chapter 4)
- $V_{m,s}$ : the variance for microcell residence times of slow MSs (Chapter 4)
- $X_y$ : the  $y$ th cell movement of the MS (Chapter 2)



# Chapter 1

## Introduction

In recent years, the number of mobile subscribers grows rapidly. The mobile access becomes an important part of human life, and there is always a need for the service providers to offer mobile services with better features (e.g., higher transmission rates, larger capacity, better quality and so on). Therefore in the past two decades, the mobile networks have evolved from the first generation (1G) to the second generation (2G) and then the third generation (3G), and are marching forward to the fourth generation (4G). In 1G systems, such as *Advanced Mobile Phone System* (AMPS) [45], analog radio transmission was in use for telephony service delivery. 2G systems, such as *Global System for Mobile communications* (GSM) [45], utilized digital radio transmission with encryption mechanism to replace the analog technology. The popular *Short Message Service* (SMS) is also first introduced to the subscribers in 2G networks. Unlike the 1G and 2G systems that are primarily designed for speech services, networks after 2G evolved to provide better data services. In 3G systems, such as *Universal Mobile Telecommunications System* (UMTS) [47], mobile subscribers are offered the enhanced mobile services of wider range and higher transmission rates. Furthermore, 4G systems are highly expected to provide the comprehensive broadband services anytime and anywhere. At present, two pre-4G solutions are being developed: the *Worldwide Interoperability for Microwave Access* (WiMAX) [75, 76, 77, 35] and the 3GPP *Long Term Evolution* (LTE) [53, 6, 30].

Figure 1.1 illustrates a simplified architecture for a mobile network, which consists of

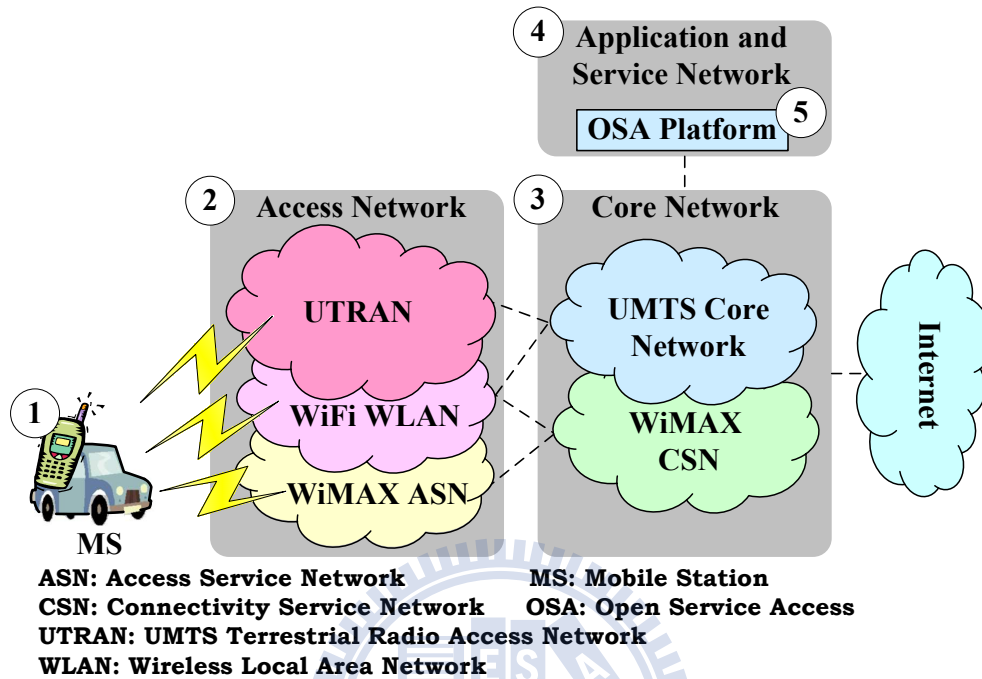


Figure 1.1: A Simplified Architecture for the Mobile Network

*Mobile Station* (MS; see Figure 1.1 (1)), *Access Network* (see Figure 1.1 (2)), *Core Network* (see Figure 1.1 (3)), and *Application and Service Network* (see Figure 1.1 (4)). An MS is the equipment through which a mobile subscriber can access services from the mobile network. The Access Network provides radio access for MSs, and the Core Network is responsible for routing MSs' calls and data from/to the access networks or the external networks, such as other *Public Land Mobile Networks* (PLMNs) [45], *Packet Switched Telephone Networks* (PSTNs) [45] and Internet. Note that the Access Network can be the *UMTS Terrestrial Radio Access Network* (UTRAN), the *WiMAX Access Service Network* (ASN) or the *Wireless Fidelity (WiFi) Wireless Local Area Network* (WLAN). The Core Network can be the *UMTS Core Network* or the *WiMAX Connectivity Service Network* (CSN). The Application and Service Network supports flexible services through a common service platform; e.g., the *Open Service Access* (OSA) platform (see Figure 1.1 (5)). OSA is defined by 3GPP CN5, ETSI SPAN12, ITU-T SG11 and the Parlay Group [52, 2, 1, 3, 4] to construct the Application and Service Network. Through the OSA platform deployed

by the mobile operators, third parties can implement and run their own applications without concerning the underlying network environment. In Appendix A, the *Push to Talk over Cellular* (PoC) service is used to illustrate how the third party programmers create a modern mobile service through OSA platform.

Many studies have been conducted to investigate various aspects of the mobile access, and *mobility management* (related to both the Access and Core Networks) is one of the most important issues. The mobility management mechanism supports MS mobility in the mobile network and can be divided into two essential functions: *location management* and *handoff management* [19, 8]. The location management function tracks the location of roaming MSs for mobile service delivery. The handoff management function maintains ongoing services when MSs move around the mobile networks to support service continuity, such as the *Voice Call Continuity* (VCC) [5]. In this dissertation, we investigate the mobility management issue in both aspects.

To track the mobility of roaming MSs, two basic location management operations, *location update* and *paging*, are utilized in most mobile networks. Location update operation is used by an MS to report its current location to the network. Paging operation is used by the network to alert an MS about its incoming data. To track MS mobility, the signalling messages for these operations cause significant traffic load to the mobile networks (see Section 1.1).

To maintain the service continuity during MS mobility, network resources would be allocated to establish a new transmission path for the handoff service. To support more handoffs, the radio channels that are the most scarce resources in mobile networks should be carefully and efficiently allocated. To increase network capacity, the deployment of the *Hierarchical Cellular Networks* (HCNs) [29, 43, 48, 32, 11] is one of the most popular solutions, such as the LTE/WiMAX *Femtocells* [24, 12, 81, 9] and the hierarchical WiMAX-WiFi networks [83, 54, 78]. Furthermore, to increase the channel utilization and reduce the waste of radio resources, many channel assignment schemes are also pro-



Figure 1.2: WiMAX Experience Buses

posed for efficient channel allocation [10, 26, 28, 50, 61, 62, 71, 73, 13, 49]. Both good cell layouts and efficient channel assignment schemes can significantly reduce the force-terminated probability for handoff services (see Section 1.2).

The location management and the handoff management issues attract great interest from both academia and industry. This dissertation will investigate both mobility management issues for WiMAX networks. In the remainder of this chapter, we first introduce the WiMAX system with the location management mechanism in Section 1.1. Then in Section 1.2, we describe an efficient channel assignment mechanism, *repacking*, for the *Hierarchical WiMAX Network* (HWN; i.e., the WiMAX system with hierarchical cell structure). Finally, we present the organization for this dissertation in Section 1.3.

## 1.1 Location Management for WiMAX System

WiMAX provides broadband wireless services with wide service coverage, high data throughput, and high mobility [75, 76, 77]. In Taiwan, an important WiMAX usage is to provide broadband access for vehicles. Figure 1.2 illustrates Taiwan WiMAX experience bus where people in the bus enjoy applications such as GPS/Navigation, portable digital TV, multimedia player, and so on.

Figure 1.3 shows a simplified WiMAX network architecture, which consists of the CSNs



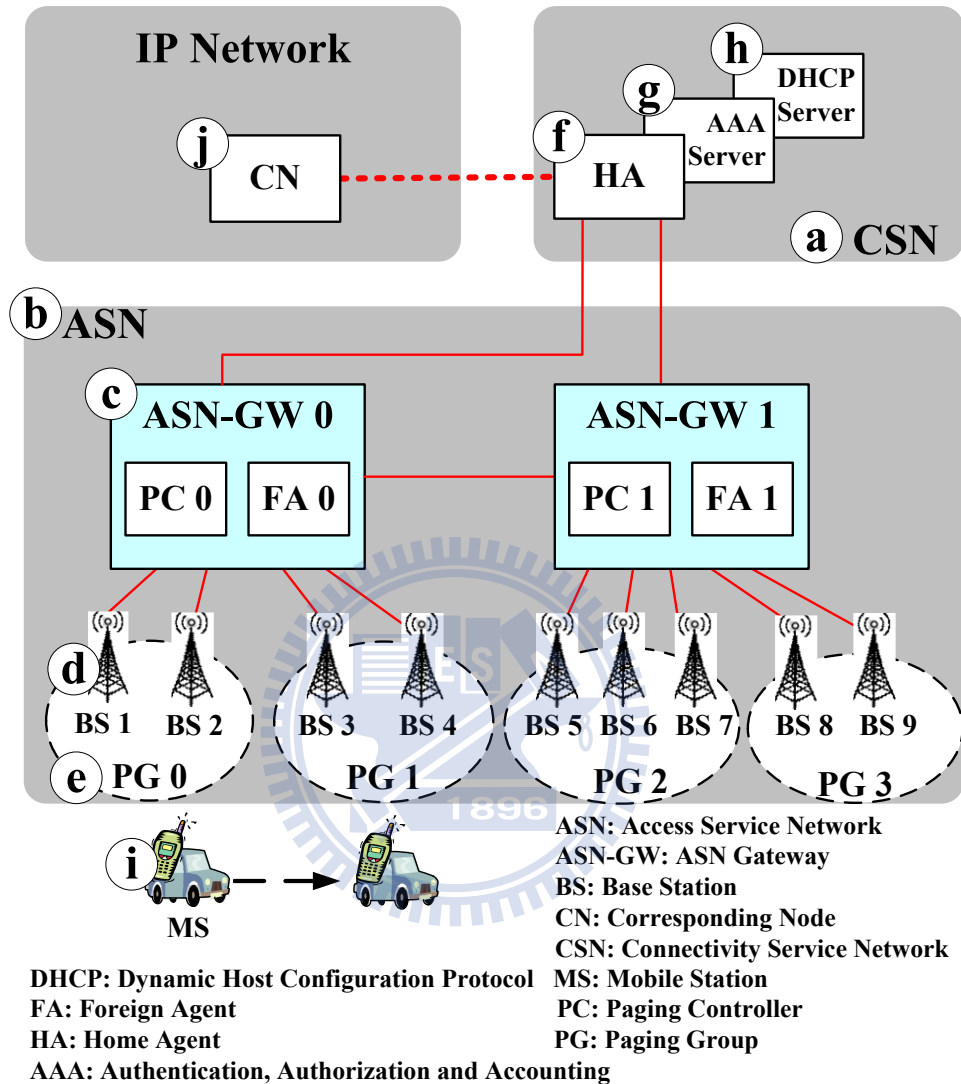


Figure 1.3: A Simplified WiMAX Network Architecture

(see Figure 1.3 (a)) and the ASNs (see Figure 1.3 (b)). An ASN provides radio access (such as radio resource management, paging and location management) to the WiMAX MS (see Figure 1.3 (i)). The ASN comprises *ASN gateways* (ASN-GWs; see Figure 1.3 (c)) and WiMAX BSs (see Figure 1.3 (d)). Every ASN-GW connects to several BSs. The ASN-GWs are also connected to each other to coordinate MS mobility. A CSN consists of network nodes such as the *Mobile IP* (MIP) [39] *Home Agent* (HA; see Figure 1.3 (f)), the *Authentication, Authorization, and Accounting* (AAA) server (see Figure 1.3 (g)) and the *Dynamic Host Configuration Protocol* (DHCP) server (see Figure 1.3 (h)). The

CSN provides IP connectivity (such as Internet access and IP address allocation) to a WiMAX MS and interworks with the ASNs to support capabilities such as AAA and mobility management. Before an MS is allowed to access WiMAX services, it must be authenticated by the ASN-GW (which serves as the *authenticator*) and the AAA server in the CSN.

In WiMAX, the *Paging Controller* (PC) in an ASN-GW (see Figure 1.3 (c)) handles the location tracking operations for the WiMAX MSs. For each roaming MS, an *Anchor PC* (APC) is assigned to handle its location tracking. To track MS location, all BSs connected to a PC are partitioned into several *Paging Groups* (PGs; see Figure 1.3 (e)), where the PG is suggested being partially overlapped with each other [35]. Note that the PG is also referred to as the *Location Area* (LA; in GSM/GPRS/UMTS), the *UTRAN Routing Area* (URA; in UMTS), the *Tracking Area* (TA; in LTE), and so on. Whenever the MS moves from one PG to another, the MS utilizes a *Location Update* (LU) operation to report its new PG to the APC. During LU procedure, the network may dynamically relocate the APC for MS mobility. Once there are incoming packets for the roaming MS, the APC will alert the MS by the *paging* operation. In Chapter 3, we will illustrate the message flows of the WiMAX location tracking operations for more details, and then investigate the performance for WiMAX location tracking mechanism.

## 1.2 Repacking for Hierarchical WiMAX Networks

One of the most important issues in cellular network operation is capacity planning. When the number of cellular subscribers grows rapidly, it is required that the cellular service provider increases its network capacity effectively. For WiMAX operators, one possible solution is to deploy the *Hierarchical WiMAX Networks* (HWNs; i.e., the WiMAX systems with hierarchical cell structure). As shown in Figure 1.4, the HWN consists of two types of *Base Stations* (BSs): micro BSs and macro BSs. A micro BS with low power transceivers provides small radio coverage (referred to as microcell), and a macro BS with high power

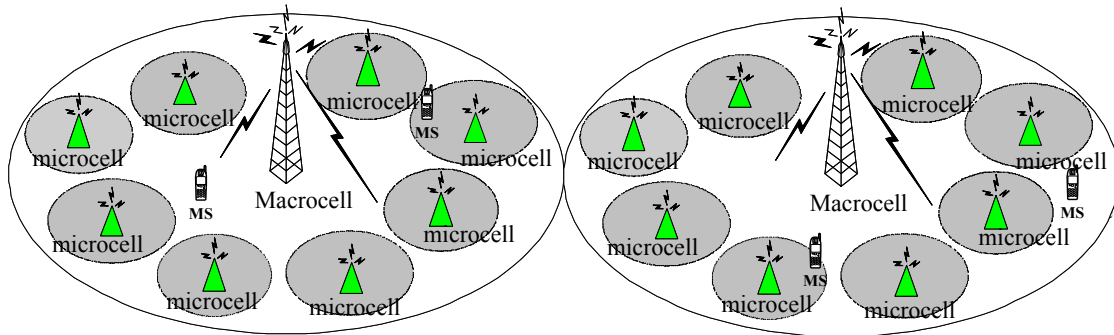


Figure 1.4: Hierarchical WiMAX Network Architecture

transceivers provides large radio coverage (referred to as macrocell). The microcells cover MSs in heavy teletraffic areas. A macrocell is overlaid with several microcells to cover all MSs in these microcells. Note that to deploy the HWNs, macrocell BSs can be the WiMAX BSs with high transmission power, and microcell BSs can be the WiMAX BSs with low transmission power, the *WiMAX Femtocell Access Points* (WFAPs) [81, 9] or the *WiFi Access Points* (APs) [54, 78, 40, 59].

In a cellular network, radio channels must be carefully assigned to reduce the numbers of new call blockings as well as handoff call force-terminations. Several channel planning and assignment approaches have been proposed for the hierarchical networks [10, 18, 26, 28, 34, 50, 61, 62, 66, 71, 73]. Some studies focused on channel assignment according to the received radio signal strength [26, 61]. Other studies [18, 28, 34, 73] investigated radio channel packing issues for channel reuse. A basic scheme called *No Repacking* (NR) was described in [62]. In this scheme, when a call attempt (either a new call or a handoff call) for an MS arrives in the HWN, the network first tries to allocate a channel in the microcell of the MS. If no idle channel is available in this microcell, the call attempt overflows to the corresponding macrocell. If the macrocell has no idle channel, the call attempt is rejected. Call blockings and force-terminations of NR can be reduced by *repacking* techniques described as follows [74]. Consider a call attempt for a microcell that has no idle channel. In NR, this call attempt is served by the corresponding macrocell. If radio channels are available in the microcell later, this call can be transferred from the macrocell

to the microcell again. The process of switching a call between the macrocell and the microcell is called the repacking. Chapter 4 will show that with repacking mechanism, channel assignment approaches can increase the number of idle channels in a macrocell so that more macrocell channels can be shared by the call attempts where no channels are available in the microcells.

### 1.3 Dissertation Organization

Mobility management is one of the most important issues for the WiMAX network. As described above, mobility management contains the location management function and the handoff management function. With these functions, mobility management enables the mobile network to locate roaming MSs for the service delivery and to maintain the ongoing communications during MS movement for the service continuity. This dissertation investigates the mobility management for WiMAX in both aspects.

For location management, we propose analytic models to study the performance of WiMAX location tracking mechanism (see Chapters 2 and 3). We first study the LU performance with overlapping LA configuration that is a suggested alternative for URA/PG/TA layout in UMTS, WiMAX and LTE systems [35, 30, 53, 6, 7]. From the performance analysis, our study indicates how to determine the appropriate overlap among LAs. Then, we further investigate the performance of the WiMAX LU procedure with/without APC relocation. The analytic results provide guidelines to utilize the APC relocation with various moving behaviors.

For handoff management, we study the performance of several channel assignment schemes with repacking mechanism for HWNs to support higher mobility, including our proposed scheme, *Repacking on Demand* (RoD; see Chapter 4). Our previous study [68] indicated that higher MS moving speeds result in more force-terminations for the numerous handoffs. To support high MS mobility in WiMAX, we propose RoD by considering MS moving speeds. Our study quantitatively indicates that RoD is less sensitive to MS

moving speeds and outperforms the other previous proposed schemes significantly.

This dissertation is organized as follows. Chapter 2 proposes an analytic model to study the LU performance with overlapping LA configuration. Chapter 3 proposes an analytic model to study the performance of the WiMAX LU procedure with/without APC relocation. Chapter 4 presents speed-sensitive RoD for the HWNs with the performance evaluation. Finally, we conclude this dissertation with some future directions.



## Chapter 2

# Performance for Mobile Network with Overlapping Location Area Configuration

As described in Section 1.1, the *Location Area* (LA) of a *Mobile Station* (MS) is tracked by the *Location Update* (LU) operation in a mobile network. To reduce the LU traffic caused by the ping-pong effect, the overlapping LA concept is introduced. In the overlapping LA configuration, an LA selection policy is required to select the new LA at an LU when the MS enters a new cell covered by multiple LAs. This chapter describes four LA selection policies and proposes an analytic model to study the performance of these LA selection policies. Our study [80] provides guidelines to determine appropriate degree of overlapping among the LAs.

### 2.1 Location Area Overlap

To track user mobility, the cells (the coverage areas of base stations) are partitioned into groups in a mobile wireless network. These groups are referred to as the *Location Areas* (LAs; in GSM/GPRS/UMTS [45, 47]), the *Routing Areas* (RAs; in GPRS/UMTS [45, 47]), the *Paging Groups* (PGs; in WiMAX [35]), *Tracking Areas* (TAs; in LTE [53, 6, 30]), and so on. Without loss of generality, we use the term LA throughout this chapter. The LA of a *Mobile Station* (MS) is tracked by the network. Whenever the MS moves from one

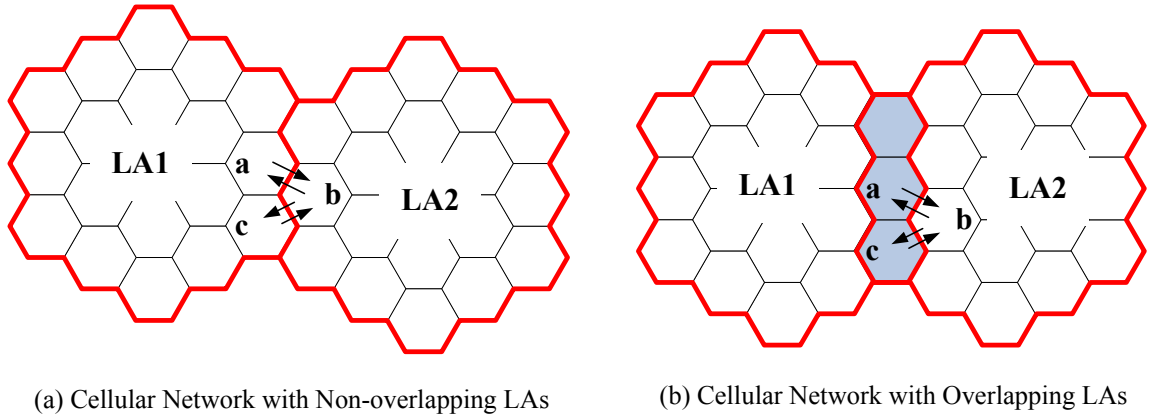


Figure 2.1: Ping-pong Effect Reduction with Overlapping LA Configuration

LA to another LA, the MS issues a *Location Update* (LU) request to inform the network that it has entered the new LA. In this way, the network keeps track of the LA where the MS resides.

A typical LA layout is illustrated in Figure 2.1 (a) where every cell is covered by exactly one LA. Recently, the overlapping LA concept (where a cell is covered by multiple LAs; see the gray areas in Figure 2.1 (b)) has been proposed to avoid the *ping-pong effect* [14, 15, 20, 21, 25, 55]. Suppose that an MS resides in cell *a* of LA 1 as illustrated in Figure 2.1. In the non-overlapping LA configuration (Figure 2.1 (a)), when the MS moves to cell *b* in LA 2, the MS performs an LU to register to LA 2. If the MS moves to cell *c* or back to cell *a* in LA 1 again, the MS performs another LU to register to LA 1. If the MS repeatedly moves back and forth between LA 1 and LA 2, many LUs are performed. This phenomenon is called the ping-pong effect. In the overlapping LA configuration, when the MS moves from cell *a* (in LA 1) to cell *b* (in LA 2), an LU is executed as in the non-overlapping LA configuration. If the MS moves to cell *c* or back to cell *a*, it still resides in LA 2 and no LU is performed. Therefore, the ping-pong effect is mitigated.

Several studies [14, 15, 25] proposed analytic models to study the performance of the mobile telecommunications network with overlapping LAs. These studies assumed that at each movement, the MS moves to any of its neighboring cells with the same probability.

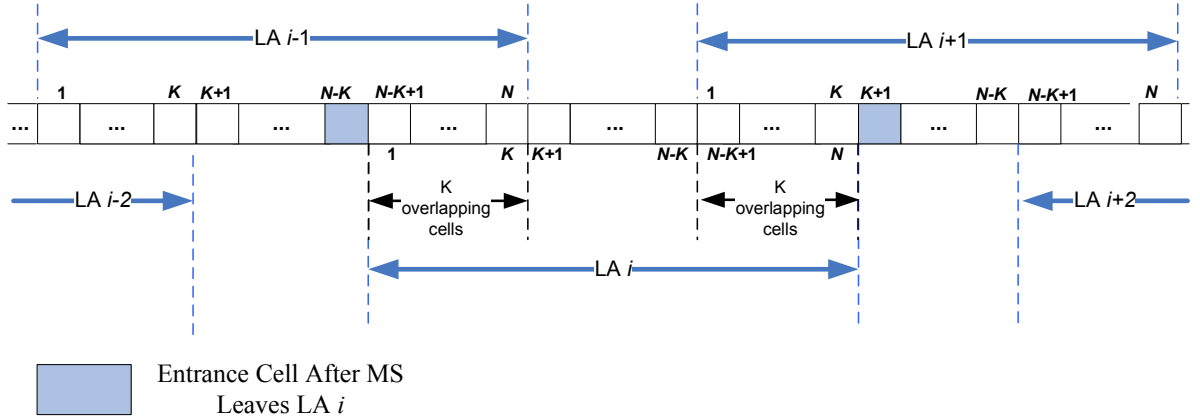


Figure 2.2: One-dimensional Overlapping LA Registration Scheme for  $0 \leq K < \frac{N}{2}$

In [25], the LA consists of odd numbers of cells. In [14, 15], an example is provided and no close-form solution was derived to evaluate the performance. Moreover, each of the previous studies investigated one LA selection algorithm.

This chapter is organized as follows. Section 2.2 introduces the system model and four overlapping LA policies. Section 2.3 proposes the analytic models for these policies. Section 2.4 quantitatively compares the four studied policies. Then Section 2.5 provides guidelines to determine appropriate degree of overlapping among the LAs.

## 2.2 System Model and LA Selection Policies

This section describes the system model and four LA selection policies in details. For the purpose of demonstration, one-dimensional overlapping LA configuration is considered. Based on this configuration, then in section 2.3, we describe a random walk model for MS movement and construct state transition diagrams to derive the LU costs.

Figures 2.2 and 2.3 illustrate the one-dimensional overlapping LA configuration, where each LA covers  $N$  cells, and is overlapped with each of its adjacent LAs by  $K$  cells ( $0 \leq K < N$ ). We say that the *overlapping degree* for this LA configuration is  $K$ . In each LA, cells are sequentially labelled from 1 to  $N$ . An MS moves to the right-hand side neighboring cell with the *routing probability*  $p$ , and moves to the left-hand side neighboring



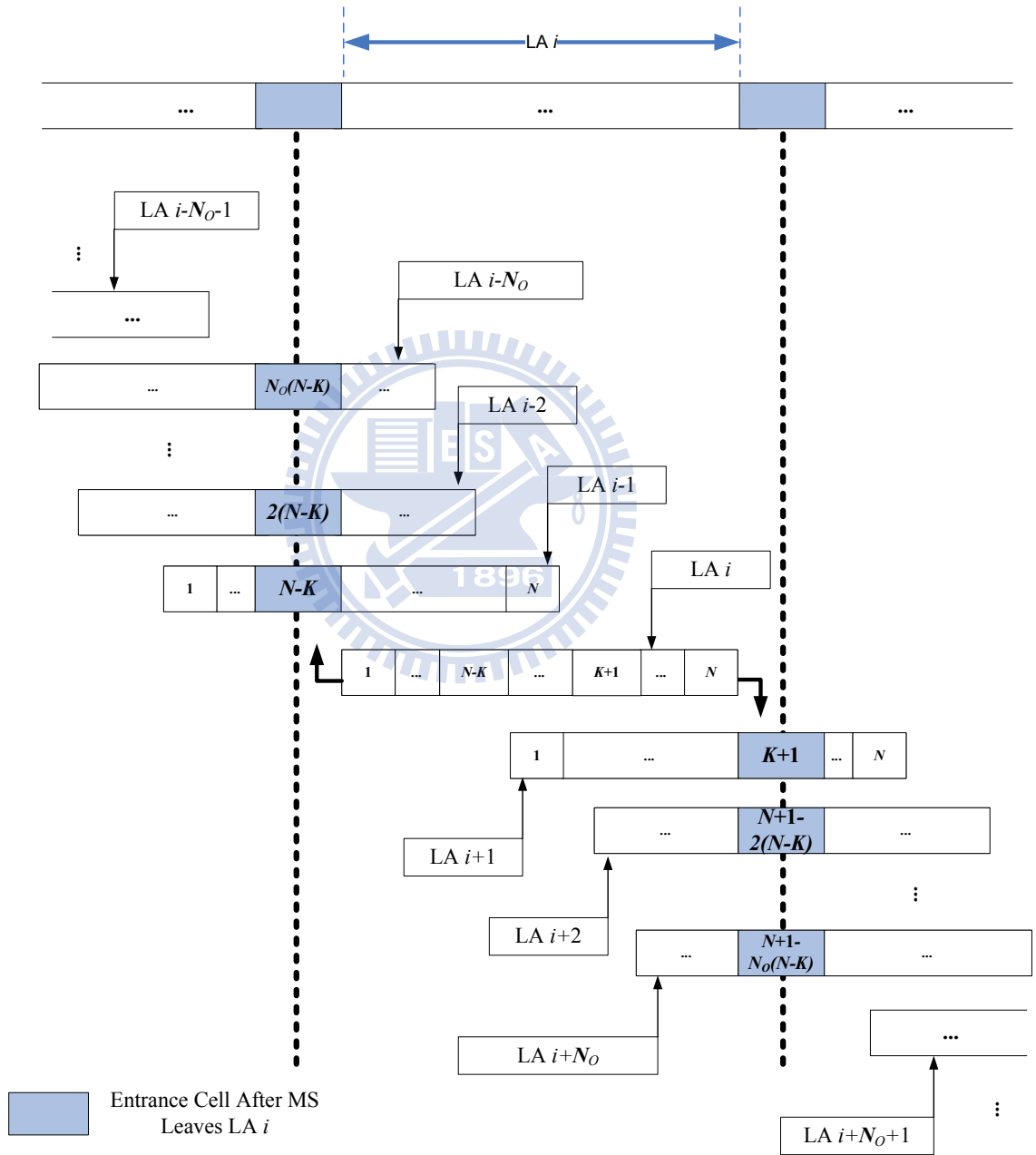


Figure 2.3: One-dimensional Overlapping LA Registration Scheme for  $\frac{N}{2} \leq K < N$

cell with probability  $1 - p$ . If the MS moves into a new cell that does not belong to the currently registered LA (i.e., the MS moves out of the current LA), it performs an LU. This new cell is called the *entrance cell* to the new LA. If  $0 \leq K < \frac{N}{2}$ , the entrance cell is covered by only one LA. When the MS moves out of LA  $i$  from the right-hand side (the left-hand side), it enters LA  $i + 1$  (LA  $i - 1$ ). The entrance cell is cell  $K + 1$  of LA  $i + 1$  (cell  $N - K$  of LA  $i - 1$ ); see the shadow boxes in Figure 2.2. On the other hand, if  $\frac{N}{2} \leq K < N$ , when an MS leaves the old LA and enters the new cell, this new cell is covered by several LAs adjacent to (or overlapping with) the old LA. As shown in Figure 2.3, when the MS leaves LA  $i$ , the new cell can be the entrance cell for each of  $N_O$  LAs, where

$$N_O = \left\lceil \frac{K + 1}{N - K} \right\rceil. \quad (2.1)$$

That is, if the MS moves out of LA  $i$  and enters a right-hand side LA, the entrance cell can be cell  $K + 1$  of LA  $i + 1$ , cell  $N + 1 - 2(N - K)$  of LA  $i + 2$ ,  $N + 1 - 3(N - K)$  of LA  $i + 3$ ,  $\dots$ , or cell  $N + 1 - N_O(N - K)$  of LA  $i + N_O$  (see the shadow boxes in Figure 2.3). Similarly, if the MS moves out of LA  $i$  and enters a left-hand side LA, the entrance cell can be cell  $N - K$  of LA  $i - 1$ , cell  $2(N - K)$  of LA  $i - 2$ ,  $\dots$ , or cell  $N_O(N - K)$  of LA  $i - N_O$ . Since the new cell is covered by more than one LAs for  $\frac{N}{2} \leq K < N$ , a policy is required to select the new LA at an LU. In this chapter, we investigate four LA selection policies described as follows.

- In the *Maximum Overlapping* (MaxOL) policy [14, 15, 25], after moving out of the current LA  $i$  from the right-hand side (the left-hand side), the MS will register to the adjacent LA  $i + 1$  (LA  $i - 1$ ). In this case, the number of cells overlapped between the old and the new LAs is maximal.
- In the *Central* policy [25], after moving out of the current LA, the MS always registers to the LA whose central cell is closest to the entrance cell.
- In the *Random* policy, the MS randomly registers to one LA covering the entrance

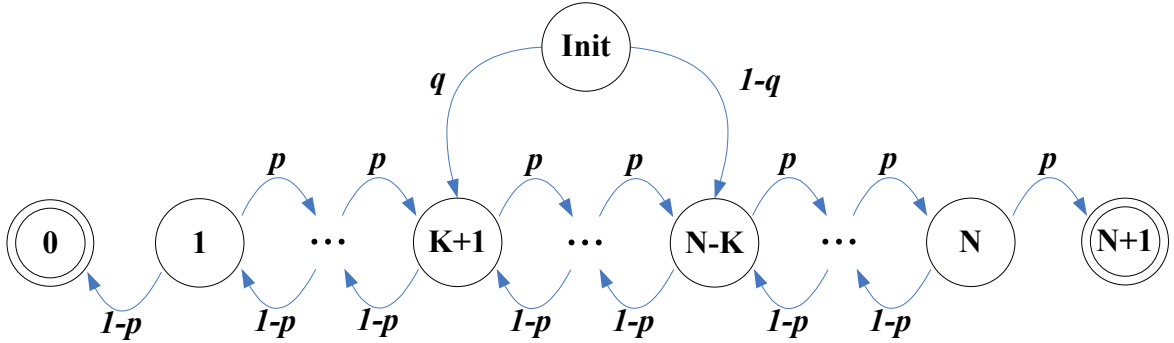


Figure 2.4: State Transition Diagram for  $K$ -degree Overlapping LA Configuration (the LA Size is  $N$ , and  $0 \leq K < \frac{N}{2}$ )

cell.

- In the *Minimum Overlapping* (MinOL) policy, after moving out of LA  $i$ , the MS chooses the farthest LA of the entrance cell from LA  $i$  (i.e., LA  $i + N_O$  in the right-hand side and LA  $i - N_O$  in the left-hand side in Figure 2.3). In this case, the number of cells overlapped between the old and the new LAs is minimal.

Note that for  $0 \leq K < \frac{N}{2}$ , the above four policies are the same; that is, the only LA covering the entrance cell is selected.

## 2.3 Analytic Model

This section proposes an analytic model to study the LU costs for mobile telecommunications networks with overlapping LAs. Suppose that an MS makes  $M$  cell movement before it leaves an LA. For each of the four policies described in section 2.2, we derive the expected number  $E[M]$ . It is clear that the larger the  $E[M]$  value, the better the performance.

### 2.3.1 Case 1: $0 \leq K < \frac{N}{2}$

Figure 2.4 illustrates the state transition diagram for MS cell movement in an LA, where  $0 \leq K < \frac{N}{2}$ . In this diagram, state *Init* represents that the MS moves into the LA in the

steady state. State  $j$  represents that the MS resides in cell  $j$  of the LA, where  $1 \leq j \leq N$ . Two virtual states, 0 and  $N + 1$ , are the absorbing states representing that the MS moves out of the LA from cell 1 and from cell  $N$ , respectively. For  $1 \leq j \leq N$ , the MS moves from state  $j$  to state  $j + 1$  with probability  $p$ , and the MS moves from state  $j$  to state  $j - 1$  with probability  $1 - p$ . As mentioned before, the entrance cell can be cell  $K + 1$  (cell  $N - K$ ) of the new LA when the MS leaves the old LA from the right-hand side (the left-hand side). Let  $q$  be the probability that the MS moves from the old LA to the new LA through the entrance cell  $K + 1$ . Then the MS moves from state  $Init$  to state  $K + 1$  with probability  $q$  and to state  $N - K$  with probability  $1 - q$ . Note that  $q$  is affected by the routing probability  $p$ , the overlapping degree  $K$  and the LA size  $N$ . We will derive  $q$  later.

Starting from the entrance cell  $j$ , let  $N_j$  be the number of cell movement before the MS leaves the LA. The expected number  $E[M]$  is

$$E[M] = qE[N_{K+1}] + (1 - q)E[N_{N-K}]. \quad (2.2)$$

We model the MS cell movement as the *Gambler's Ruin Problem* [64] to solve  $E[N_j]$ .

Let  $\alpha_j$  be the probability that starting from cell  $j$ , the MS will reach state  $N + 1$  before reaching state 0 (i.e., the MS moves out from the right-hand side). From Figure 2.4, we obtain the following recurrence relation for  $\alpha_j$

$$\alpha_j = p\alpha_{j+1} + (1 - p)\alpha_{j-1} \quad \text{for } j = 1, 2, \dots, N. \quad (2.3)$$

Since  $\alpha_0 = 0$  and  $\alpha_{N+1} = 1$ , (2.3) is solved to yield

$$\alpha_j = \begin{cases} \frac{1 - \left(\frac{1-p}{p}\right)^j}{1 - \left(\frac{1-p}{p}\right)^{N+1}} & \text{for } p \neq \frac{1}{2} \\ \frac{j}{N+1} & \text{for } p = \frac{1}{2} \end{cases}. \quad (2.4)$$

Define a random variable  $X_y$  as follows:

$$X_y = \begin{cases} -1 & \text{if the MS moves left at the } y\text{th cell movement} \\ 1 & \text{if the MS moves right at the } y\text{th cell movement} \end{cases}.$$

Then

$$N_j = \min \left\{ n : \sum_{y=1}^n X_y = -j \quad \text{or} \quad \sum_{y=1}^n X_y = N + 1 - j \right\}.$$

Note that  $E[X_y] = 1 \times p + (-1)(1 - p) = 2p - 1$  and  $N_j$  is a stopping time for  $X_y$ 's. The  $E[X_y]$  value can be a positive or a negative number, and the sign of  $E[X_y]$  indicates the direction of MS movement. By using the *Wald's Equation* [64], we have

$$E \left[ \sum_{y=1}^{N_j} X_y \right] = (2p - 1)E[N_j]. \quad (2.5)$$

Consider the left-hand side of (2.5). We have

$$\sum_{y=1}^{N_j} X_y = \begin{cases} N + 1 - j & \text{with probability } \alpha_j \\ -j & \text{with probability } 1 - \alpha_j \end{cases},$$

or

$$E \left[ \sum_{y=1}^{N_j} X_y \right] = (N + 1 - j)\alpha_j + (-j)(1 - \alpha_j) = (N + 1)\alpha_j - j. \quad (2.6)$$

Substituting (2.6) into (2.5) to yield

$$E[N_j] = \frac{(N + 1)\alpha_j - j}{2p - 1}. \quad (2.7)$$

If  $p$  approaches  $\frac{1}{2}$ ,  $E[N_j]$  can be derived by applying the *L'Hospital's Rule* [67] to (2.7), which yields

$$\lim_{p \rightarrow \frac{1}{2}} E[N_j] = (N + 1)j - j^2. \quad (2.8)$$

To derive  $q$ , Figure 2.5 modifies the state diagram in Figure 2.4 by removing the absorbing states 0 and  $N + 1$ , and adding the transitions from state  $N$  to state  $K + 1$  (with probability  $p$ ) and from state 1 to state  $N - K$  (with probability  $1 - p$ ). When the MS moves out of the current LA from the right-hand side (the left-hand side), the process moves from state  $N$  to state  $K + 1$  (from state 1 to state  $N - K$ ). In other words, the MS moves from cell  $N$  (cell 1) of the old LA to cell  $K + 1$  (cell  $N - K$ ) of the new LA. In this case, the MS

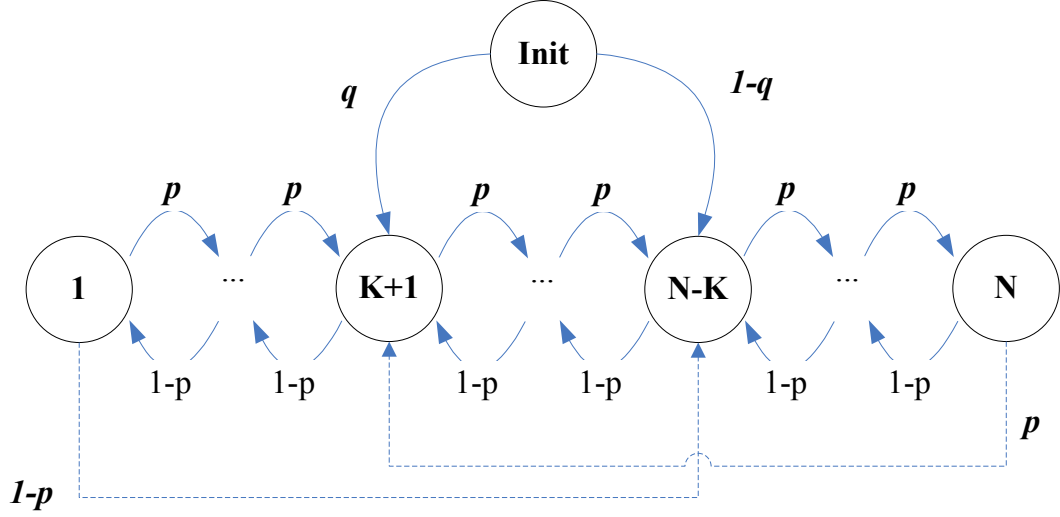


Figure 2.5: Modified State Transition Diagram for  $K$ -degree Overlapping LA Configuration (the LA Size is  $N$ , and  $0 \leq K < \frac{N}{2}$ )

would leave the current LA from the right-hand side boundary and move to cell  $K + 1$  of new LA with probability  $q\alpha_{K+1}$  (i.e., the probability that the MS moves into entrance cell  $K + 1$  and then moves out the LA from the right-hand side) plus  $(1 - q)\alpha_{N-K}$  (i.e., the probability that the MS moves into entrance cell  $N - K$  and then moves out the LA from the right-hand side). Since the MS moves from state  $Init$  to state  $K + 1$  with probability  $q$ , we have the following equation

$$q = q\alpha_{K+1} + (1 - q)\alpha_{N-K},$$

or equivalently

$$q = \frac{\alpha_{N-K}}{1 - \alpha_{K+1} + \alpha_{N-K}}. \quad (2.9)$$

Substituting (2.4) and (2.7) - (2.9) into (2.2),  $E[M]$  is expressed as

$$E[M] = \begin{cases} \left( \frac{\alpha_{N-K}}{1 - \alpha_{K+1} + \alpha_{N-K}} \right) \left[ \frac{(N+1)\alpha_{K+1} - K - 1}{2p - 1} \right] \\ \quad + \left( \frac{1 - \alpha_{K+1}}{1 - \alpha_{K+1} + \alpha_{N-K}} \right) \left[ \frac{(N+1)\alpha_{N-K} - N + K}{2p - 1} \right] & \text{for } p \neq \frac{1}{2} \quad , \\ (N - K) \times (K + 1) & \text{for } p = \frac{1}{2} \end{cases} \quad (2.10)$$

where

$$\alpha_j = \begin{cases} \frac{1 - \left(\frac{1-p}{p}\right)^j}{1 - \left(\frac{1-p}{p}\right)^{N+1}} & \text{for } p \neq \frac{1}{2} \\ \frac{j}{N+1} & \text{for } p = \frac{1}{2} \end{cases}.$$

### 2.3.2 Case 2: $\frac{N}{2} \leq K < N$

In this case, an entrance cell is covered by two or more LAs. Therefore, after the MS leaves the old LA, an LA selection policy is required to select the new LA. The  $E[M]$  values for the four policies are derived as follows.

- **MaxOL:** The MS always chooses a new LA with maximum overlapping with the old LA. When the MS moves out of LA  $i$  from the right-hand side (the left-hand side), it registers to LA  $i + 1$  (LA  $i - 1$ ). Clearly, the LA selected in this policy is the same as that selected in case  $0 \leq K < \frac{N}{2}$  described in Section 2.3.1. Therefore, the expected number of MS cell movement in an LA is expressed in (2.10).
- **Central:** After moving out of LA  $i$ , the MS always registers to the LA whose central cell is closest to the entrance cell. The selected LA is the  $\left\lceil \frac{N_O}{2} \right\rceil$ -th LA away from LA  $i$ . That is, the entrance cell is cell  $N + 1 - \left\lceil \frac{N_O}{2} \right\rceil (N - K)$  of LA  $i + \left\lceil \frac{N_O}{2} \right\rceil$  in the right-hand side or cell  $\left\lceil \frac{N_O}{2} \right\rceil (N - K)$  of LA  $i - \left\lceil \frac{N_O}{2} \right\rceil$  in the left-hand side. The state transition diagram for the Central policy is shown in Figure 2.6, where the MS moves from state *Init* to state  $N + 1 - \left\lceil \frac{N_O}{2} \right\rceil (N - K)$  with probability  $q'$  and to state  $\left\lceil \frac{N_O}{2} \right\rceil (N - K)$  with probability  $1 - q'$ . Following the derivation in Section 2.3.1, we have

$$q' = \frac{\alpha_{\left\lceil \frac{N_O}{2} \right\rceil (N-K)}}{1 - \alpha_{N+1 - \left\lceil \frac{N_O}{2} \right\rceil (N-K)} + \alpha_{\left\lceil \frac{N_O}{2} \right\rceil (N-K)}}$$

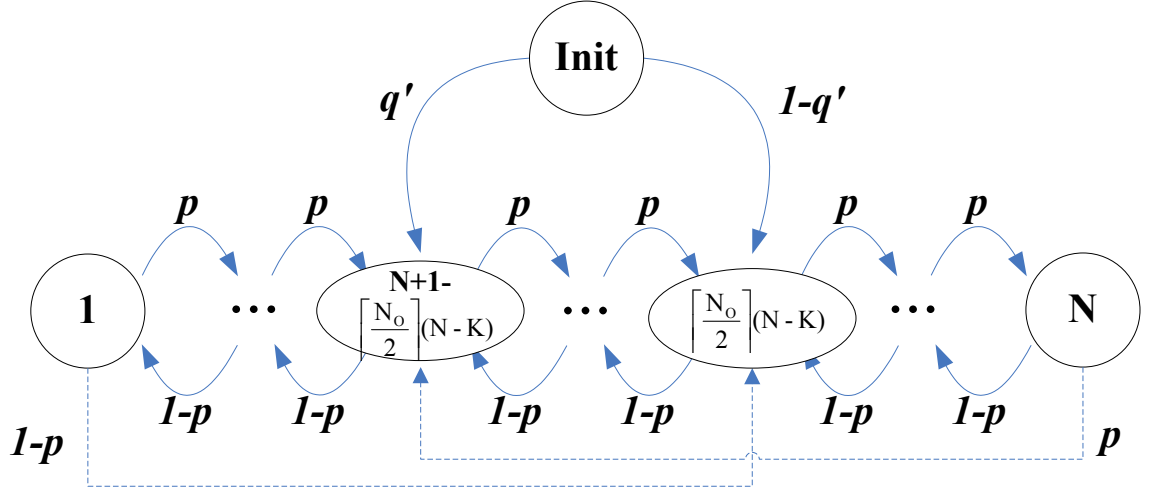


Figure 2.6: State Transition Diagram for the Central Policy ( $\frac{N}{2} \leq K < N$ )

and the expected number

$$\begin{aligned}
 E[M] &= q' E \left[ N_{N+1 - \lfloor \frac{N_O}{2} \rfloor (N-K)} \right] + (1-q') E \left[ N_{\lfloor \frac{N_O}{2} \rfloor (N-K)} \right] \\
 &= \left\{ \begin{aligned} & \left[ \frac{\alpha_{\lfloor \frac{N_O}{2} \rfloor (N-K)}}{1 - \alpha_{N+1 - \lfloor \frac{N_O}{2} \rfloor (N-K)} + \alpha_{\lfloor \frac{N_O}{2} \rfloor (N-K)}} \right] \\ & \times \left\{ \frac{(N+1) \left( \alpha_{N+1 - \lfloor \frac{N_O}{2} \rfloor (N-K)} - 1 \right) + \lfloor \frac{N_O}{2} \rfloor (N-K)}{2p-1} \right\} \\ & + \left[ \frac{1 - \alpha_{N+1 - \lfloor \frac{N_O}{2} \rfloor (N-K)}}{1 - \alpha_{N+1 - \lfloor \frac{N_O}{2} \rfloor (N-K)} + \alpha_{\lfloor \frac{N_O}{2} \rfloor (N-K)}} \right] \\ & \times \left[ \frac{(N+1) \alpha_{\lfloor \frac{N_O}{2} \rfloor (N-K)} - \lfloor \frac{N_O}{2} \rfloor (N-K)}{2p-1} \right] \text{ for } p \neq \frac{1}{2} \\ & \left[ \left[ \frac{N_O}{2} \right] (N-K) \right] \times \left[ N+1 - \left[ \frac{N_O}{2} \right] (N-K) \right] \text{ for } p = \frac{1}{2} \end{aligned} \right\}. \quad (2.11)
 \end{aligned}$$



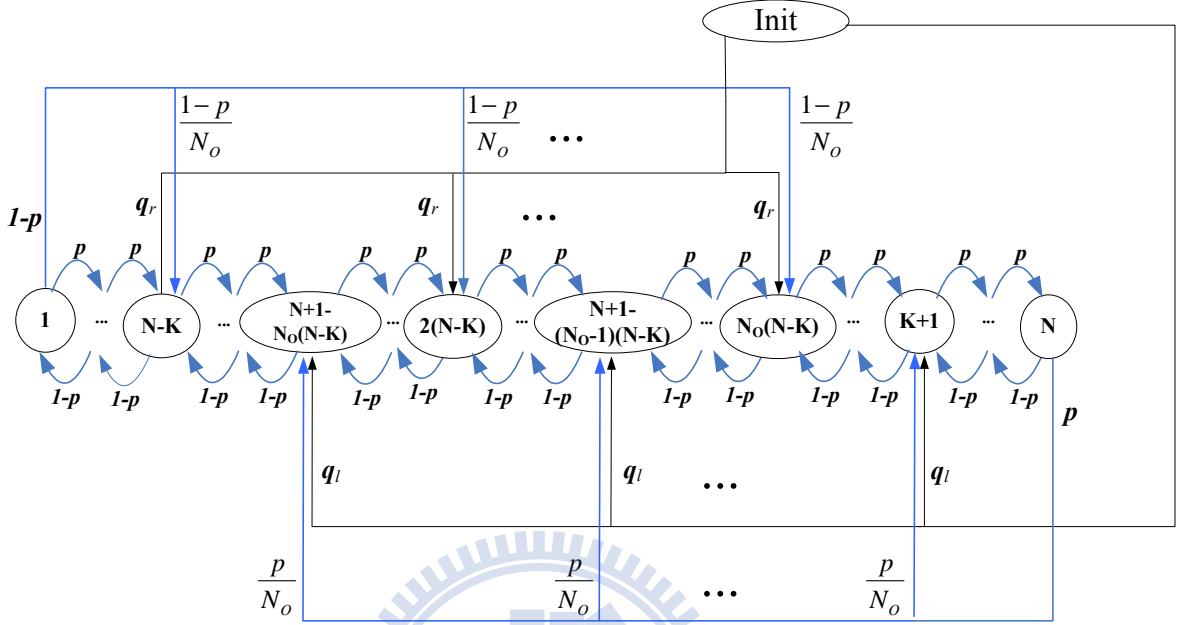


Figure 2.7: State Transition Diagram for the Random Policy ( $\frac{N}{2} \leq K < N$ )

- Random: The MS randomly registers to one LA covering the entrance cell. Let  $q_r$  ( $q_l$ ) be the probability that the MS moves from a left-hand side LA (right-hand side LA) to the new LA through the entrance cell. The state transition diagram for the Random policy is shown in Figure 2.7, where the MS moves from state *Init* to state  $N + 1 - m(N - K)$  with probability  $q_l$  and to state  $m(N - K)$  with probability  $q_r$ , where  $1 \leq m \leq N_o$ . From Figure 2.7,  $E[M]$  is expressed as

$$E[M] = q_l \left\{ \sum_{m=1}^{N_o} E \left[ N_{N+1-m(N-K)} \right] \right\} + q_r \left\{ \sum_{m=1}^{N_o} E \left[ N_{m(N-K)} \right] \right\}. \quad (2.12)$$

Since the entrance cell is covered by  $N_o$  LAs, when the MS leaves the old LA, the process moves from state  $N$  (state 1) to state  $N + 1 - m(N - K)$  (state  $m(N - K)$ ) with probability  $\frac{p}{N_o}$  ( $\frac{1-p}{N_o}$ ), where  $1 \leq m \leq N_o$ ; see Figure 2.7. The balance

equations for probabilities  $q_l$  and  $q_r$  are

$$\begin{aligned}
q_l &= \left( \frac{1}{N_O} \right) \left[ q_l \sum_{m=1}^{N_O} \alpha_{N+1-m(N-K)} + q_r \sum_{m=1}^{N_O} \alpha_{m(N-K)} \right] \\
q_r &= \left( \frac{1}{N_O} \right) \left\{ q_l \sum_{m=1}^{N_O} [1 - \alpha_{N+1-m(N-K)}] + q_r \sum_{m=1}^{N_O} [1 - \alpha_{m(N-K)}] \right\} \\
1 &= N_O (q_l + q_r)
\end{aligned}$$

or equivalently

$$\left. \begin{aligned}
q_l &= \frac{\sum_{m=1}^{N_O} \alpha_{m(N-K)}}{N_O \left\{ N_O + \sum_{m=1}^{N_O} [\alpha_{m(N-K)} - \alpha_{N+1-m(N-K)}] \right\}} \\
q_r &= \frac{1}{N_O} - q_l
\end{aligned} \right\}. \quad (2.13)$$

Substituting (2.13) into (2.12),  $E[M]$  is expressed as

$$E[M] = \begin{cases} \sum_{m=1}^{N_O} \left\{ q_l \left( \frac{(N+1)\alpha_{N+1-m(N-K)} - [N+1-m(N-K)]}{2p-1} \right) + \left( \frac{1}{N_O} - q_l \right) \left[ \frac{(N+1)\alpha_{m(N-K)} - m(N-K)}{2p-1} \right] \right\} & \text{for } p \neq \frac{1}{2} \\ \sum_{m=1}^{N_O} \frac{[m(N-K)] \times [N+1-m(N-K)]}{N_O} & \text{for } p = \frac{1}{2} \end{cases}, \quad (2.14)$$

where

$$q_l = \frac{\sum_{m=1}^{N_O} \alpha_{m(N-K)}}{N_O \left\{ N_O + \sum_{m=1}^{N_O} [\alpha_{m(N-K)} - \alpha_{N+1-m(N-K)}] \right\}}.$$

- MinOL: After leaving LA  $i$ , the MS chooses the farthest LA of the entrance cell from LA  $i$ . The entrance cell is cell  $N+1 - N_O(N-K)$  of LA  $i + N_O$  in the right-hand side or cell  $N_O(N-K)$  of LA  $i - N_O$  in the left-hand side. The state transition diagram for the MinOL policy is shown in Figure 2.8. In this figure,

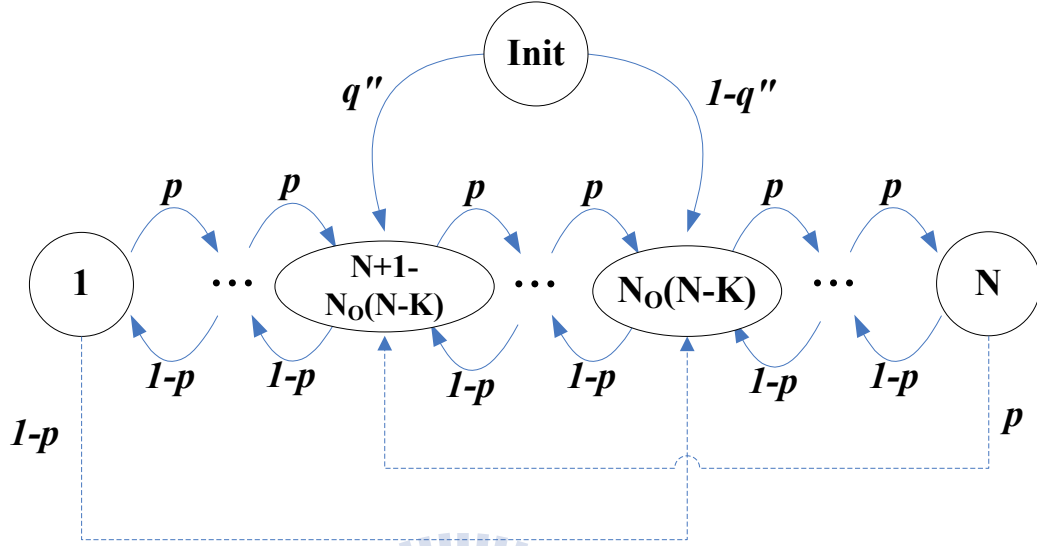


Figure 2.8: State Transition Diagram for the MinOL Policy ( $\frac{N}{2} \leq K < N$ )

$$q'' = \frac{\alpha_{N_O(N-K)}}{1 - \alpha_{N+1-N_O(N-K)} + \alpha_{N_O(N-K)}}, \quad (2.15)$$

and  $E[M]$  is expressed as

$$E[M] = q'' E[N_{N+1-N_O(N-K)}] + (1 - q'') E[N_{N_O(N-K)}]$$

$$= \begin{cases} \left( \frac{\alpha_{N_O(N-K)}}{1 - \alpha_{N+1-N_O(N-K)} + \alpha_{N_O(N-K)}} \right) \times \left\{ \frac{(N+1)\alpha_{N+1-N_O(N-K)} - [N+1 - N_O(N-K)]}{2p-1} \right\} \\ + \left( \frac{1 - \alpha_{N+1-N_O(N-K)}}{1 - \alpha_{N+1-N_O(N-K)} + \alpha_{N_O(N-K)}} \right) \times \left[ \frac{(N+1)\alpha_{N_O(N-K)} - N_O(N-K)}{2p-1} \right] & \text{for } p \neq \frac{1}{2} \\ [N_O(N-K)] \times [N+1 - N_O(N-K)] & \text{for } p = \frac{1}{2} \end{cases} \quad (2.16)$$

Note that our analytic results have been validated against the simulation experiments (see Table 2.1). The errors between the analytic and simulation models are under 1%.

## 2.4 Performance Evaluation

This section studies the performance of the LA selection policies (i.e., MaxOL, Central, Random and MinOL). Specifically, we investigate the expected number  $E[M]$  of cell

Table 2.1: Analytic and Simulation Results ( $N = 15$ )

K	0	4	8	12
$p = 0.5$				
E[M] (Analytic)	15	55	63	39
E[M] (Simulation)	15.022	54.979	62.913	38.845
Error	-0.152%	0.037%	0.136%	0.396%
$p = 0.7$				
E[M] (Analytic)	15	26.716	17.482	7.499
E[M] (Simulation)	15.032	26.622	17.458	7.501
Error	-0.214%	0.351%	0.141%	-0.023%

(a) The MaxOL Policy

K	0	4	8	12
$p = 0.5$				
E[M] (Analytic)	15	55	63	63
E[M] (Simulation)	14.987	55.060	62.925	62.927
Error	0.084%	-0.109%	0.118%	0.115%
$p = 0.7$				
E[M] (Analytic)	15	26.716	17.482	22.380
E[M] (Simulation)	15.032	26.622	17.465	22.330
Error	-0.214%	0.351%	0.100%	0.223%

(b) The Central Policy

K	0	4	8	12
$p = 0.5$				
E[M] (Analytic)	15	55	45.5	45
E[M] (Simulation)	15.003	54.899	45.129	44.833
Error	-0.020%	0.181%	0.814%	0.370%
$p = 0.7$				
E[M] (Analytic)	15	26.716	21.818	18.608
E[M] (Simulation)	15.025	26.738	21.992	18.579
Error	-0.169%	-0.083%	-0.798%	0.157%

(c) The Random Policy

K	0	4	8	12
$p = 0.5$				
E[M] (Analytic)	15	55	28	15
E[M] (Simulation)	15.003	54.899	27.969	14.995
Error	-0.020%	0.181%	0.107%	0.031%
$p = 0.7$				
E[M] (Analytic)	15	26.716	24.137	15
E[M] (Simulation)	15.025	26.738	24.136	15.008
Error	-0.169%	-0.083%	0.007%	-0.056%

(d) The MinOL Policy

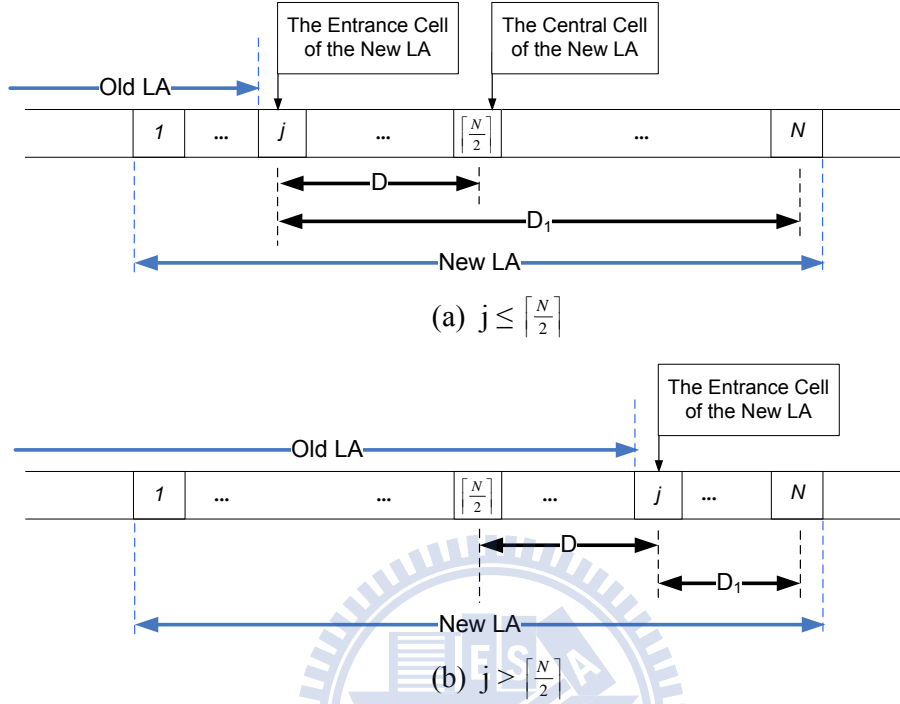


Figure 2.9: Distances  $D$  and  $D_1$  in the New LA

movement in an LA before an MS leaves the LA. It is clear that the larger the  $E[M]$  value, the better the performance. In our numerical examples, we show the results for LA size  $N = 15$  and  $N = 100$ . The results for other  $N$  values are similar and are omitted.

We first note that due to the symmetric cell structure in each LA, the effect for  $p$  is identical to that for  $1 - p$ . Therefore, it suffices to consider  $0.5 \leq p \leq 1$ . Denote  $D$  as the distance (the number of cells) between the entrance cell (cell  $j$  in Figure 2.9) and the central cell of the new LA (cell  $\lfloor \frac{N}{2} \rfloor$  in Figure 2.9). Denote  $D_1$  as the distance between the entrance cell and the new LA's right-hand side (left-hand side) boundary cell if the MS enters the new LA from the left-hand side (right-hand side) of the LA; i.e., cell  $N$  (cell 1) in Figure 2.9. Note that  $E[M]$  is affected by the ping-pong effect and moving-to-one-direction effect. Besides  $p$ , these effects are determined by  $D$  and  $D_1$ . The smaller the  $D$  value, the less significant the ping-pong effect. The larger the  $D_1$  value, the less significant the moving-to-one-direction effect. Tables 2.2 and 2.3 list  $D$  and  $D_1$  as functions of  $K$  for  $N = 15$ . These  $D$  and  $D_1$  values are computed from the analytic

Table 2.2: The Distance  $D$  between the Entrance Cell and the Cental Cell of the New LA ( $N = 15$ )

K	0	1	2	3	4	5	6	7	8	9	10	11	12	13	14
MaxOL	7	6	5	4	3	2	1	0	1	2	3	4	5	6	7
Cental	7	6	5	4	3	2	1	0	1	2	2	0	1	0	0
Random	7	6	5	4	3	2	1	0	3.5	3	4	2.7	3.8	3.4	3.7
MinOL	7	6	5	4	3	2	1	0	6	4	7	4	7	6	7

Table 2.3: The Distance  $D_1$  ( $N = 15$ )

K	0	1	2	3	4	5	6	7	8	9	10	11	12	13	14
MaxOL	14	13	12	11	10	9	8	7	6	5	4	3	2	1	0
Cental	14	13	12	11	10	9	8	7	6	5	9	7	8	7	7
Random	14	13	12	11	10	9	8	7	9.5	8	9	7	8	7	7
MinOL	14	13	12	11	10	9	8	7	13	11	14	11	14	13	14

model, and are validated by the simulation experiments.

Figures 2.10 - 2.13 plot  $E[M]$  as a function of  $K$  and  $p$ , where  $N = 15$ . Consider  $0.5 \leq p \leq 1$ . When  $p$  is small, the ping-pong effect is significant, and  $E[M]$  is likely to increase as  $D$  decreases. When  $p = 0.5$ ,  $E[M]$  is a decreasing function of  $D$  (see Figure 2.10 and Table 2.2). When  $p = 1$ , the MS always moves to one direction. Therefore,  $E[M]$  increases as  $D_1$  increases (see Figure 2.13 and Table 2.3). When  $p$  increases, the ping-pong effect (impact of  $D$ ) becomes insignificant, and the moving-to-one-direction effect (impact of  $D_1$ ) becomes significant. Consider the MaxOL policy,  $E[M]$  increases and then decreases as  $K$  increases. For  $p = 0.5, 0.7, 0.9, 1$ , the maximal  $E[M]$  values occur when  $K = 7, 3, 1, 0$ , respectively. For a maximal  $E[M]$  value, the corresponding  $K$  value is called the *best overlapping degree*. As  $p$  increases, the impact of  $D_1$  becomes more significant, and the best overlapping degree decreases. Figures 2.14 - 2.17 plot  $E[M]$  as a function of  $K$  and  $p$  with  $N = 100$ . The effects of  $K$  and  $p$  on  $E[M]$  are similar to that for  $N = 15$ , and the details are omitted.

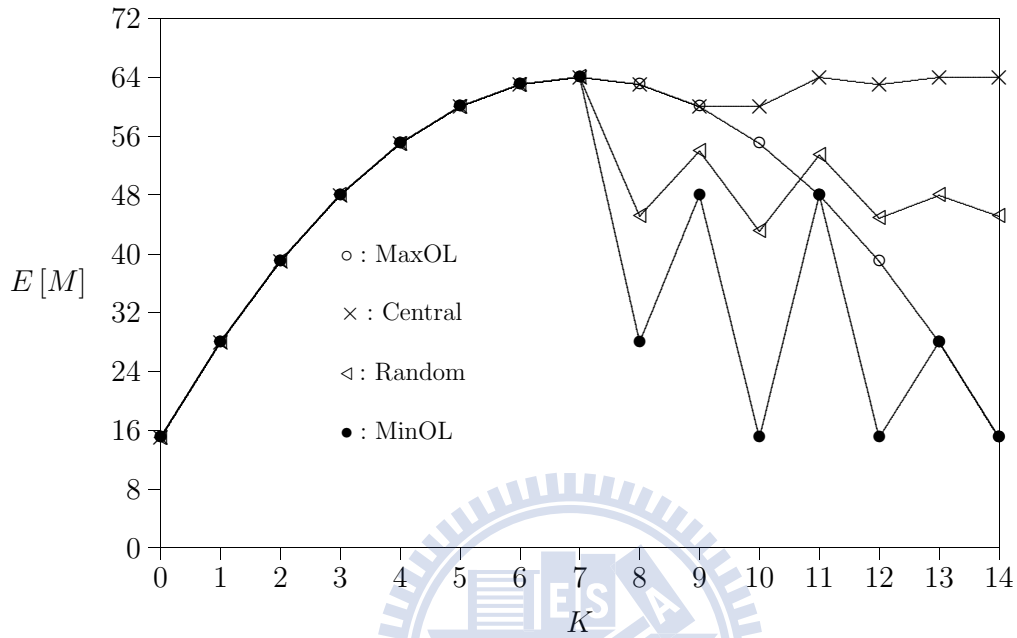


Figure 2.10: Effect of  $K$  on  $E[M]$  for  $p = 0.5$  and  $N = 15$

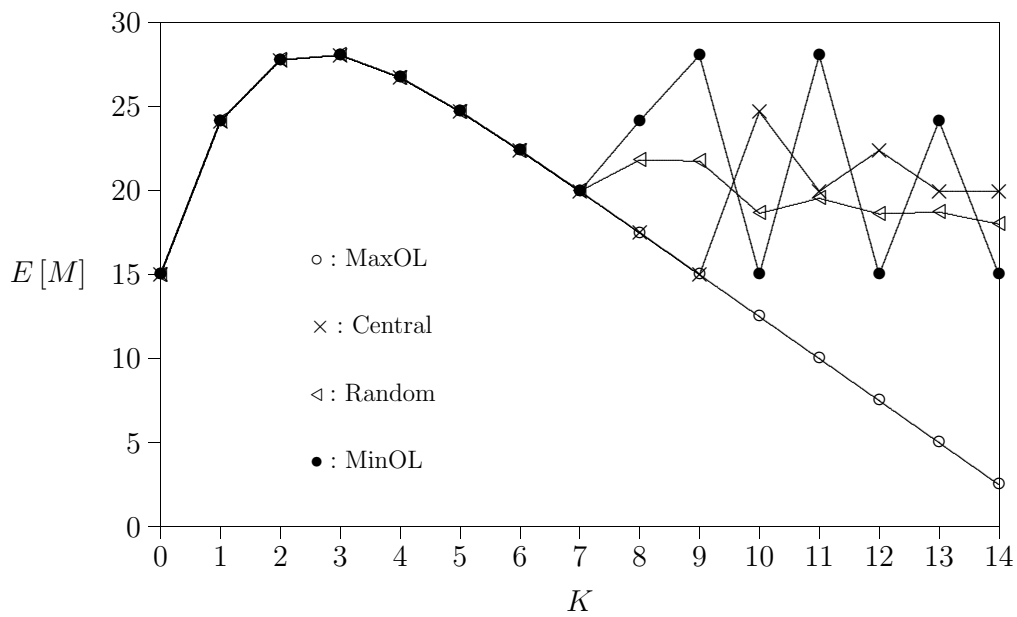


Figure 2.11: Effect of  $K$  on  $E[M]$  for  $p = 0.7$  and  $N = 15$

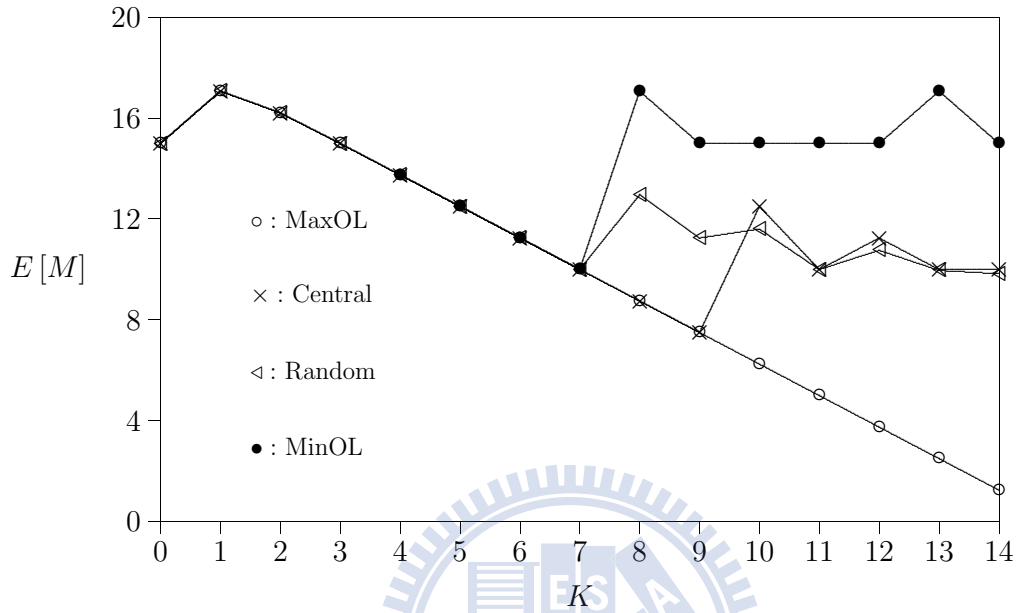


Figure 2.12: Effect of  $K$  on  $E[M]$  for  $p = 0.9$  and  $N = 15$

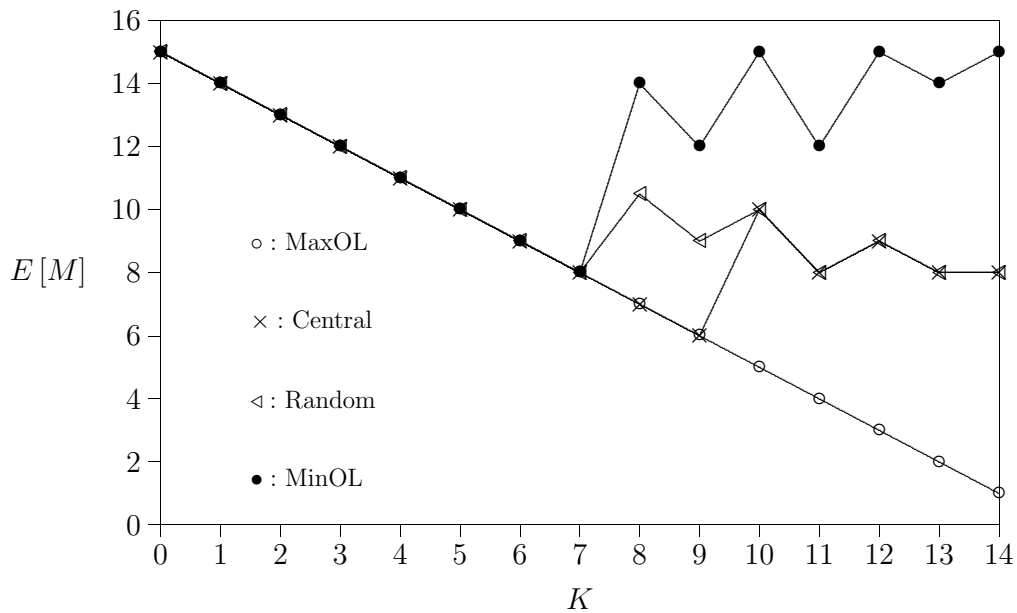


Figure 2.13: Effect of  $K$  on  $E[M]$  for  $p = 1.0$  and  $N = 15$



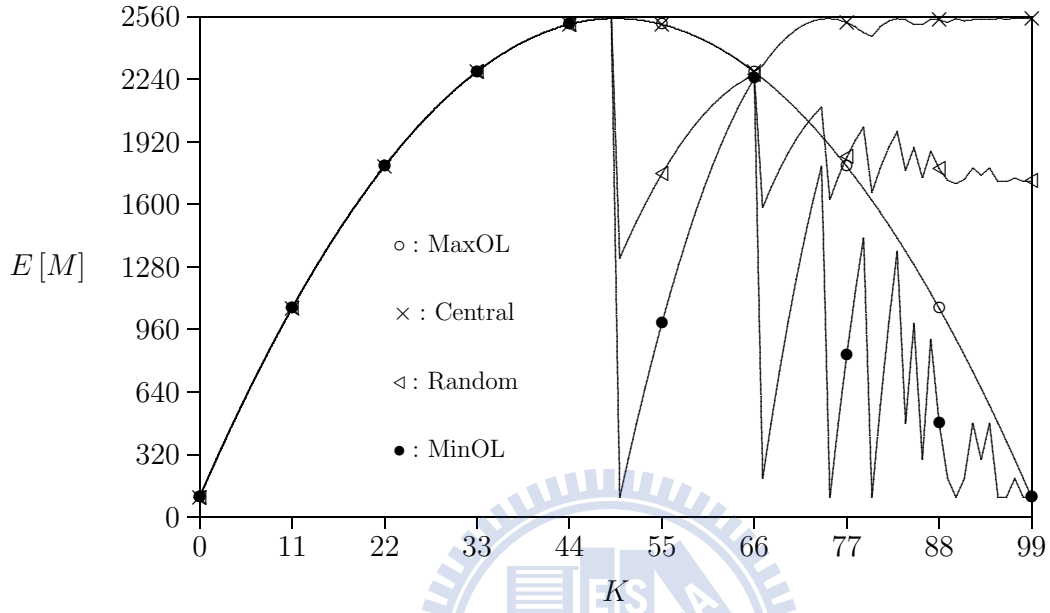


Figure 2.14: Effect of  $K$  on  $E[M]$  for  $p = 0.5$  and  $N = 100$

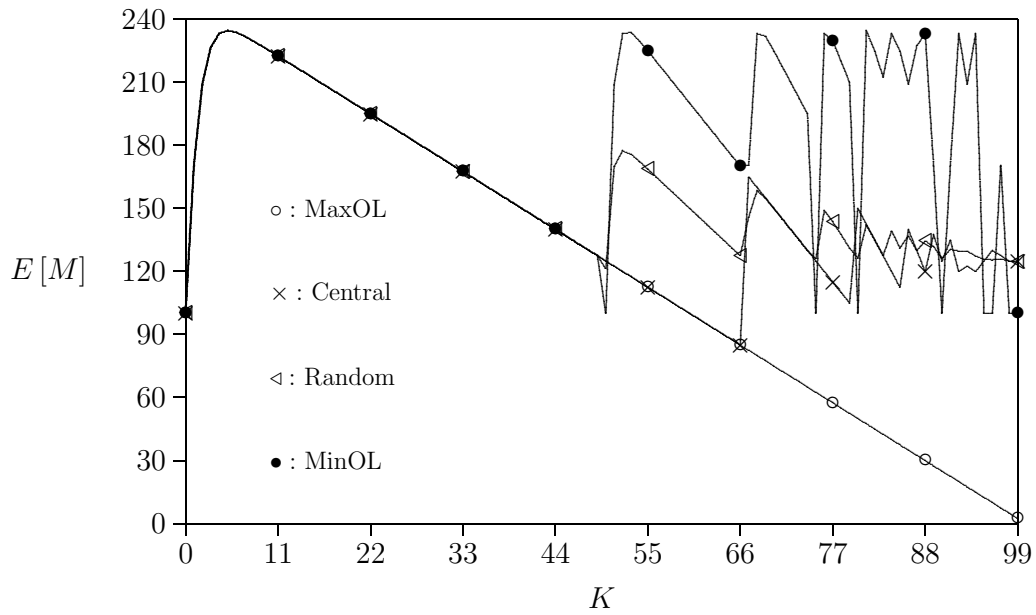


Figure 2.15: Effect of  $K$  on  $E[M]$  for  $p = 0.7$  and  $N = 100$

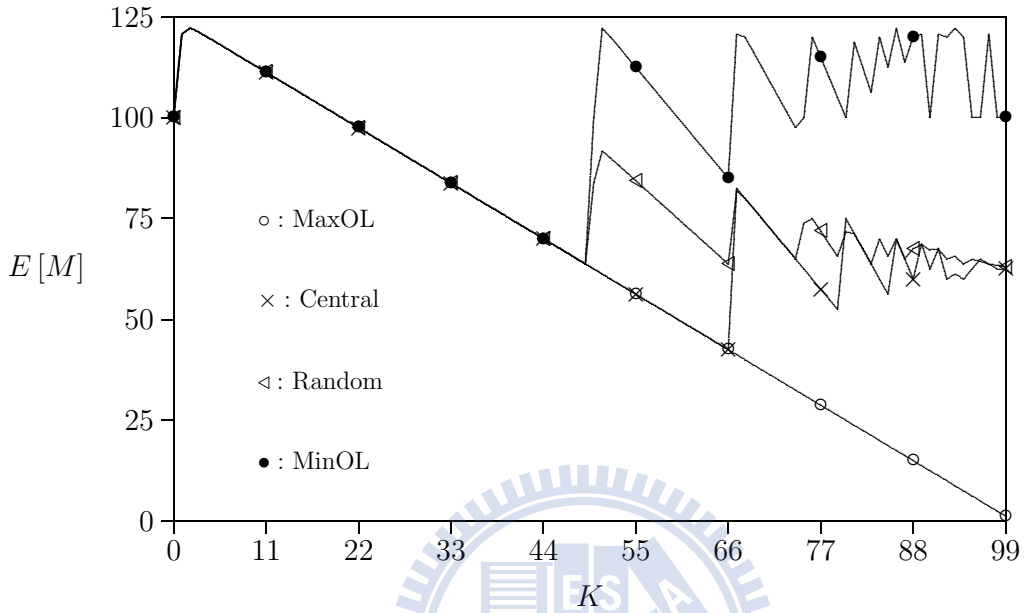


Figure 2.16: Effect of  $K$  on  $E[M]$  for  $p = 0.9$  and  $N = 100$

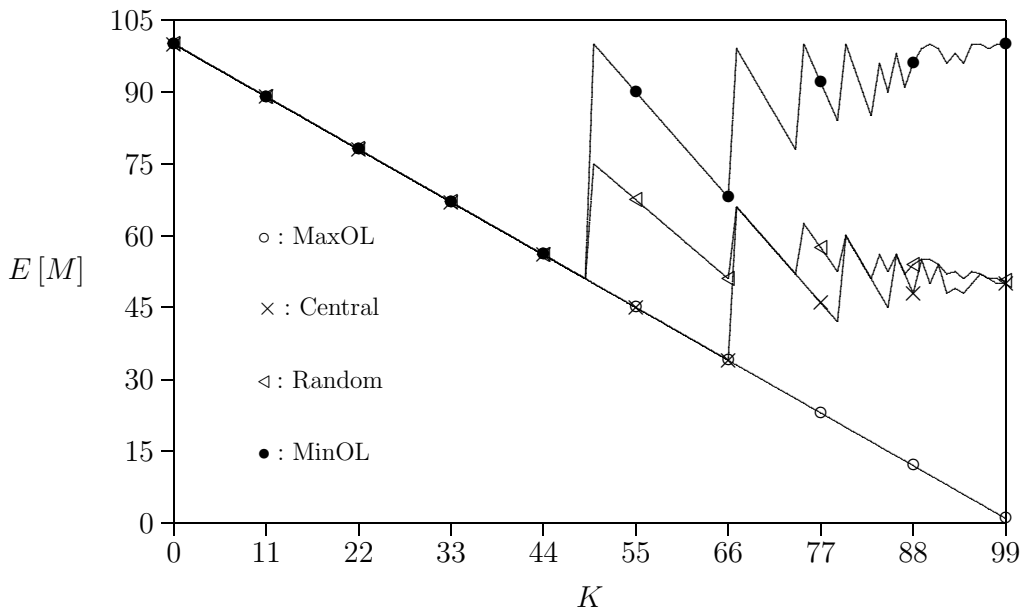


Figure 2.17: Effect of  $K$  on  $E[M]$  for  $p = 1.0$  and  $N = 100$

From Figures 2.10 - 2.17, we observe that when  $0 \leq K < N/2$ , all four policies result in same performance. When  $N/2 \leq K < N$ , the *Central* policy makes sense for  $p = 0.5$ , while the *MinOL* policy is more appropriate for  $p = 1.0$ . For all policies, these figures show an apparent result that for the same  $K$  value,  $E[M]$  decreases as  $p$  increases. By differentiating the analytic equations (equations (10), (11), (14) and (16)), we can formally prove that the best overlapping degree always occurs when  $0 \leq K < \frac{N}{2}$ . That is, in one-dimensional overlapping LA configuration, it suffices to consider the configurations for  $K < \frac{N}{2}$ .

## 2.5 Summary

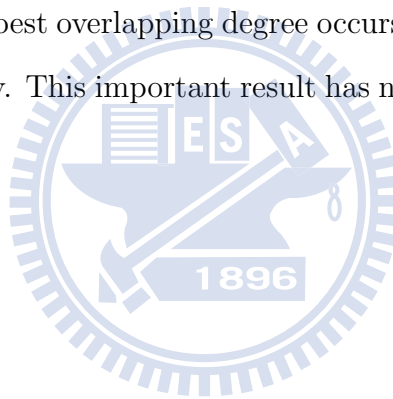
This chapter studied four LA selection policies for overlapping LA configuration: Maximum Overlapping (MaxOL), Central, Random and Minimum Overlapping (MinOL) policies. We proposed an analytic model to investigate the  $E[M]$  performance of these policies for the one-dimensional overlapping LA configuration. The analytic results were validated against the simulation experiments.

Our study for the one-dimensional overlapping LA configuration is more general than the previous studies [14, 15, 25]. For specific scenarios in the previous studies, their results are consistent with ours (which validates that our results are correct). The major difference between our model and those in the previous studies is the setup for the routing probability  $p$ . All previous studies assumed that at each movement, the MS moves to any of its neighboring cells with the same routing probability. In our study, we assume that the MS moves to each of its neighboring cells with different probabilities (i.e.,  $0 < p \leq 1.0$ ). Furthermore, the overlapping degree  $K$  in our study can be arbitrary (i.e.,  $0 \leq K < N$ ). The previous studies made restrictive assumption where  $0 \leq K < \frac{N}{2}$ . We note that there is a typo in equation (11) of [25]. Specifically, the  $(2d - w + 1)$  term in the right-hand side of the equation should be rewritten as  $(2d - w - 1)$ .

Our study indicates the following results.

- It suffices to consider the configurations for  $0 \leq K < \frac{N}{2}$ , and all four policies result in same performance in these configurations. When  $N/2 \leq K < N$ , the *Central* policy makes sense for  $p = 0.5$ , while the *MinOL* policy is more appropriate for  $p = 1.0$ .
- When the routing probability  $p \in [0.5, 1]$ , the  $E[M]$  value decreases as  $p$  increases. When  $p = 1$  (i.e., the mobile telecommunications network is deployed in the highway), the  $E[M]$  performance for  $K = 0$  is always better than that for  $K > 0$ .

From the numerical comparison of the four LA selection policies, our study indicates that in practical scenarios, the best overlapping degree occurs for  $0 \leq K < \frac{N}{2}$ , and it suffices to consider the MaxOL policy. This important result has not been reported in the literature.



# Chapter 3

## WiMAX Location Update for Vehicle Applications

In IEEE 802.16e mobile *Worldwide Interoperability for Microwave Access* (WiMAX), *Paging Groups* (PGs; groups of *base stations*) are used to identify the locations of *Mobile Stations* (MSs). In WiMAX systems, an *Anchor Paging Controller* (APC) is assigned to an MS to handle location tracking for the MS. During *Location Update* (LU), the WiMAX network may or may not relocate the APC. This chapter considers a linear WiMAX base station layout for vehicle applications, where a base station serves as a roadside unit, and a WiMAX MS installed in a vehicle serves as an onboard unit. In these vehicle applications, APC relocation may significantly affect the network traffic. This chapter proposes an analytic model to study the performance of the location update with/without APC relocation. Our study provides guidelines to utilize the APC relocation for vehicles with various moving behaviors.

### 3.1 WiMAX Location Tracking Mechanism

IEEE 802.16e mobile *Worldwide Interoperability for Microwave Access* (WiMAX) provides broadband wireless services with wide service coverage, high data throughput, and high mobility [75, 76, 77]. The WiMAX network architecture can be simplified as shown in Figure 3.1, which consists of the *Connectivity Service Networks* (CSNs; see Figure 3.1

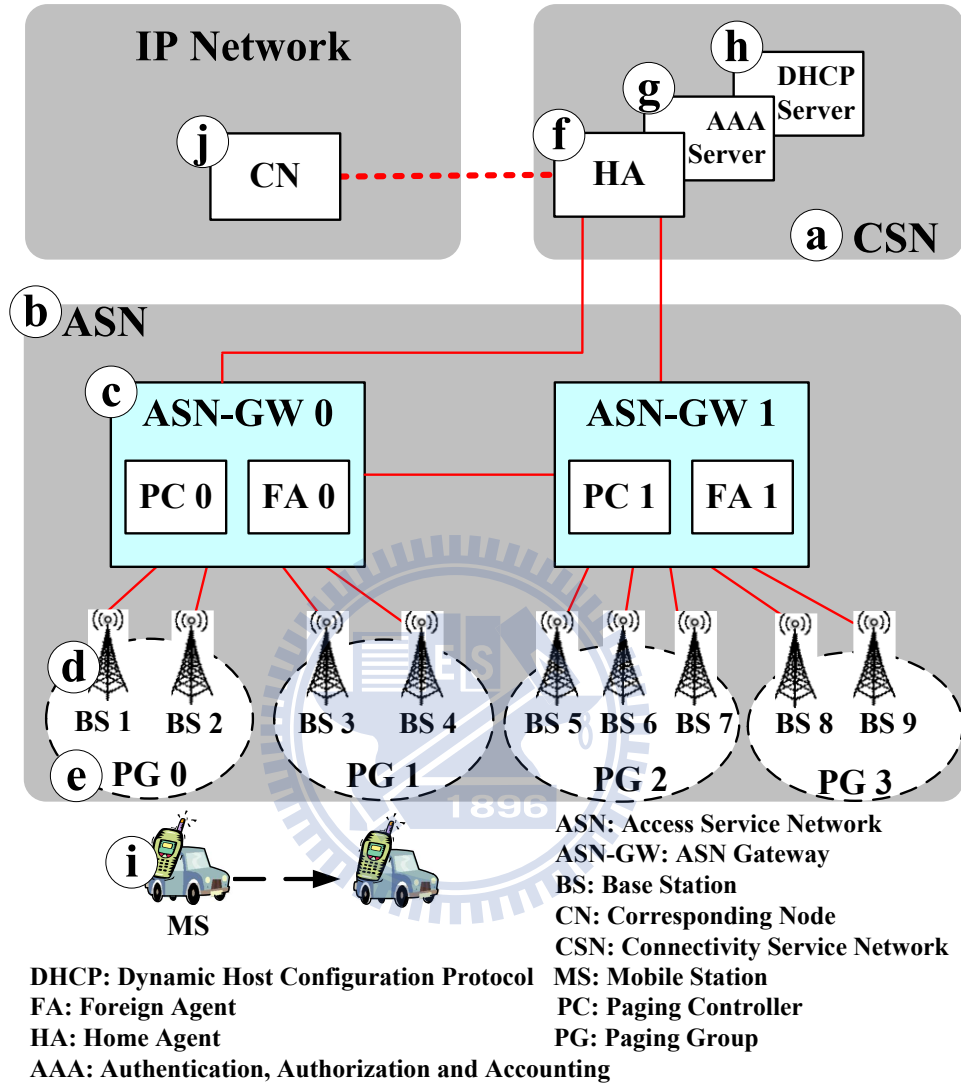


Figure 3.1: A Simplified WiMAX Network Architecture

(a) and the *Access Service Networks* (ASNs; see Figure 3.1 (b)). An ASN that comprises *ASN Gateways* (ASN-GWs; see Figure 3.1 (c)) and *WiMAX Base Stations* (BSs; see Figure 3.1 (d)) provides radio access (such as radio resource management, paging and location management) to the *WiMAX Mobile Station* (MS; Figure 3.1 (i)). Every ASN-GW connects to several BSs. The ASN-GWs are also connected to each other to coordinate MS mobility. A CSN consists of network nodes such as the *Mobile IP* (MIP) [39] *Home Agent* (HA; see Figure 3.1 (f)), the *Authentication, Authorization, and Accounting* (AAA) server (see Figure 3.1 (g)) and the *Dynamic Host Configuration Protocol* (DHCP) server

(see Figure 3.1 (h)). The CSN provides IP connectivity (such as Internet access and IP address allocation) to a WiMAX MS and interworks with the ASNs to support capabilities such as AAA and mobility management. Before an MS is allowed to access WiMAX services, it must be authenticated by the ASN-GW (which serves as the *authenticator*) and the AAA server in the CSN.

In Taiwan, a linear layout with 27 WiMAX BSs has been deployed from Taipei to Taoyuan International Airport to cover highway and local road traffics (the distance is 30km). The network is anticipated to extend to 679 BSs in north Taiwan for more general broadband wireless applications [44]. One of the applications aims for *Intelligent Transportation Systems* (ITS) where the WiMAX BSs can be viewed as roadside units and the MSs are onboard units [36, 37, 51, 82]. In ITS applications, high mobility of vehicles may significantly affect network signalling overhead for location tracking, which is investigated in this chapter.

We first introduce the WiMAX location tracking mechanism. In WiMAX, two *subscriber modes* characterize the activities of an MS attached to the network. In the *normal* mode, the MS sends or receives packets to/from a BS. When there is no data transmission for a period, the MS switches from the normal mode to the *idle* mode to conserve resources.

Several procedures defined in WiMAX are exercised when the MS is in the idle mode. For example, the *Location Update* (LU) procedure is exercised for location tracking of an MS [27]. When there are incoming packets for the idle MS, the *paging* procedure is exercised to alert the MS. Then the MS performs the *idle mode exit* procedure to return to the normal mode and starts data transmission. In the control plane, the *Paging Controller* (PC) in an ASN-GW (see Figure 3.1 (c)) handles the location tracking and the paging operations for the idle MSs. All BSs connected to a PC are partitioned into several *Paging Groups* (PGs; see Figure 3.1 (e)). The PGs are used for MS tracking. For each MS in the idle mode, the network assigns a PC called the *Anchor PC* (or APC) to the MS.

Every APC is associated with a database called *Location Register* (LR) that contains the MS tracking and paging information of the idle mode MSs. The information includes the current PG where the MS resides, the paging parameters, the QoS profiles, etc. Suppose that an MS in the normal mode enters the idle mode through PG 0 in Figure 3.1, and PC 0 serves as the APC of the MS. When this idle MS moves from PG 1 to PG 2, it performs LU procedure to inform its APC (i.e., PC 0) of the new location through PC 1. After location update, PC 1 serves as the *relay PC* for the MS and all PC-related control messages are delivered between PC 0 (the APC) and the MS indirectly through PC 1.

When the MS enters the normal mode, data transmission with handover is supported by the MIP. In Figure 3.1, assume that an MS first enters the WiMAX network (in the normal mode) and obtains an IP address through ASN-GW 0. The MS then registers to the HA (see Figure 3.1 (f)) in the CSN to indicate that the *Foreign Agent* (FA) is FA 0 associated with ASN-GW 0 (see Figure 3.1 (c)). At this point, the MS can start data transmission with a *Corresponding Node* (CN; see Figure 3.1 (j)). When the MS moves from BS 4 to BS 5, the local ASN-GW is changed from ASN-GW 0 to ASN-GW 1. The data between FA 0 and the MS is then delivered through ASN-GW 0, ASN-GW 1 and BS 5.

In WiMAX, the APC is only defined in the idle mode and does not play any role in the normal mode. When an MS switches from the idle mode to the normal mode, the APC is no longer associated with the MS; i.e., the MS information is removed from the LR of the APC (through the idle mode exit procedure). When the MS enters the idle mode again, a new APC is assigned to the MS by exercising the *idle mode entry* procedure. In the idle mode, WiMAX provides two alternatives to reassign the APC during the MS movement: *static* or *dynamic*. When the MS moves from an old PG to a new PG, the APC can be dynamically reassigned during the LU procedure. If the APC reassignment occurs frequently, these APC/LR relocations result in extra network signalling overhead. On the other hand, if the APC reassignment occurs infrequently, the APC may be far



away from the MS after several movements. In this case, long delays for message exchange will be expected in the LU procedures. This chapter analyzes the cost for the APC/LR reassignment under Taiwan's linear WiMAX BS layout for ITS.

This chapter is organized as follows. In Section 3.2, we describe the LU procedure. Section 3.3 illustrates two scenarios to study the cost for the APC/LR relocation due to MS (vehicle) mobility. Section 3.4 numerically compares these two scenarios.

## 3.2 The Location Update Procedure

This section describes the location update (LU) procedure exercised in the idle mode [76, 77]. Figure 3.2 (a) illustrates how the LU procedure is performed when an idle MS moves from a BS in PG 1 to another BS in PG 2. Without loss of generality, we assume that PC 0 is the MS's APC, and both the APC (PC 0) and the FA (FA 0) are collocated in ASN-GW 0. We also assume that a specific ASN-GW serves as the idle MS's authenticator. When the idle MS moves to ASN-GW 1, the relay PC (e.g., PC 1 in Figure 3.2 (a)) may become the APC. For the description purpose, let  $S_R$  be the LU scenario with APC relocation and  $S_W$  be the LU scenario without APC relocation. The LU procedure with APC relocation scheme  $S_R$  is described as follows (see  $S_R$  in Figure 3.2 (a)):

**Step 1.** The MS moves from PC 0 to PC 1. Through the new BS, the MS sends an **LU Request** message to PC 1.

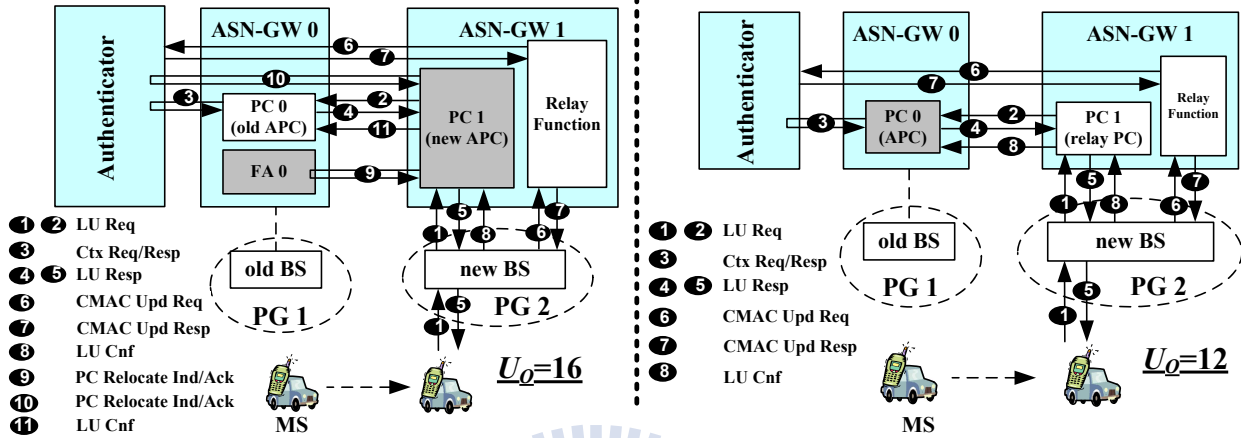
**Step 2.** PC 1 decides to relocate the APC and selects itself as the APC. The **LU Request** message is forwarded to PC 0 with a relocation indicator.

**Step 3.** PC 0 retrieves the *Authorization Key* (AK) context from the authenticator through the **Context Request/Response** message exchange.

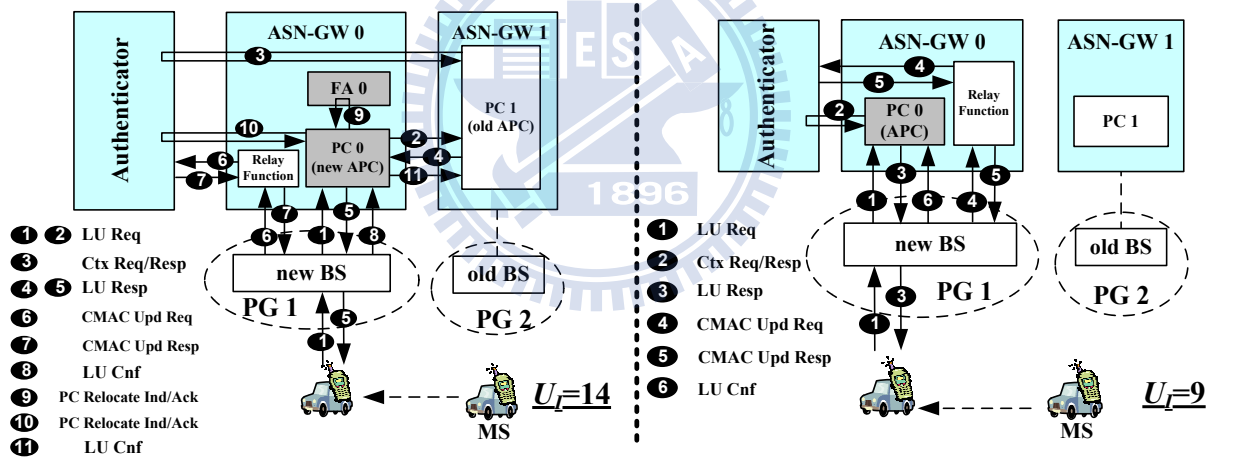
**Steps 4 and 5.** The LU result (with the AK context and the MS's record data) is delivered to PC 1 by the **LU Response** message. PC 1 stores the received information (including the MS's new location) in its LR. The **LU Response** message

## $S_R$ (APC Relocation)

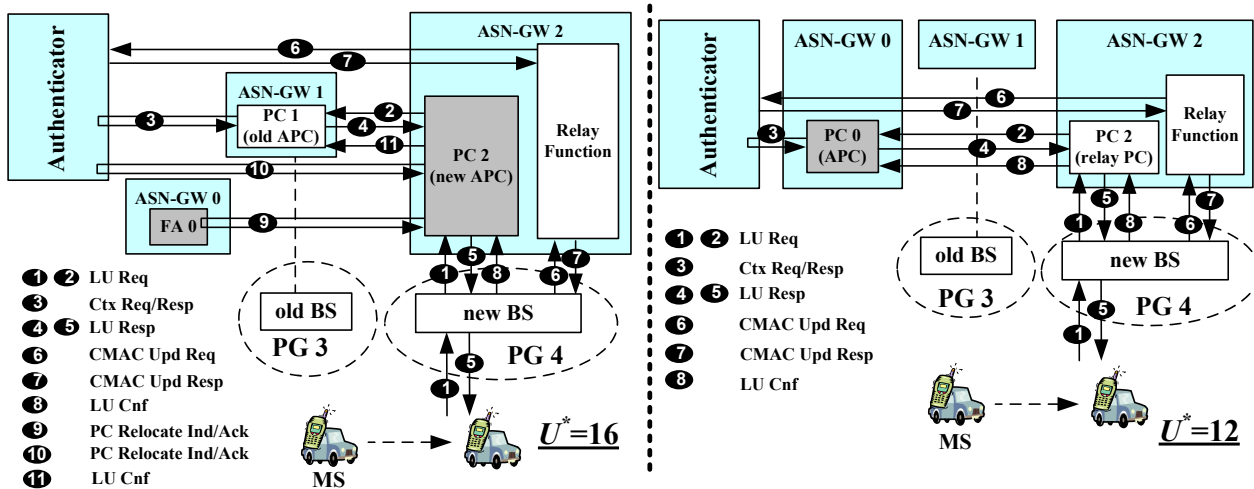
## $S_W$ (Without APC Relocation)



(a) Inter-PC LU "Out" from PC 0 to PC 1



(b) Inter-PC LU from PC 1 "Into" PC 0



(c) Inter-PC LU from PC 1 to PC 2

Figure 3.2: Flows of Inter-PC LUs with Signalling Costs

then carries the AK context (to be retrieved by the new BS) and the LU result (for the MS).

**Steps 6 and 7.** To prevent the replay attack, the new BS updates *Cipher-based Message Authentication Code (CMAC) Key Count* (the latest counter value for the MS's request message) with the authenticator through the **CMAC Update Request/Response** message exchange.

**Step 8.** The new BS notifies PC 1 of the completion of the LU procedure by an **LU Confirm** message.

**Steps 9 and 10.** PC 1 informs both the MS's FA (i.e., FA 0) and authenticator about the APC relocation through the **PC Relocation Indication/Acknowledge** message exchange.

**Step 11.** PC 1 informs PC 0 that the LU procedure is completed by the **LU Confirm** message. After receiving the message, PC 0 removes the MS's record from its LR.

The LU procedure without APC relocation (see  $S_W$  in Figure 3.2 (a)) is similar to that with APC relocation, except that Steps 9 and 10 are eliminated. For  $S_W$  in Figure 3.2 (a), PC 1 serves as the relay PC, and no relocation indicator is added in the **LU Request** message in Step 2. Therefore, the network needs not to transfer the MS data to the new APC/LR in Step 4.

### 3.3 Analytic Analysis

This section studies the expected location update cost during the idle period. When the MS enters the idle mode, we assume that PC 0 is assigned as its APC and is collocated with its FA (FA 0). A location update can be an inter-PC LU (e.g., from BS 4 to BS 5 in Figure 3.1) or an intra-PC LU (e.g., from BS 2 to BS 3 in Figure 3.1), and the associated

costs are elaborated below. In our study, the network signalling cost is measured through the messages exchanged between the network nodes.

- $U_O$ : the cost of an inter-PC LU “Out” from PC 0 (to any neighboring PC; see Figure 3.2 (a)). For  $S_R$ ,  $U_O = 16$ . For  $S_W$ ,  $U_O = 12$ .
- $U_I$ : the cost of an inter-PC LU from the neighboring PCs “Into” PC 0 (see Figure 3.2 (b)). For  $S_R$ ,  $U_I = 14$ . For  $S_W$ ,  $U_I = 9$ .
- $U^*$ : the cost of an inter-PC LU without involving PC 0 (see Figure 3.2 (c)). For  $S_R$ ,  $U^* = 16$ . For  $S_W$ ,  $U^* = 12$ .
- $u$ : the cost of an intra-PC LU within PC 0 (see Figure 3.3 (a)). For both  $S_R$  and  $S_W$ ,  $u = 9$ .
- $u^*$ : the cost of an intra-PC LU in any PC other than PC 0 (see Figure 3.3 (b)). For  $S_R$ ,  $u^* = 9$ . For  $S_W$ ,  $u^* = 12$ .
- $U$ : the expected cost of an LU in the idle mode.

We propose an analytic model to study the expected LU cost  $U$  for both  $S_R$  and  $S_W$ . Figure 3.4 shows the MS movement state-transition diagram with the linear configuration of PGs and PCs. Figure 3.4 (a) illustrates the state-transition diagram for the MS movement among PGs. We use a one-dimensional linear layout of PGs to represent an extension of Taiwan’s WiMAX-based ITS deployment described in Section 3.1, where state  $i$  represents that the MS visits PG  $i$  ( $-\infty < i < \infty$ ). The MS moves from state  $i$  to states  $i + 1$  and  $i - 1$  with probabilities  $p$  and  $1 - p$ , respectively. Let  $P_j^k$  be the probability that from PG 0, the MS visits PG  $j$  after  $k$  PG movements, where  $k \geq 0$ . From the state-transition diagram in Figure 3.4 (a),  $P_j^k$  is derived as follows. For  $j \geq 0$

$$P_j^k = \begin{cases} \binom{k}{\frac{k-j}{2}} p^j [p(1-p)]^{\frac{k-j}{2}}, & k \geq j \geq 0 \text{ and } k-j \text{ is even} \\ 0, & \text{otherwise} \end{cases} \quad (3.1)$$

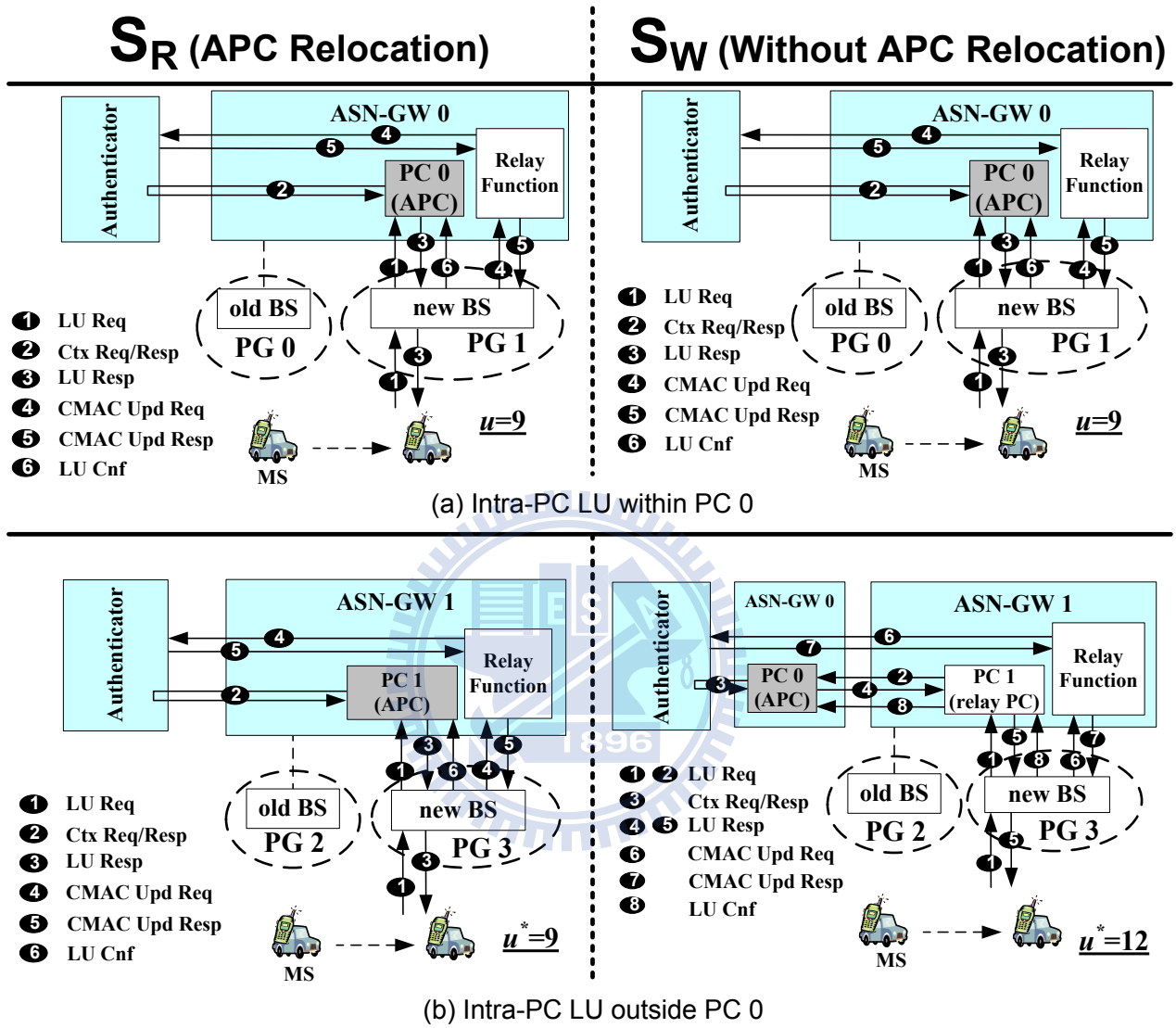


Figure 3.3: Flows of Intra-PC LUs with Signalling Costs

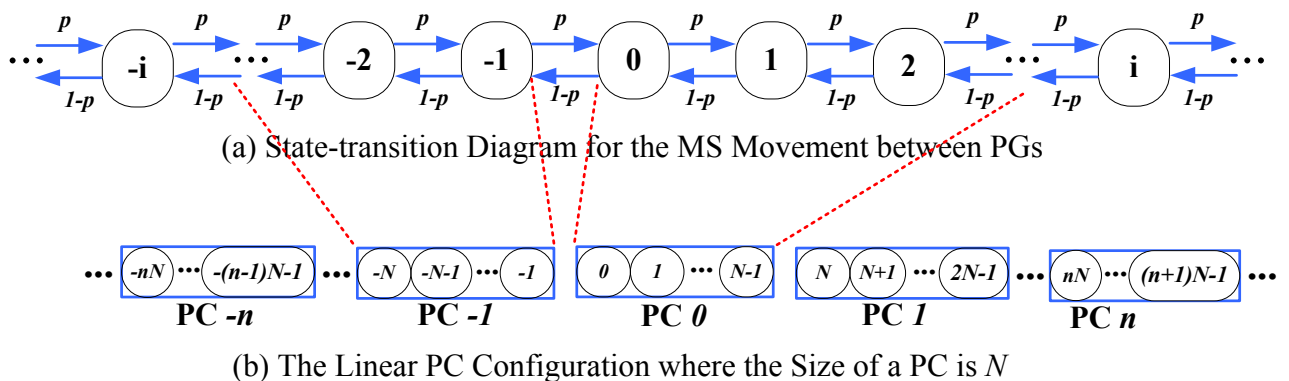


Figure 3.4: The MS Movement State-transition Diagram with Linear Configuration of PGs and PCs

Note that (3.1) is partially validated for  $j = 0$  and  $p = 1 - p = 0.5$  [64]. Due to the symmetric PG layout, from (3.1),  $P_j^k$  for  $j < 0$  can be expressed as

$$P_j^k = \begin{cases} \binom{k}{\frac{k+j}{2}} (1-p)^{-j} [p(1-p)]^{\frac{k+j}{2}}, & k \geq -j > 0 \text{ and } k+j \text{ is even} \\ 0, & \text{otherwise} \end{cases} \quad (3.2)$$

Let  $P_{i,j}^k$  be the probability that starting from PG  $i$ , the MS visits PG  $j$  after  $k$  PG movements. From (3.1) and (3.2), the probability  $P_{i,j}^k$  can be generalized as

$$P_{i,j}^k = \begin{cases} \binom{k}{\frac{k-(j-i)}{2}} p^{j-i} [p(1-p)]^{\frac{k-(j-i)}{2}}, & j \geq i, k \geq |j-i| \geq 0 \text{ and} \\ & k - |j-i| \text{ is even} \\ \binom{k}{\frac{k+(j-i)}{2}} (1-p)^{-(j-i)} [p(1-p)]^{\frac{k+(j-i)}{2}}, & j < i, k \geq |j-i| > 0 \text{ and} \\ & k - |j-i| \text{ is even} \\ 0, & \text{otherwise} \end{cases} \quad (3.3)$$

Based on the above model, we define five parameters to compute  $U$  as follows:

- $\Pi_O(k)$ : the expected number of the inter-PC movements “Out” from PC 0 (to PC  $-1$  or PC 1) during  $k$  PG movements of the MS.
- $\Pi_I(k)$ : the expected number of the inter-PC movements from PC  $-1$  or PC 1 “Into” PC 0 during  $k$  PG movements of the MS.
- $\Pi^*(k)$ : the expected number of the inter-PC movements without visiting PC 0 during  $k$  PG movements of the MS.
- $\pi(k)$ : the expected number of the intra-PC movements within PC 0 during  $k$  PG movements of the MS.
- $\pi^*(k)$ : the expected number of the intra-PC movements in any PC other than PC 0 during  $k$  PG movements of the MS.

Figure 3.4 (b) illustrates a PC configuration with linear PG layout to derive the above five parameters. In this figure, every PC consists of  $N$  PGs ( $N \geq 1$ ). For example, PC  $n$  covers the PGs from  $nN$  to  $(n+1)N - 1$ , and PC  $-n$  covers the PGs from  $-nN$  to  $-(n-1)N - 1$ .

$\Pi_O(k)$  is derived as follows. Starting from PG  $i$ , the probability that the MS moves out from PC 0 (i.e., from PG 0 to PG  $-1$  or from PG  $N-1$  to PG  $N$ ) at the  $m$ -th PG movement is  $(1-p)P_{i,0}^{m-1} + pP_{i,N-1}^{m-1}$ . Therefore, during  $k$  PG movements, the expected number of inter-PC movements out from PC 0 can be expressed as  $\sum_{m=1}^k [(1-p)P_{i,0}^{m-1} + pP_{i,N-1}^{m-1}]$ . For simplicity, assume that the MS initially resides in any of the  $N$  PGs in PC 0 with the same probability  $1/N$ . Then

$$\Pi_O(k) = \left(\frac{1}{N}\right) \left\{ \sum_{i=0}^{N-1} \sum_{m=1}^k [(1-p)P_{i,0}^{m-1} + pP_{i,N-1}^{m-1}] \right\}. \quad (3.4)$$

Similar to the derivation of (3.4), we have

$$\Pi_I(k) = \left(\frac{1}{N}\right) \left\{ \sum_{i=0}^{N-1} \sum_{m=1}^k [pP_{i,-1}^{m-1} + (1-p)P_{i,N}^{m-1}] \right\}. \quad (3.5)$$

$\Pi^*(k)$  is derived as follows. Starting from PG  $i$  ( $0 \leq i < N$ ), after  $k$  PG movements, PCs  $\pm \lceil \frac{k}{N} \rceil$  are the farthest PCs that can be visited by the MS, and the probability to make an inter-PC movement between PCs  $-l, -l+1$  or between PCs  $l, l-1$  at the  $m$ -th movement is  $[pP_{i, -(l-1)N-1}^{m-1} + (1-p)P_{i, -(l-1)N}^{m-1}] + [pP_{i, lN-1}^{m-1} + (1-p)P_{i, lN}^{m-1}]$ , where  $2 \leq l \leq \lceil \frac{k}{N} \rceil$ . In this case, the probability that at the  $m$ -th movement, the MS makes an inter-PC LU without involving PC 0 can be expressed as

$$\sum_{l=2}^{\lceil \frac{k}{N} \rceil} \left\{ [pP_{i, -(l-1)N-1}^{m-1} + (1-p)P_{i, -(l-1)N}^{m-1}] + [pP_{i, lN-1}^{m-1} + (1-p)P_{i, lN}^{m-1}] \right\}. \quad (3.6)$$

From the definition for  $\Pi^*(k)$  and (3.6), we have

$$\Pi^*(k) = \left(\frac{1}{N}\right) \left\{ \sum_{i=0}^{N-1} \sum_{m=1}^k \sum_{l=2}^{\lceil \frac{k}{N} \rceil} \left\{ p [P_{i, -(l-1)N-1}^{m-1} + P_{i, lN-1}^{m-1}] + (1-p) [P_{i, -(l-1)N}^{m-1} + P_{i, lN}^{m-1}] \right\} \right\}. \quad (3.7)$$

Note that for  $\lceil \frac{k}{N} \rceil \leq 1$ ,  $\Pi^*(k) = 0$ .

To compute  $\pi(k)$ , we classify the intra-PC movements inside PC 0 into two types.

- First-type: the MS moves to the boundary PGs of PC 0 (i.e., the MS moves from PG  $N-2$  to PG  $N-1$  or from PG 1 to PG 0 in Figure 3.4 (b)).

- Second-type: the MS moves to the non-boundary PGs (e.g., the MS moves from PG  $N - 1$  to PG  $N - 2$  or from PG 0 to PG 1 in Figure 3.4 (b) with  $N \geq 3$ ).

For  $N = 1$ , there are no intra-PC movements and  $\pi(k) = 0$ . For  $N = 2$ , all PGs are boundary PGs, and no second-type movements are made. For  $N \geq 2$ , starting from PG  $i$ , the expected number of the first-type movements during  $k$  PG movements is  $\sum_{m=1}^k [(1-p)P_{i,1}^{m-1} + pP_{i,N-2}^{m-1}]$ . For  $N \geq 3$ , the expected number of the second-type movements during  $k$  PG movements is  $\sum_{m=1}^k \sum_{j=1}^{N-2} P_{i,j}^m$ . Therefore,  $\pi(k)$  can be expressed as

$$\pi(k) = \begin{cases} 0, & N = 1 \\ \left(\frac{1}{N}\right) \left\{ \sum_{i=0}^{N-1} \sum_{m=1}^k [(1-p)P_{i,1}^{m-1} + pP_{i,N-2}^{m-1}] \right\}, & N = 2 \\ \left(\frac{1}{N}\right) \left\{ \sum_{i=0}^{N-1} \sum_{m=1}^k \left[ (1-p)P_{i,1}^{m-1} + pP_{i,N-2}^{m-1} + \sum_{j=1}^{N-2} P_{i,j}^m \right] \right\}, & N \geq 3 \end{cases} \quad (3.8)$$

From (3.4), (3.5), (3.7) and (3.8), we have

$$\pi^*(k) = k - \Pi_O(k) - \Pi_I(k) - \Pi^*(k) - \pi(k). \quad (3.9)$$

Equations (3.4), (3.5), (3.7) and (3.8) are validated against the simulation experiments (see Table 3.1) [79], where the differences are within 2%. Note that due to the symmetric PG structure in each PC, the effect for  $p$  is identical to that for  $1-p$ . Therefore, it suffices to consider  $0.5 \leq p \leq 1$  in our study. Our simulation program is written in C++, which works as follows:

- Step 1.** Decide the PC size  $N$ , the right move probability  $p$  and the number  $k$  of PG movements. (e.g.,  $k = 39$  for Table 3.1).
- Step 2.** An MS is initially assigned to the PGs in PC 0 with the same probability.
- Step 3.** According to the right move probability  $p$ , we randomly generate a series of PG movements for the MS.
- Step 4.** Log the numbers of each type of the LUs during the  $k$  PG movements.



**Step 5.** Repeat Steps 2 - 4 for one million times.

**Step 6.** Use the numbers of LU types obtained from Step 4 to calculate  $\Pi_I(k)$ ,  $\Pi_O(k)$ ,  $\Pi^*(k)$ ,  $\pi(k)$  and  $\pi^*(k)$ .

Let  $P(k)$  be the probability that during the idle period  $t$ , the MS makes  $k$  PG movements. Let  $t$  have the Gamma distribution [70, 79] with density function  $f(\cdot)$ , mean  $1/\gamma$ , variance  $V$  and Laplace transform

$$f^*(s) = \left( \frac{1}{Vs\gamma + 1} \right)^{\frac{1}{V\gamma^2}}. \quad (3.10)$$

Suppose that the residence time of the MS at a PG is exponentially distributed with the mean  $1/\eta$ . Then,  $P(k)$  can be expressed as

$$\begin{aligned} P(k) &= \int_{t=0}^{\infty} \Pr[k \text{ LUs in } t] f(t) dt \\ &= \int_{t=0}^{\infty} \left[ \frac{(\eta t)^k}{k!} \right] e^{-\eta t} f(t) dt \\ &= \left( \frac{\eta^k}{k!} \right) \int_{t=0}^{\infty} e^{-\eta t} t^k f(t) dt \\ &= \left[ \frac{(-\eta)^k}{k!} \right] \left[ \frac{d^k f^*(s)}{ds^k} \right] \Big|_{s=\eta}. \end{aligned} \quad (3.11)$$

From (3.10), for  $k \geq 1$ , we have

$$\frac{d^k f^*(s)}{ds^k} = (-1)^k V^k \gamma^k \left( \frac{1}{Vs\gamma + 1} \right)^{\frac{1}{V\gamma^2} + k} \prod_{l=1}^k \left( \frac{1}{V\gamma^2} + l - 1 \right). \quad (3.12)$$

Substituting (3.12) into (3.11),  $P(k)$  is expressed as

$$\begin{aligned} P(k) &= \begin{cases} \left( \frac{1}{V\gamma\eta + 1} \right)^{\frac{1}{V\gamma^2}}, & \text{for } k = 0 \\ \left( \frac{\eta^k}{k!} \right) V^k \gamma^k \left( \frac{1}{V\gamma\eta + 1} \right)^{\frac{1}{V\gamma^2} + k} \prod_{l=1}^k \left( \frac{1}{V\gamma^2} + l - 1 \right), & \text{for } k \geq 1 \end{cases} \\ &= \begin{cases} \left( \frac{1}{V\gamma\eta + 1} \right)^{\frac{1}{V\gamma^2}}, & \text{for } k = 0 \\ \left( \frac{1}{V\gamma^2} \right)^{\frac{1}{V\gamma^2} + k} (V\gamma\eta)^k \left( \frac{1}{V\gamma\eta + 1} \right)^{\frac{1}{V\gamma^2} + k}, & \text{for } k \geq 1 \end{cases}. \end{aligned} \quad (3.13)$$

From (3.4), (3.5), (3.7) - (3.9) and (3.13), the normalized expected cost  $U$  of an LU can be expressed as

$$U = \sum_{k=1}^{\infty} \left( \frac{1}{k} \right) \left\{ U_O \Pi_O(k) + U_I \Pi_I(k) + U^* \Pi^*(k) + u\pi(k) + u^*\pi^*(k) \right\} P(k). \quad (3.14)$$

Table 3.1: Comparison between Analytic and Simulation Results ( $k = 39$ )

$p$	0.5	0.6	0.7	0.8	0.9	1.0
$N = 1$						
$\Pi_O(k)$ (Analytic)	5.0148	3.9794	2.4783	1.6666	1.25	1
$\Pi_O(k)$ (Simulation)	4.9899	3.9488	2.473	1.6729	1.2513	1
Error(%)	0.50	0.77	0.21	0.38	0.54	0
$\Pi_I(k)$ (Analytic)	4.0148	2.9794	1.4783	0.6666	0.25	0
$\Pi_I(k)$ (Simulation)	3.9899	2.9488	1.473	0.6729	0.2513	0
Error(%)	0.62	1.03	0.36	0.54	0.54	0
$\Pi^*(k)$ (Analytic)	29.9703	32.0412	35.0434	36.6668	37.50	38
$\Pi^*(k)$ (Simulation)	30.0203	32.1024	35.054	36.6541	37.4973	38
Error(%)	0.16	0.19	0.03	0.03	0.01	0
$N = 2$						
$\Pi_O(k)$ (Analytic)	4.5148	3.6036	2.2599	1.5416	1.1944	1
$\Pi_O(k)$ (Simulation)	4.4939	3.5678	2.2529	1.5452	1.1961	1
Error(%)	0.46	0.99	0.31	0.23	0.14	0
$\Pi_I(k)$ (Analytic)	3.6402	2.6613	1.2645	0.5416	0.1944	0
$\Pi_I(k)$ (Simulation)	3.6179	2.6246	1.258	0.5452	0.1961	0
Error(%)	0.61	1.38	0.51	0.66	0.87	0
$\Pi^*(k)$ (Analytic)	11.345	13.2352	15.9756	17.4168	18.1111	18.50
$\Pi^*(k)$ (Simulation)	11.3908	13.3037	15.988	17.4095	18.1086	18.50
Error(%)	0.40	0.52	0.08	0.04	0.01	0
$\pi(k)$ (Analytic)	4.5148	3.4794	1.9783	1.1666	0.75	0.50
$\pi(k)$ (Simulation)	4.4921	3.4449	1.9755	1.1714	0.7517	0.50
Error(%)	0.05	0.99	0.14	0.41	0.22	0
$N = 9$						
$\Pi_O(k)$ (Analytic)	2.312	2.1995	1.7973	1.3815	1.1406	1
$\Pi_O(k)$ (Simulation)	2.3131	2.1983	1.7931	1.3810	1.1406	1
Error(%)	0.05	0.06	0.23	0.03	0.01	0
$\Pi_I(k)$ (Analytic)	1.7991	1.4715	0.8366	0.3822	0.1406	0
$\Pi_I(k)$ (Simulation)	1.7974	1.4678	0.8339	0.382	0.1406	0
Error(%)	0.09	0.25	0.32	0.04	0.04	0
$\Pi^*(k)$ (Analytic)	0.2222	0.6623	1.6995	2.5697	3.0521	3.3333
$\Pi^*(k)$ (Simulation)	0.2219	0.6675	1.7063	2.5698	3.052	3.3333
Error(%)	0.17	0.79	0.40	0	0	0
$\pi(k)$ (Analytic)	23.0427	18.8287	11.7555	7.4215	5.2461	4
$\pi(k)$ (Simulation)	22.9828	18.7273	11.7141	7.4246	5.2476	4
Error(%)	0.26	0.54	0.35	0.04	0.03	0

We note that equation (3.14) is affected by  $\eta/\gamma$  (the update rate or the speed to move out of a PG) and  $p$  (the moving direction of a vehicle). An MS with large  $\eta/\gamma$  and  $p$  represents a vehicle moving in highway. An MS with small  $\eta/\gamma$  and  $p$  represents a vehicle moving in local roads.

### 3.4 Performance Evaluation

This section studies the performance for both  $S_R$  and  $S_W$ . We investigate the effects of parameters  $N$  (the PC size),  $p$  (the right move probability),  $\eta/\gamma$  (the update rate or the speed of the vehicle) and  $V$  (the variance of idle period) on the expected signalling cost of a location update (LU) operation. Let  $U_R$  and  $U_W$  be the LU costs (the expected number of messages sent in an LU) for  $S_R$  and  $S_W$ , respectively. We note that the costs of the paging and idle mode exit procedures for both  $S_R$  and  $S_W$  are the same and are not considered in this chapter.

Figure 3.5 plots  $U_R$  and  $U_W$  as functions of  $N$ ,  $p$  and  $\eta/\gamma$ , where the idle period is exponentially distributed ( $V = 1/\gamma^2$ ). In this figure,  $\eta/\gamma = 1.85, 24, 240$ ,  $p = 0.5, 0.8$ , and  $N$  ranges from 1 to 20. We first point out several facts. From Figure 3.5, we have

**Fact 1.** As  $N$  increases, more intra-PC LUs (with lower costs) and less inter-PC LUs (with higher costs) are exercised.

**Fact 2.** When  $\eta/\gamma$  is very small, few LUs occur in an idle period, and it is more likely that the MS only makes intra-PC LUs within PC 0. When  $\eta/\gamma$  is large, more LUs outside PC 0 occur.

**Fact 3.** If an MS makes more inter-PC LUs (with costs  $U_I$ ,  $U_O$  or  $U^*$ ; see Figure 3.2), then  $U_R > U_W$ .

**Fact 4.** If an MS makes more intra-PC LUs outside PC 0 (with cost  $u^*$ ; see Figure 3.3), then  $U_R < U_W$ .

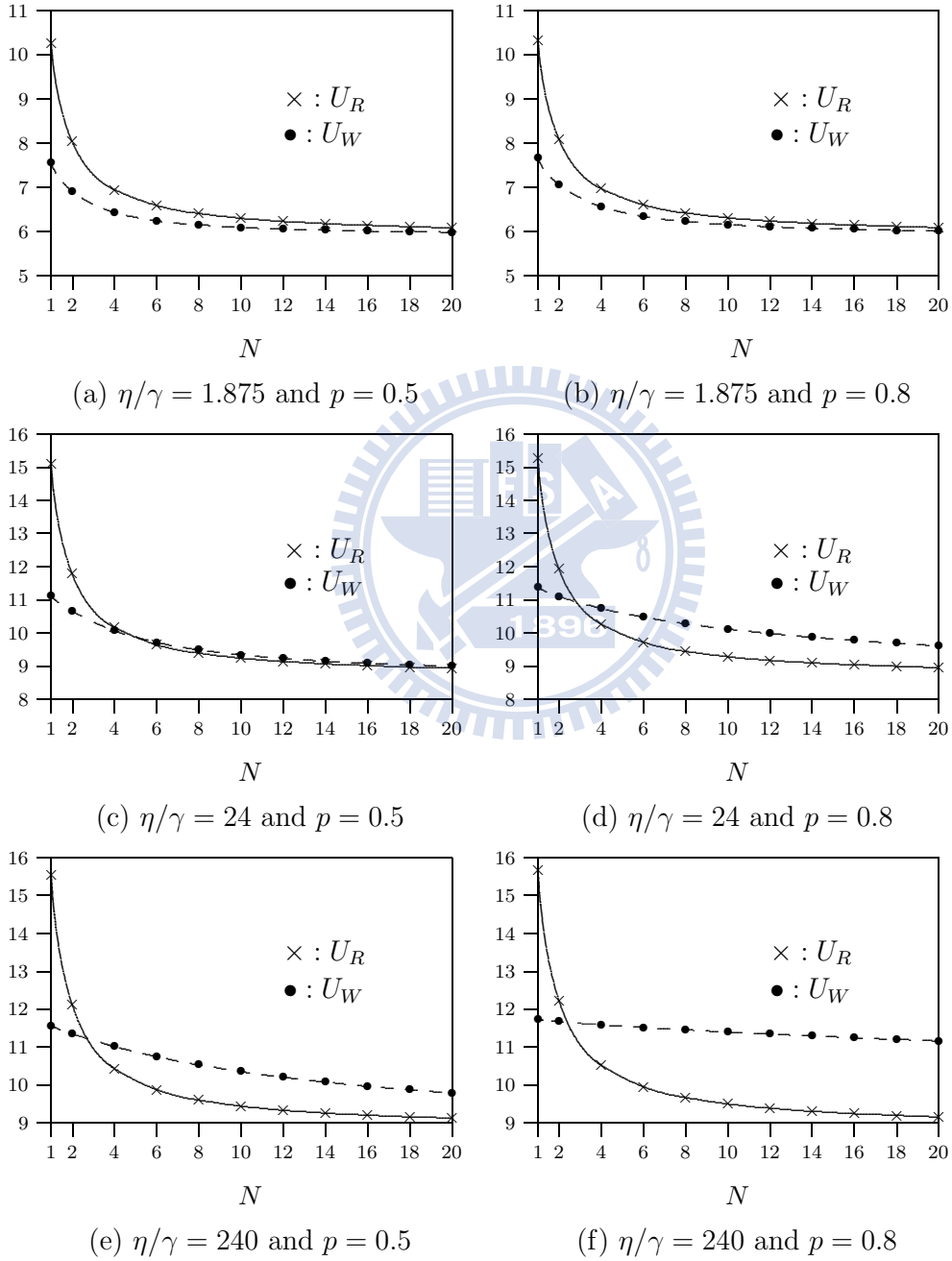


Figure 3.5:  $U_R$  and  $U_W$  for  $V = 1/\gamma^2$

**Effect of  $p$ .** In practice, a small  $p$  (e.g.,  $p = 0.5$  in Figures 3.5 (a), (c) and (e)) represents the movement of a pedestrian or a vehicle in local roads, and a large  $p$  (e.g.,  $p = 0.8$  in Figures 3.5 (b), (d) and (f)) represents the movement of a vehicle in highways. When  $p$  increases, the MS tends to move to one direction, and more LUs without involving PC 0 are exercised. That is, Fact 4 becomes more significant as  $p$  increases, and  $U_W$  increases faster than  $U_R$  does.

**Effects of  $N$  and  $\eta/\gamma$ .** Figure 3.5 shows an intuitive result that  $U_R$  and  $U_W$  decrease as  $N$  increases (Fact 1). This figure also shows that  $U_R$  and  $U_W$  increase as  $\eta/\gamma$  increases. When  $\eta/\gamma$  is very small (see Figures 3.5 (a) and (b)), the expected LU cost is small (Fact 2). The increase of  $\eta/\gamma$  results in more LUs with higher costs. Figure 3.5 indicates that  $S_W$  outperforms  $S_R$  when  $N$  or  $\eta/\gamma$  are small. Conversely,  $S_R$  is better than  $S_W$  when both  $N$  and  $\eta/\gamma$  are large. When  $N$  is small,  $U_R > U_W$  (Facts 1 and 3). When  $\eta/\gamma$  is small, more LUs around PC 0 are exercised (Fact 3), and  $U_R > U_W$ . When both  $\eta/\gamma$  and  $N$  are large, more intra-PC LUs outside PC 0 are exercised, and  $U_R < U_W$  (Facts 1, 2 and 4). Therefore, for highway traffic (i.e.,  $\eta/\gamma$  and  $p$  are large) and when the PC size is sufficiently large (e.g.,  $N > 3$  in our examples),  $S_R$  is better than  $S_W$ . For local road traffic (i.e.,  $\eta/\gamma$  and  $p$  are small),  $S_W$  outperforms  $S_R$ .

**Effect of  $V$ .** Figure 3.6 shows that  $U_R$  and  $U_W$  are decreasing functions of the variance  $V$  of idle periods. When  $V$  is small, less long and short idle periods are observed, and  $U_R/U_W$  are mainly affected by the parameters  $N$ ,  $p$  and  $\eta/\gamma$  as previously described. When  $V$  is large, many short idle periods with few LUs are observed (i.e.,  $P(0)$  is large in equation (3.14)), and  $U_R/U_W$  significantly decrease as  $V$  increases. In this case,  $U_R \approx U_W$ .

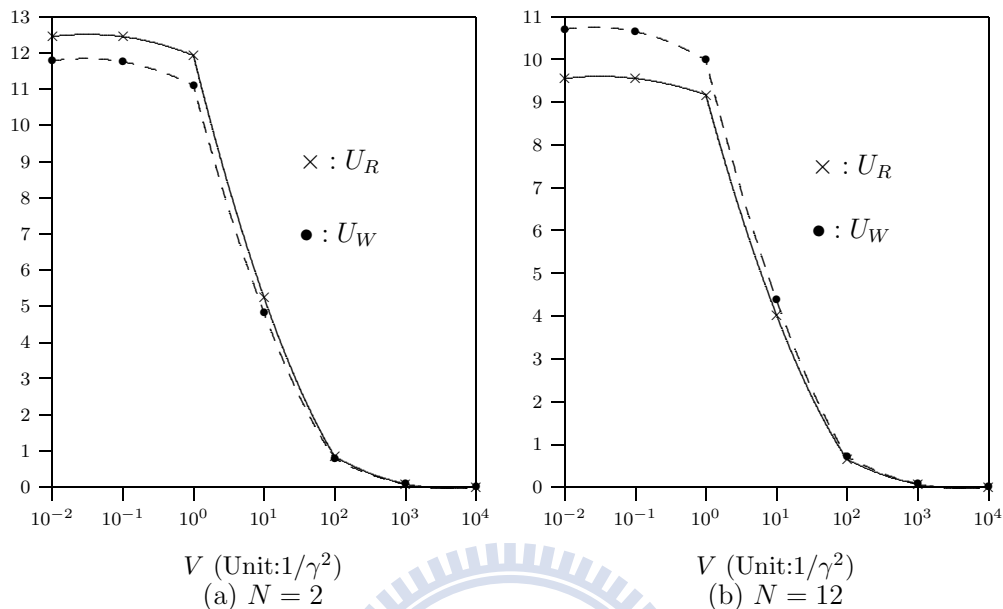


Figure 3.6:  $U_R$  and  $U_W$  for  $p = 0.8$  and  $\eta/\gamma = 24$

### 3.5 Summary

This chapter studied the WiMAX-based ITS systems where the base stations serve as roadside units and the mobile stations installed in vehicles serve as the onboard units. We investigated the impact of vehicle mobility on location update of two APC relocation scenarios for WiMAX-based ITS: with APC relocation ( $S_R$ ) and without APC relocation ( $S_W$ ). An analytic model was proposed to model the expected location update cost  $U$  for the one-dimensional WiMAX paging group configuration. The analytic results were validated against the simulation experiments. Our study indicates the following results:

- For a vehicle or a pedestrian in local roads,  $S_W$  outperforms  $S_R$ .
- For a vehicle in highway,  $S_R$  outperforms  $S_W$  when the PC size is sufficiently large.

These results provide guidelines to activate the APC relocation mechanism for vehicles with various moving behaviors.

## Chapter 4

# Repacking on Demand for the Hierarchical WiMAX Networks

As described in Section 1.2, radio channels are limited resources that should be carefully allocated in mobile telecommunications networks. To increase network capacity for WiMAX, operators can deploy the *Hierarchical WiMAX Networks* (HWNs). To further increase the channel utilization, the *repacking* mechanism that switches calls between macrocells and microcells can be applied in the HWNs. Based on the repacking mechanism, our previous work proposed *Repacking on Demand* (RoD) [33, 68] to improve the network performance. To support much faster *Mobile Stations* (MSs), we extend RoD by considering the moving speeds of MSs. A simulation model is developed to investigate the performance of RoD and some previously proposed repacking approaches. Our study [69] quantitatively shows that speed-sensitive RoD is less sensitive to MS moving speeds and significantly outperforms the previous proposed approaches.

### 4.1 Channel Repacking for the HWNs

Capacity planning is one of the most important issues in cellular network operation. To effectively increase network capacity in WiMAX systems, mobile operators can deploy the HWN (Figure 4.1), the WiMAX network with the hierarchical cell structure. As shown in Figure 4.1, the HWN consists of two types of *Base Stations* (BSs): micro BSs

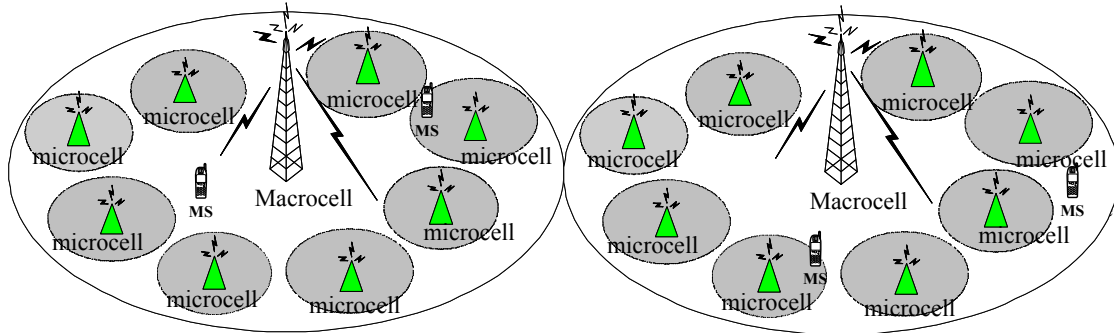


Figure 4.1: Hierarchical WiMAX Network Architecture

and macro BSs. A micro BS with low power transceivers provides small radio coverage (referred to as microcell), and a macro BS with high power transceivers provides large radio coverage (referred to as macrocell). The microcells cover MSs in heavy teletraffic areas. A macrocell is overlaid with several microcells to cover all MSs in these microcells. For an HWN, macrocell BSs can be the WiMAX BSs with high transmission power, and microcell BSs can be the WiMAX BSs with low transmission power or the WiFi *Access Points* (APs) [54, 78, 40, 59].

In the HWNs, *repacking* is the process of switching a connected call from a macrocell to a microcell and vice versa. With repacking mechanism, operators can increase the number of idle channels in a macrocell so that more macrocell channels can be shared by the call attempts where no channels are available in their microcells. Moreover, the performance of repacking can be enhanced by considering the moving speeds of the MSs [38, 71, 72]. Speed-sensitive channel assignment and repacking (including Macro-to-micro and micro-to-Macro repacking) are exercised to satisfy the following criteria:

**Criterion 1.** Calls for slow MSs tend to be assigned with microcell channels so that the “global resources” of macrocells can be effectively shared by calls in the blocked microcells (i.e., the microcells without any idle channel).

**Criterion 2.** Calls for fast MSs tend to be assigned with macrocell channels so that the number of handoffs can be reduced.



Following Criterion 1, *Macro-to-micro* (M-to-m) repacking may be exercised to switch a call for a slow MS from the macrocell to the microcell. In this case, the “global resources” of macrocells can be effectively shared by calls in the blocked microcells. Following Criterion 2, the *micro-to-Macro* (m-to-M) repacking may be exercised to switch a call for a fast MS from the microcell to the macrocell. In this case, the number of handoffs can be reduced.

In this study, we consider several speed-sensitive channel assignment with repacking approaches: *Always Repacking* (AR; or *take-back* in [10, 38, 50]) always exercises repacking as soon as some specific events (e.g., a channel is released at the microcell/macrocell) occur to reduce the number of handoffs for calls of fast MSs. However, always exercising repacking may degrade the system performance on call blocking probability and force-termination probability in some cases (e.g., the number of macrocell channels is small). In *Partial Repacking on Demand* (PRoD; or *preemption* in [71, 72]), only calls with slow speeds are repacked on demand. When the proportion of fast calls increases, the effect of slow-call repacking on performance improvement becomes insignificant. Therefore, in order to further reduce call blocking and force-termination, this study improves the RoD approach by considering repacking for both slow and fast MSs.

This chapter is organized as follows. In Section 4.2, we describe speed-sensitive channel assignment approaches including AR, PRoD and RoD. In Section 4.3, input parameters and output measures for these channel assignment approaches are described. Section 4.4 compares RoD with AR and PRoD. Our study quantitatively shows that RoD outperforms AR and PRoD.

## 4.2 Speed-sensitive Channel Assignment for HWNs

Based on the moving speeds of MSs, several speed-sensitive channel assignment approaches have been proposed. In these approaches, a call for a fast MS is referred to as a *fast call*, and a call for a slow MS is referred to as a *slow call*.

*No Repacking (NR)* [62]: This approach does not perform repacking. Based on Criteria 1 and 2, the slow and fast calls are handled differently.

**NR for Slow Calls (Figure 4.2).** When a slow call attempt is newly generated at or handed off to the  $i$ th microcell in HWN, the network first tries to assign a channel in the  $i$ th microcell (following Criterion 1) to the call attempt (Steps 1 and 2 in Figure 4.2). If no idle channel is available in the  $i$ th microcell, the call attempt overflows to the macrocell that is overlaid with the  $i$ th microcell. If the macrocell has an idle channel, the HWN accepts the call (Steps 3 and 4). Otherwise, the call attempt is rejected; i.e., the new call is blocked or the handoff call is forced to terminate (Step 5). Steps 1 - 4 in Figure 4.2 are called the *NR Slow MS Channel Assignment Procedure*.

**NR for Fast Calls (Figure 4.3).** When a new or handoff fast call attempt occurs in the  $i$ th microcell, the HWN first tries to assign the call attempt a channel in the macrocell (following Criterion 2) that is overlaid with the  $i$ th microcell (Steps 1 and 2 in Figure 4.3). If no idle channel is available in the macrocell, the call attempt overflows to the  $i$ th microcell, and the HWN tries to allocate the call a channel in the  $i$ th microcell (Steps 3 and 4). If no idle channel is available in the microcell, the call attempt is rejected (Step 5).

When a call is complete or the MS moves out of a cell, the radio channel is reclaimed to the idle channel pool of the corresponding micro (macro) cell.

*Always Repacking (AR)* [10, 38, 50]: Two repacking procedures are exercised in AR to reduce the force-termination probability of fast calls. In Macro-to-micro (M-to-m) repacking, a slow call occupying a macrocell channel is switched to an idle channel in the microcell where the MS resides (following Criterion 1). In micro-to-Macro (m-to-M) repacking, a fast call occupying a microcell channel is switched to an idle channel of the overlay macrocell (following Criterion 2). During repacking,

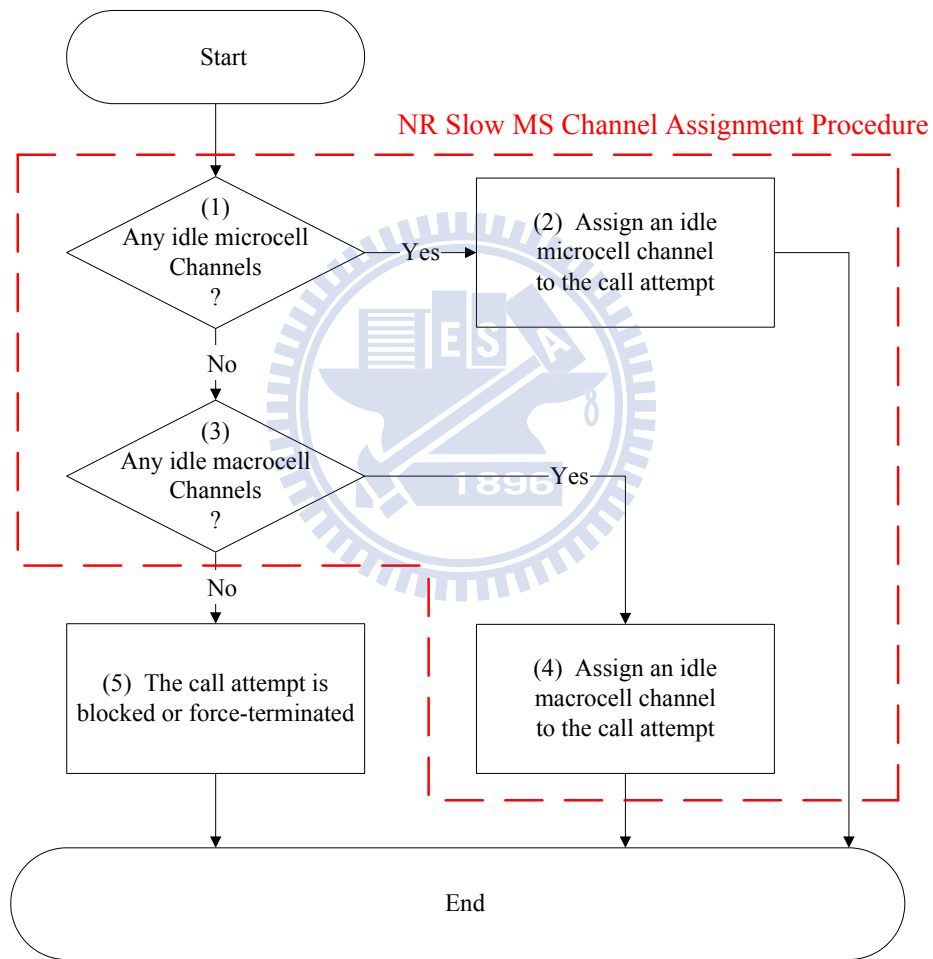


Figure 4.2: No Repacking for Slow MSs

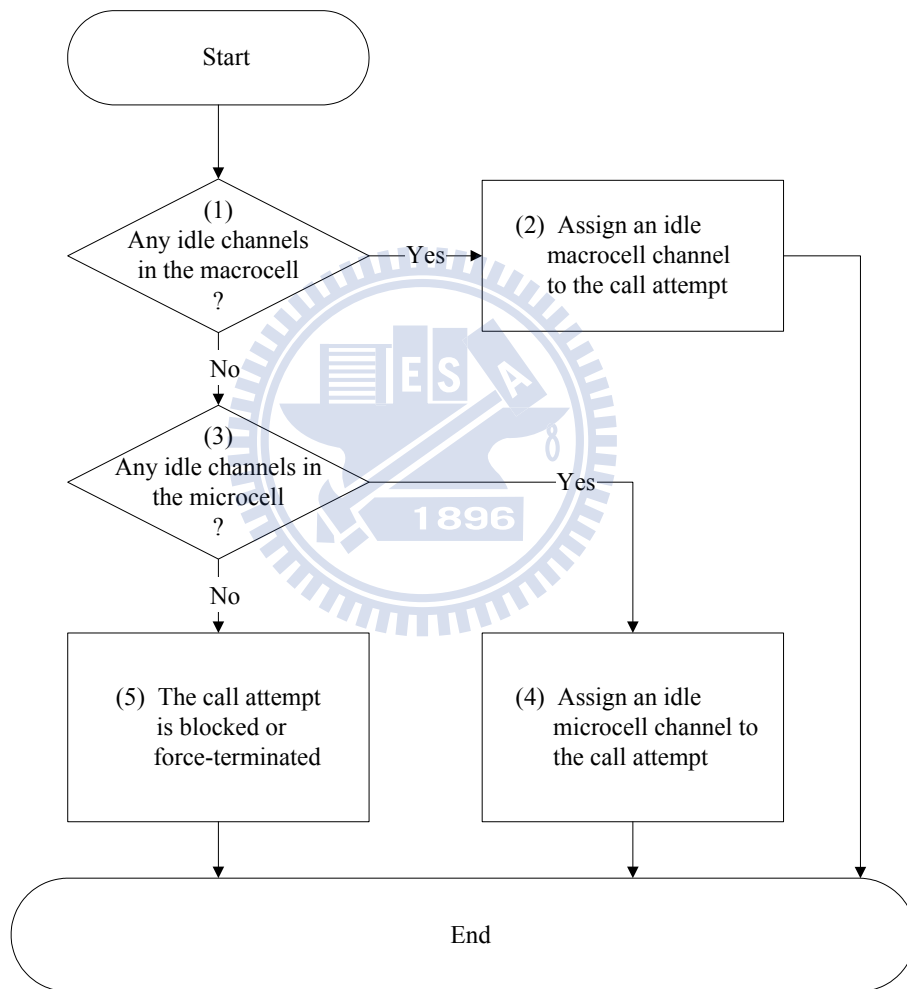


Figure 4.3: No Repacking for Fast MSs

one or more calls may be available for switching. These calls are referred to as the *repacking candidates*.

The AR channel assignment is the same as that for NR (see Figures 4.2 and 4.3). The AR repacking procedures (Figures 4.4 (a) and (b)) are repeatedly executed to check if one of the following situations occurs.

**M-to-m Repacking (Figure 4.4 (a)):** When a channel is released at a microcell (Step 1 in Figure 4.4 (a)), the HWN checks if there is any slow M-to-m repacking candidate (which is a slow call) in the corresponding macrocell (Step 2). If so, M-to-m repacking is exercised to switch one of the slow repacking candidates from the macrocell to the microcell (Steps 3 and 4).

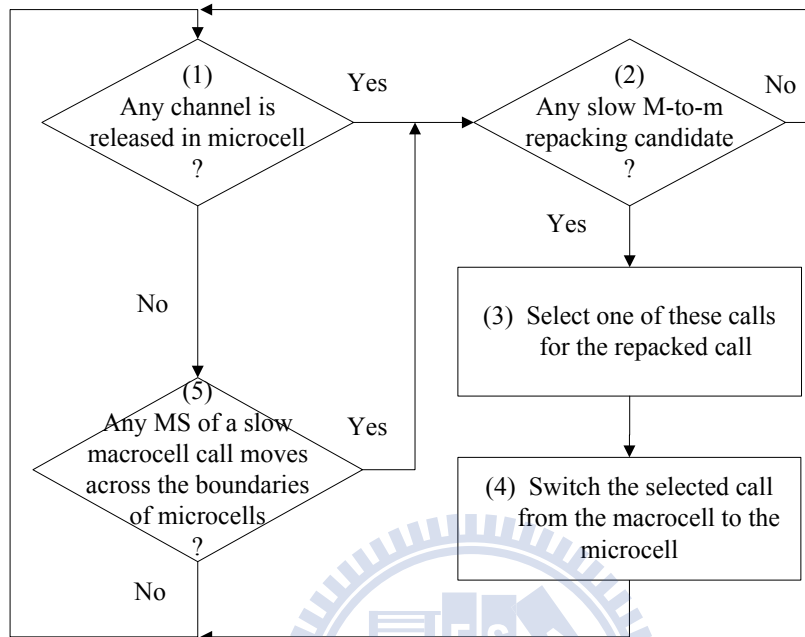
When an MS of a slow macrocell call moves across the boundary of two microcells in that macrocell (Step 5 in Figure 4.4 (a)), the HWN checks if the call can be a slow M-to-m repacking candidate (Step 2 in Figure 4.4 (a)). If so, Steps 3 and 4 in Figure 4.4 (a) are executed to perform M-to-m repacking.

**m-to-M Repacking (Figure 4.4 (b)):** When a channel is released in a macrocell (Step 1 in Figure 4.4 (b)), the HWN checks if there is any m-to-M repacking candidate (which is a fast call ; Step 2). If so, m-to-M repacking is exercised (Steps 3 and 4).

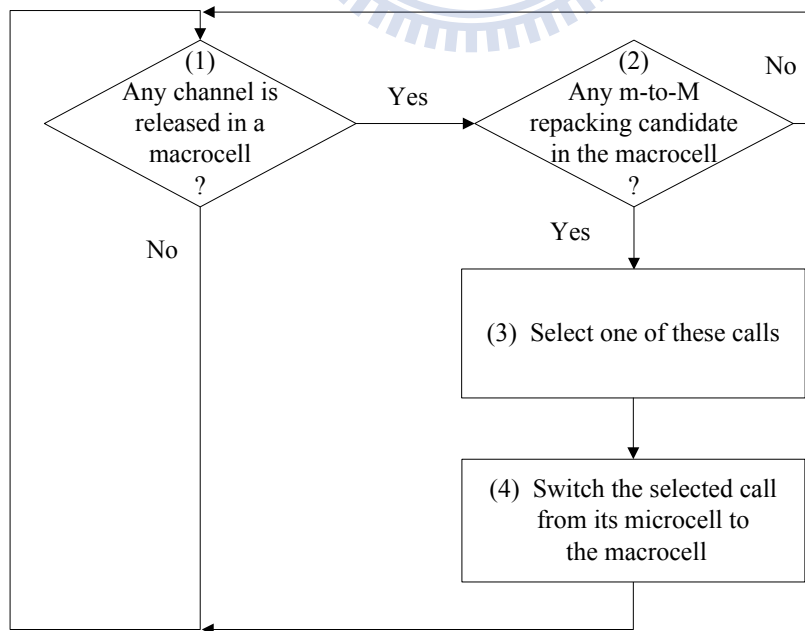
*Repacking on Demand (RoD):* This chapter proposes the RoD, where the HWN may trigger the M-to-m repacking when a call assignment (for a new call or a handoff call) occurs (following Criterion 1). Note that Criterion 2 is used in channel assignment for fast calls, but is not used in repacking.

#### **RoD I: RoD for Slow Calls (Figure 4.5).**

**Step RoD I.1:** When a slow call attempt  $C_s$  is newly generated at or handed off to the  $i$ th microcell, the HWN first exercises the NR slow MS channel



(a) M-to-m Repacking Procedure for AR



(b) m-to-M Repacking Procedure for AR

Figure 4.4: Channel Repacking Procedures for AR

assignment procedure. If the call attempt  $C_s$  is assigned a channel, the procedure exits.

**Step RoD I.2:** If no idle channel is found in Step RoD I.1, then following Criterion 1, the HWN checks if there is any slow M-to-m repacking candidate. If so, Step RoD I.3 is executed. Otherwise, Step RoD I.5 is executed.

**Steps RoD I.3 and 4:** The HWN selects one of these calls (i.e., the found M-to-m repacking candidates) to exercise M-to-m repacking, and the reclaimed macrocell channel is assigned to the slow call attempt  $C_s$ . The procedure exits.

**Steps RoD I.5 and 6:** If no slow M-to-m repacking candidate is found, the HWN checks if there is any fast M-to-m repacking candidate. If so, go to Step RoD I.3. Otherwise, the call attempt  $C_s$  is rejected.

## **RoD II: RoD for Fast Calls (Figure 4.6).**

**Steps RoD II.1 and 2:** When a fast call attempt  $C_f$  is newly generated at or handed off to the  $i$ th microcell, the HWN first tries to assign a channel in the macrocell that is overlaid with the  $i$ th microcell (following Criterion 2) to the call attempt. If the call attempt  $C_f$  is assigned a channel, the RoD procedure exists.

**Step RoD II.3:** If no idle macrocell channel is found in Step RoD II.1, then following Criterion 1, the HWN checks if there is any slow M-to-m repacking candidate. If so, the procedure proceeds to Step RoD II.4. Otherwise, Step II.6 is executed.

**Steps RoD II.4 and 5:** The HWN performs M-to-m repacking to generate a free macrocell channel for  $C_f$  and the procedure exits.

**Steps RoD II.6 and 7:** If no slow M-to-m repacking candidate is found,

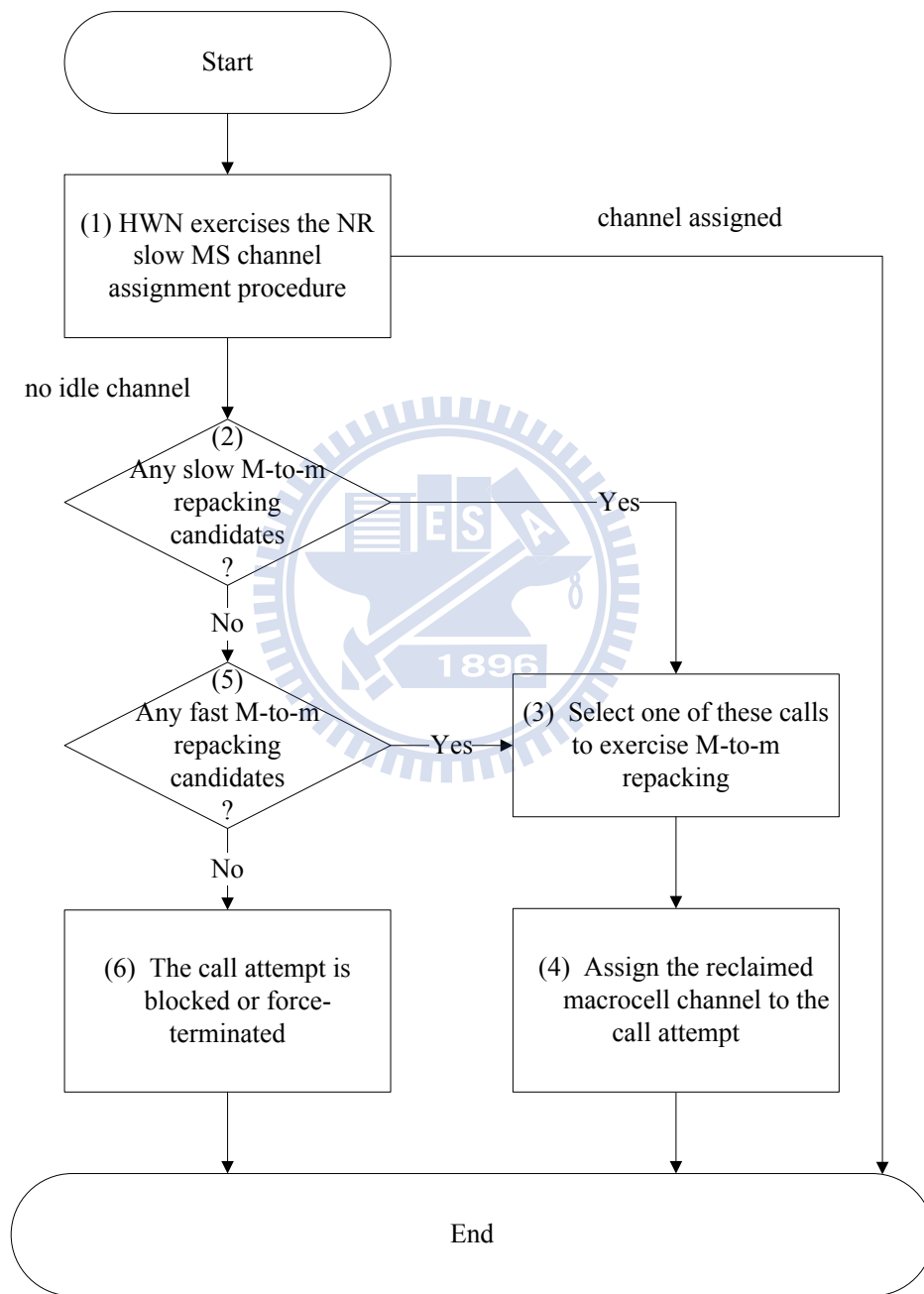


Figure 4.5: RoD I: RoD for Slow MSs



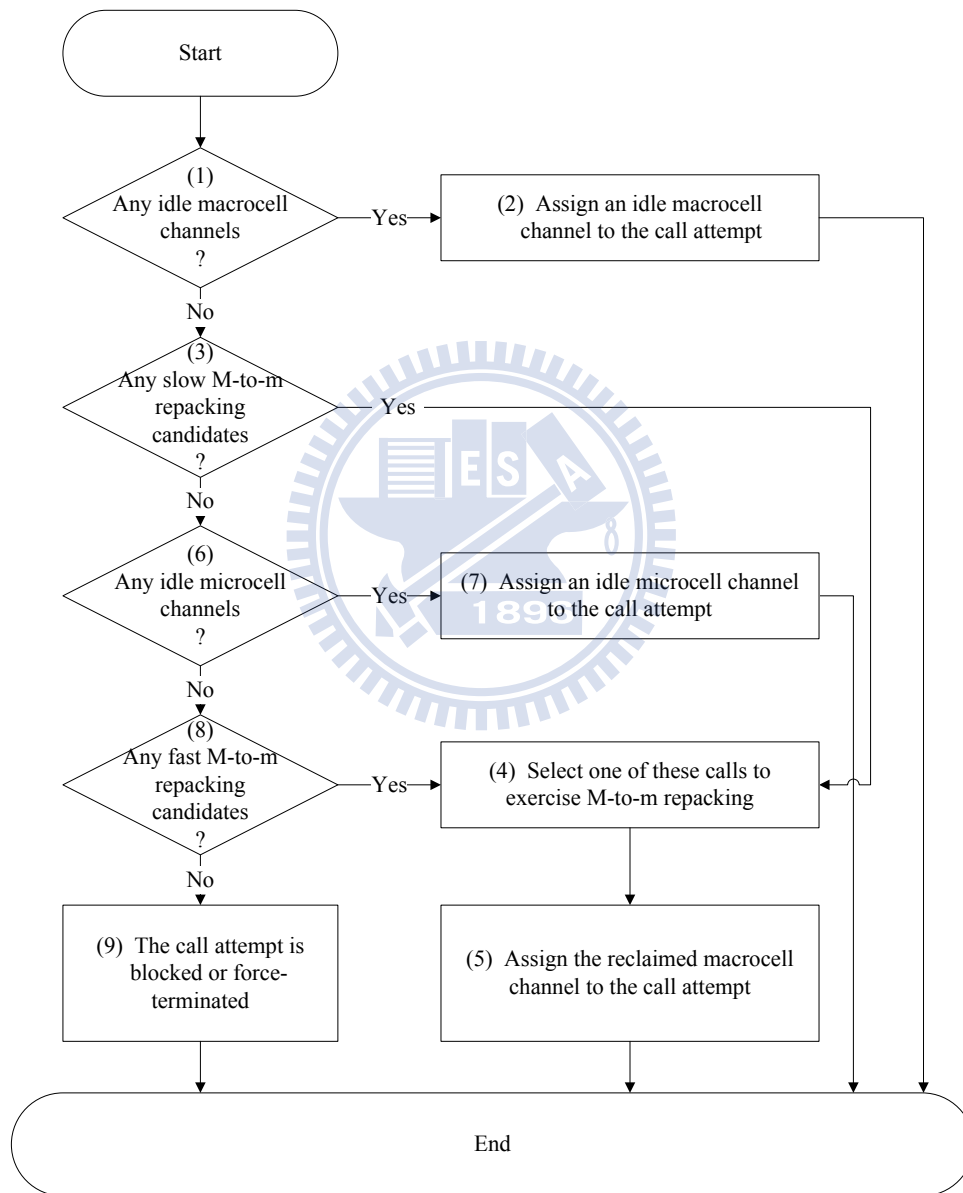


Figure 4.6: RoD II: RoD for Fast MSs

the HWN tries to allocate a channel in the  $i$ th microcell to the call.

**Steps RoD II.8 and 9:** If no idle channel is available in the microcell, the HWN checks if there is any fast M-to-m repacking candidate. If so, go to Step RoD II.4. Otherwise, the call attempt  $C_f$  is rejected.

In RoD, there are two alternatives to select the M-to-m repacking candidate at Steps RoD I.3 and RoD II.4. *Random RoD* (RoD-R) randomly selects a repacking candidate with the same probability. *Load Balancing RoD* (RoD-L) selects the repacking candidate whose microcell has the least traffic load.

*Partial RoD* (PRoD; or *preemption* in [71, 72]) is a special case of RoD, where Steps RoD I.5 (for slow calls) and RoD II.8 (for fast calls) are not executed. That is, PRoD only repacks slow calls.

Note that for both PRoD and RoD, Criterion 2 is used in channel assignment, but not in repacking. Only AR uses Criterion 2 in repacking. The primary purpose is to reduce the number of force-terminations for fast calls. Our study in Section 4.4 indicates that AR does not achieve its goal to reduce the force-termination probability as compared with RoD.

### 4.3 System Model for HWN Channel Assignment

This section describes the input parameters and output measures for the HWN channel assignment model. For the demonstration purpose, we consider a wrapped mesh cell configuration as shown in Figure 4.7. This configuration consists of four macrocells. Each macrocell covers  $4 \times 4$  microcells. The wrapped topology simulates unbounded HWN so that the boundary cell effects can be ignored [46]. Without loss of generality, the MS moves to one of the four neighbor microcells with the same probability (i.e., 0.25). Three types of input parameters are considered.

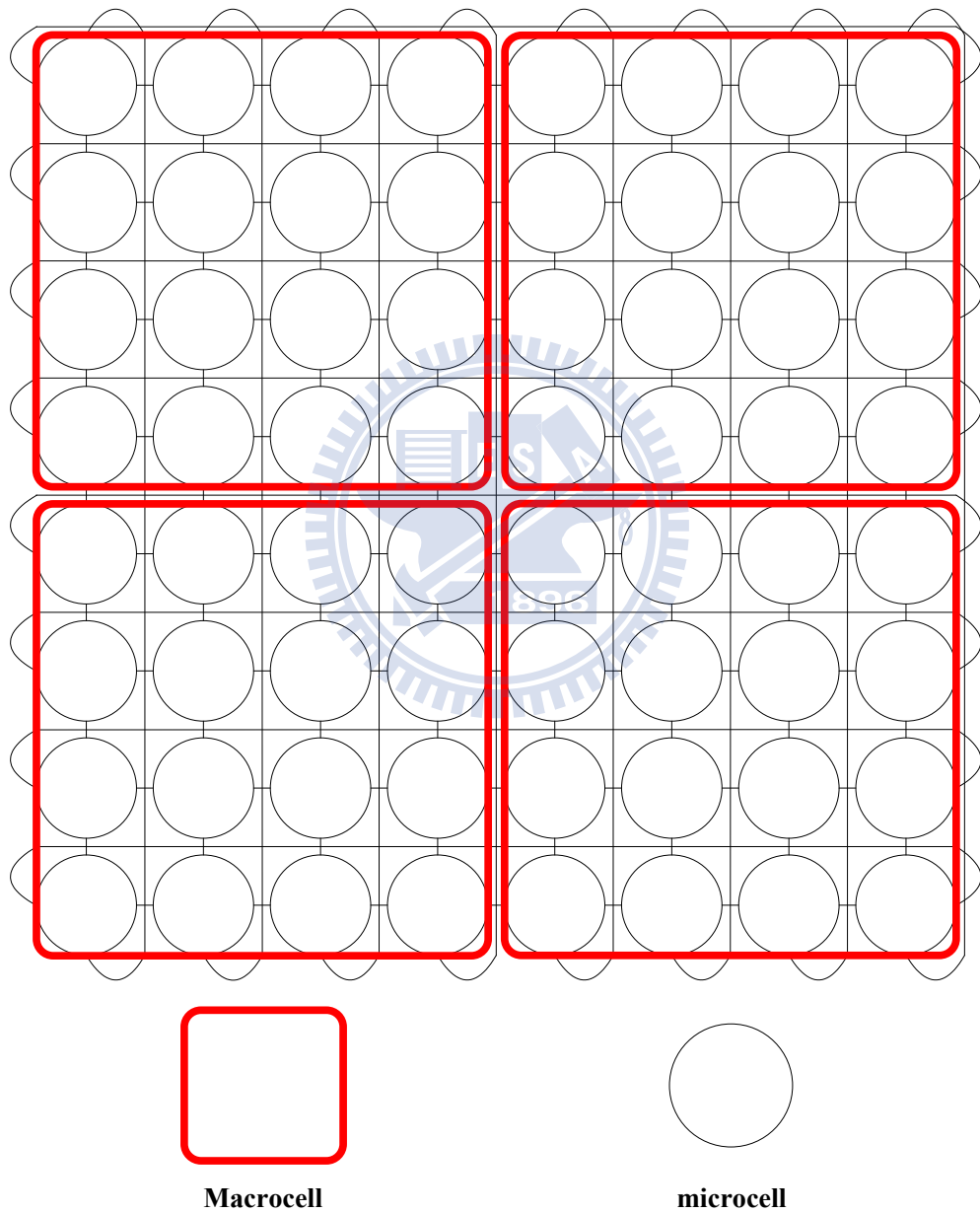


Figure 4.7: Hierarchical WiMAX Network with Wrapped Mesh Configuration

**System Parameters:** Each macrocell has  $C$  radio channels, and each microcell has  $c$  radio channels.

**Traffic Parameters:** The call arrivals to a microcell (for both incoming and outgoing calls) form a Poisson stream with rate  $\lambda$ . For fast MSs and slow MSs, the call arrivals rates are  $\beta\lambda$  and  $(1 - \beta)\lambda$ , respectively, where  $0 \leq \beta \leq 1$ . The call holding times have a Gamma distribution with mean  $1/\mu$  and variance  $V_c$  (the typical value for  $1/\mu$  is 1 minute).

**Mobility Parameters:** The microcell residence times of slow (fast) MSs have a Gamma distribution with mean  $1/\eta_s$  ( $1/\eta_f$ ) and variance  $V_{m,s}$  ( $V_{m,f}$ ).

The Gamma distribution is often used in mobile telecommunications network modeling (call blocking analysis for PCS networks under general cell residence time [16], teletraffic analysis and mobility modeling for PCS network [22], analytical results for optimal choice of location update interval for mobility database failure restoration in PCS networks [23]). It has been shown that the distribution of any positive random variable can be approximated by a mixture of Gamma distributions (see Lemma 3.9 in reversibility and stochastic networks [41]). Several output measures are defined in this study:

$P_b$ : the probability that a new call is blocked

$P_f$ : the probability that a successfully connected call is forced to terminate because of handoff failure

$P_{ff}$ : the probability that a successfully connected fast call is forced to terminate because of handoff failure

$P_{nc}$ : the probability that a new call is blocked or a connected call is forced to terminate

$H$ : the expected number of handoffs (including repackings) occurred during a call

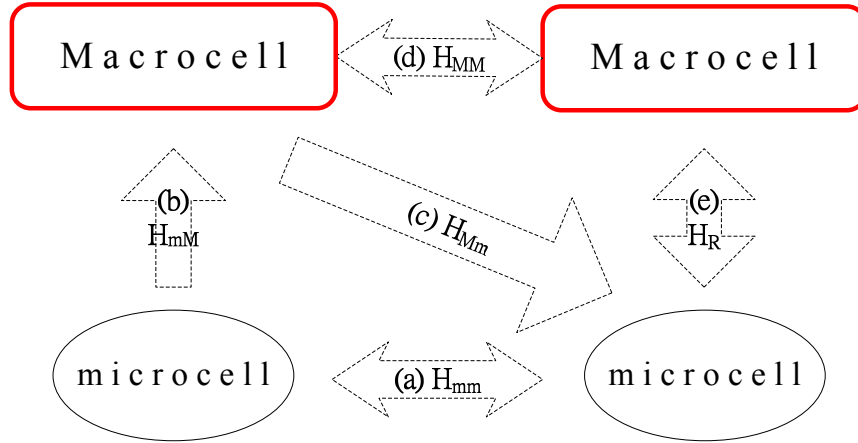


Figure 4.8: Handoff Types

Figure 4.8 shows five types of handoffs. Handoff measures for these handoff types are defined as follows.

$H_{mm}$ : the expected number of handoffs from a microcell to another microcell during a call (Figure 4.8 (a))

$H_{mM}$ : the expected number of handoffs from a microcell to a macrocell during a call (Figure 4.8 (b))

$H_{Mm}$ : the expected number of handoffs from a macrocell to a microcell during a call (Figure 4.8 (c))

$H_{MM}$ : the expected number of handoffs from a macrocell to another macrocell during a call (Figure 4.8 (d))

$H_R$ : the expected number of repackings (including m-to-M and M-to-m repackings) during a call (Figure 4.8 (e))

From the above description,  $H$  can be expressed as

$$H = H_{mm} + H_{mM} + H_{Mm} + H_{MM} + H_R. \quad (4.1)$$

Based on above discussions, a discrete event simulation model for RoD-R is described in Appendix B. Other strategies (such as NR, AR, PRoD and RoD-L) can be studied by similar simulation models, and the details are omitted.

## 4.4 Results and Discussions

We compare NR, AR, PRoD, RoD-R and RoD-L in terms of the output measures described above. In our numerical examples, the radio channel number is  $c = 10$  for every microcell and the expected microcell residence time for slow MSs is 5 times the value for fast MSs (i.e.,  $1/\eta_s = 5/\eta_f$ ). In most cases, we have the input parameters with the default setup: the call holding times are exponentially distributed with mean  $1/\mu = 1$  minute (i.e.,  $V_c = 1/\mu^2$ ), the microcell residence times for slow MSs are exponentially distributed with mean  $1/\eta_s = 10/\mu$  (i.e.,  $V_{m,s} = 100/\mu^2$  and  $V_{m,f} = V_{m,s}/25 = 4/\mu^2$ ), the number of macrocell channel is  $C = 8$ , the call arrival rate to a microcell is  $\lambda = 7/\mu$ , and the proportion of fast calls is  $\beta = 9\%$ . The effects of the input parameters are described as follows.

**Effect of the Macrocell Channel Number  $C$ .** Figures 4.9 (a) - (d) plot  $P_{ff}$ ,  $P_b$ ,  $P_f$  and  $P_{nc}$  as functions of  $C$ , where the values for the input parameters except  $C$  follow the default values listed above. These figures show an intuitive result that for all approaches,  $P_{ff}$ ,  $P_b$ ,  $P_f$  and  $P_{nc}$  decrease as  $C$  increases. We also observe that the  $P_{ff}$ ,  $P_b$ ,  $P_f$  and  $P_{nc}$  are more sensitive to the change of  $C$  for small  $C$  values than for large  $C$  values. Since the macrocell channels are the bottleneck resources when  $C$  is small, increasing  $C$  significantly reduces  $P_{ff}$ ,  $P_b$ ,  $P_f$  and  $P_{nc}$ . Figures 4.10 (a) - (d) plot  $H_{mm}$ ,  $H_{mM}$ ,  $H_R$  and  $H$  as functions of  $C$ , where the values for the input parameters except  $C$  follow the default values listed above. Figure 4.10 (a) shows that for all approaches,  $H_{mm}$  is a decreasing function of  $C$ . This phenomenon is due to the fact that when  $C$  increases, more calls (especially fast calls) will occupy macrocell channels, and the number of microcell to microcell handoffs will decrease.

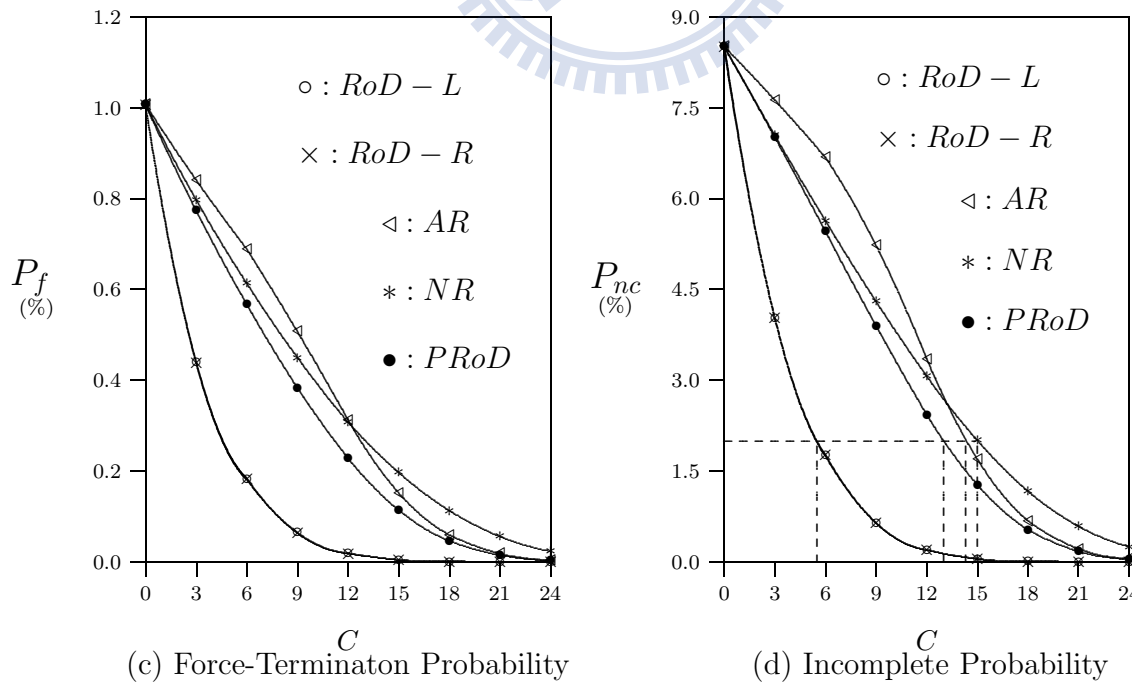
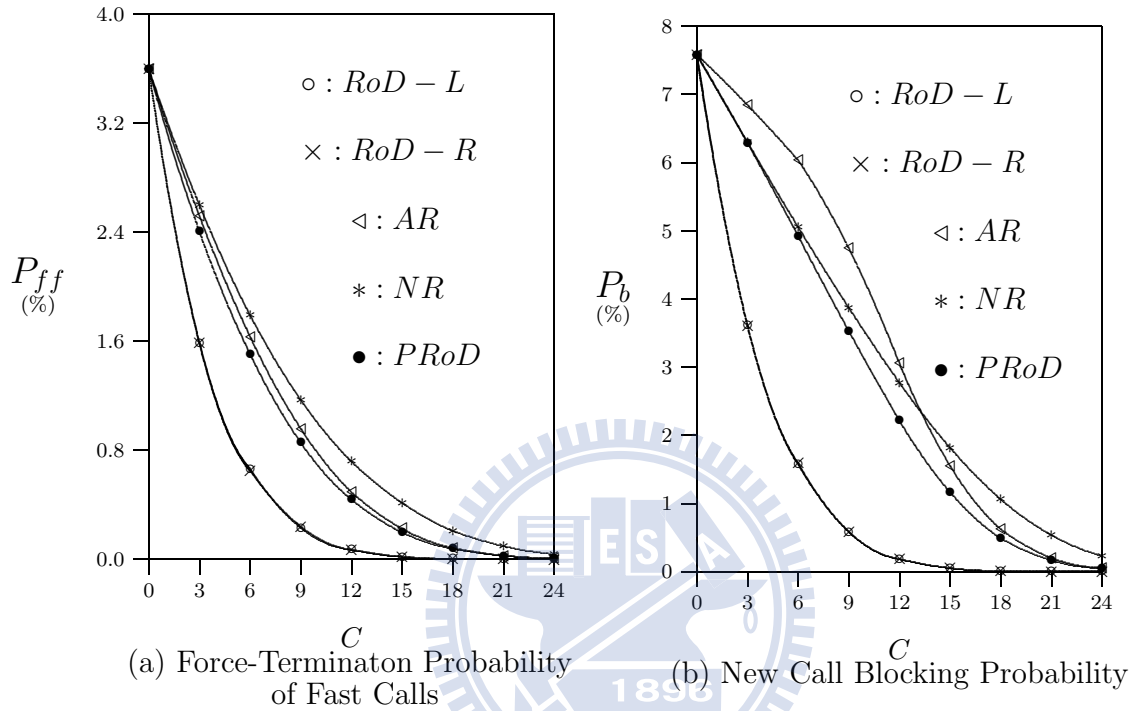


Figure 4.9: Effects of Macrocell Channel Number  $C$

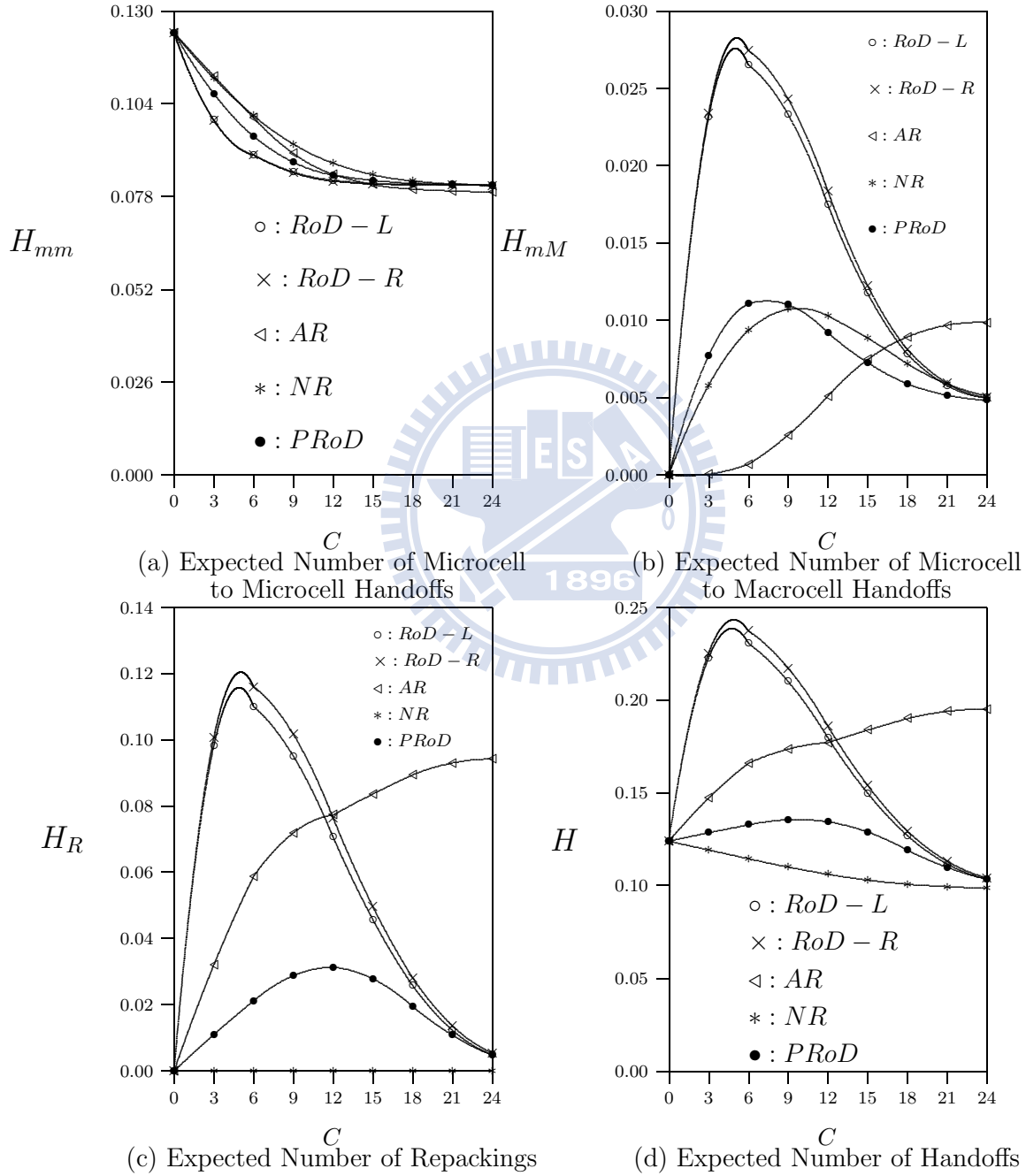


Figure 4.10: Effects of the Macrocell Channel Number  $C$



Figure 4.10 (b) shows that for AR,  $H_{mM}$  is an increasing function of  $C$ . Increasing  $C$  results in more idle macrocell channels, and more calls (especially slow calls) will be handed off from microcells to macrocells. For NR, PRoD and RoD,  $H_{mM}$  increases and then decreases as  $C$  increases. When  $C$  is small, macrocell channels are the bottleneck resources and increasing  $C$  results in more calls handed off from microcells to macrocells (especially fast calls that overflow to microcells). When  $C$  is large ( $C > 5$  in Figure 4.10 (b)), macrocell channels are no longer the bottleneck resources and less fast calls overflow to microcells. In this case, increasing  $C$  results in decreasing of  $H_{mM}$ . The performance figures for  $H_{Mm}$  and  $H_{MM}$  are similar to that for  $H_{mM}$ , and the details are omitted. Figure 4.10 (c) shows that for AR,  $H_R$  increases as  $C$  increases. Increasing  $C$  results in more slow calls that would overflow to macrocells, and thus more calls are repacked. On the other hand, for PRoD and RoD,  $H_R$  increases and then decreases as  $C$  increases. This non-trivial phenomenon is explained as follows. When  $C$  is small ( $C < 5$  for RoD and  $C < 12$  for PRoD in Figure 4.10 (c)), increasing  $C$  results in more M-to-m repacking candidates, and more on-demand repackings are exercised. When  $C$  is large, macrocell channels are no longer the bottleneck resources. Increasing  $C$  results in less blockings as well as force-terminations, and less on-demand repackings are needed. Therefore  $H_R$  decreases as  $C$  increases in this case. Figure 4.10 (d) shows the net effects of repackings and all types of handoffs. In this figure, as  $C$  increases,  $H$  decreases for NR and increases for AR. For PRoD and RoD,  $H$  increases and then decreases as  $C$  increases.

**Comparison of NR, AR, PRoD, RoD-R and RoD-L.** Figures 4.9 (a) - (d) compare NR, AR, PRoD, RoD-R and RoD-L on  $P_{ff}$ ,  $P_b$ ,  $P_f$  and  $P_{nc}$ , respectively. These figures show that RoD-R and RoD-L have smaller  $P_{ff}$ ,  $P_b$ ,  $P_f$  and  $P_{nc}$  values than NR, AR and PRoD. Furthermore, AR has higher  $P_{nc}$  than NR when  $C$  is small, and the opposite result is observed when  $C$  is large ( $C > 12.5$  in Figure 4.9

(d)). This non-trivial phenomenon is explained as follows. Consider the case when  $C$  is much less than the number of fast calls. In AR, m-to-M repacking is always exercised, and therefore macrocells have less idle channels in AR than in NR. In this case, the  $P_{nc}$  value is higher for AR than for NR. On the other hand, when  $C$  is large, the effect of M-to-m repacking for slow calls becomes more significant. Thus macrocells have more idle channels in AR than in NR. Specifically, if the HWN is engineered at  $P_{nc} = 2\%$  (see the horizontal dashed line in Figure 4.9 (d)),  $C = 5.5$  for RoD,  $C = 13$  for PRoD,  $C = 14.5$  for AR, and  $C = 15$  for NR. Thus RoD can save at least 7 macrocell channels over other approaches.

Figure 4.10 (c) shows that  $H_{R,RoD-R} > H_{R,RoD-L} > H_{R,AR} > H_{R,PRoD} > H_{R,NR} = 0$  when  $C$  is small ( $C < 12$ ). When  $C$  is large ( $C > 12$ ),  $H_{R,AR} > H_{R,RoD-R} > H_{R,RoD-L} > H_{R,PRoD} > H_{R,NR} = 0$ . Similar phenomena for  $H$  are observed in Figure 4.10 (d). Although NR, AR and PRoD have smaller  $H_R$  and  $H$  values than RoD, the increase of  $H_R$  and  $H$  does not result in the increase of  $P_{ff}$ ,  $P_b$ ,  $P_f$  and  $P_{nc}$  in RoD (see Figures 4.9 (a) - (d)).

**Effect of the Proportion  $\beta$  of Fast MSs.** Figure 4.11 plots  $P_{nc}$  as a function of  $\beta$ , where the values for the input parameters except  $\beta$  follow the default values listed above. In the figure, the call arrival rates for fast and slow MSs are  $\beta\lambda$  and  $(1 - \beta)\lambda$ , respectively. This figure shows that for all approaches,  $P_{nc}$  increases as  $\beta$  increases. Increasing of fast calls results in the increase of handoffs and hence force-terminations. This figure also shows that RoD approaches (i.e., RoD-R and RoD-L) are less sensitive to  $\beta$  than other approaches. Furthermore, when  $\beta$  is large ( $\beta > 8\%$  for AR and  $\beta > 18\%$  for PRoD), AR and PRoD have higher  $P_{nc}$  values than NR. The reason is that for AR, when  $\beta$  is large, the effect of m-to-M repackings is more significant than that of M-to-m repackings. Thus, less idle channels are available in macrocells for AR than for NR, and more calls are blocked or forced to terminate in

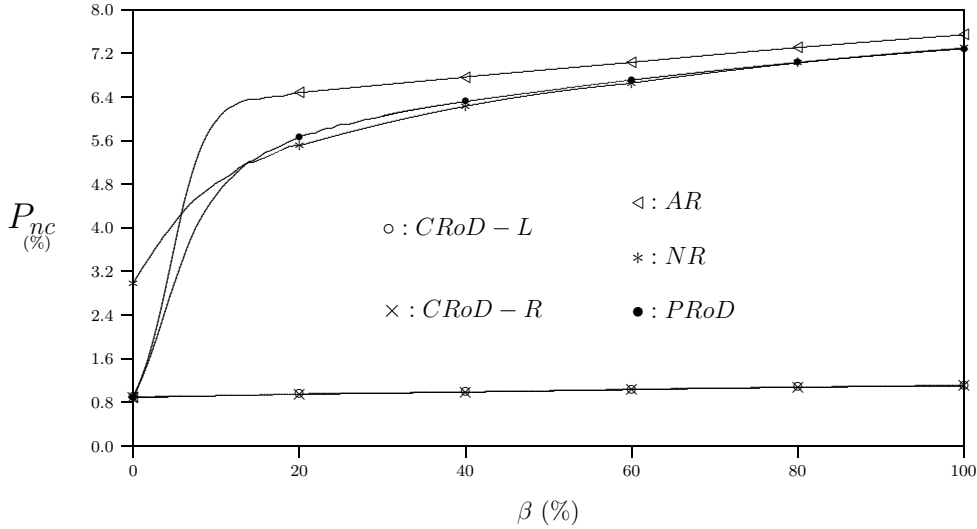


Figure 4.11: Effect of the Proportion  $\beta$  of Fast MSs on Incomplete Probability  $P_{nc}$

AR. For PRoD, when  $\beta$  is large, more fast calls repack slow calls, which occupy more macrocell channels. Therefore, more slow calls are blocked or forced to terminate.

**Effect of the MS Mobility (i.e., Mean Microcell Residence Times).** Figure 4.12 plots  $P_{nc}$  as a function of the microcell mobility rates (i.e.,  $\eta_s$  for slow MSs and  $\eta_f = 5\eta_s$  for fast MSs), where the values for the input parameters except  $1/\eta_s$  and  $1/\eta_f$  follow the default values listed above. This figure shows that  $P_{nc}$  increases as  $\eta_s$  increases. This figure also shows that to keep the same  $P_{nc}$  performance, (e.g.,  $P_{nc} = 7\%$ ), RoD can support much faster MSs (at least  $2^3$  times the  $\eta_s$  value) than other approaches.

**Effect of the Arrival Rate  $\lambda$ .** Figure 4.13 plots  $P_{nc}$  as a function of  $\lambda$ , where the values for the input parameters except  $\lambda$  follow the default values listed above. This figure shows that  $P_{nc}$  increases as  $\lambda$  increases. It also shows that to keep the same  $P_{nc}$  performance (e.g.,  $P_{nc} = 2\%$ ), RoD can support more call arrivals (at least 18%) than other approaches.

**Effect of the Variance  $V_c$  for the Call Holding Times.** Figure 4.14 plots  $P_{nc}$  and  $H$  as functions of  $V_c$ , where the values for the input parameters except  $V_c$  follow

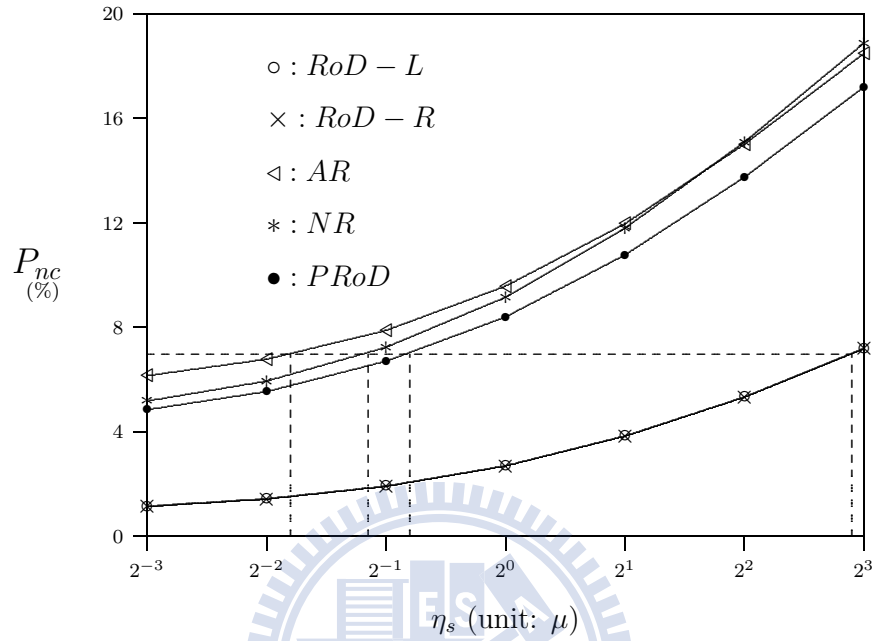


Figure 4.12: Effect of MS Mobility on Incomplete Probability  $P_{nc}$

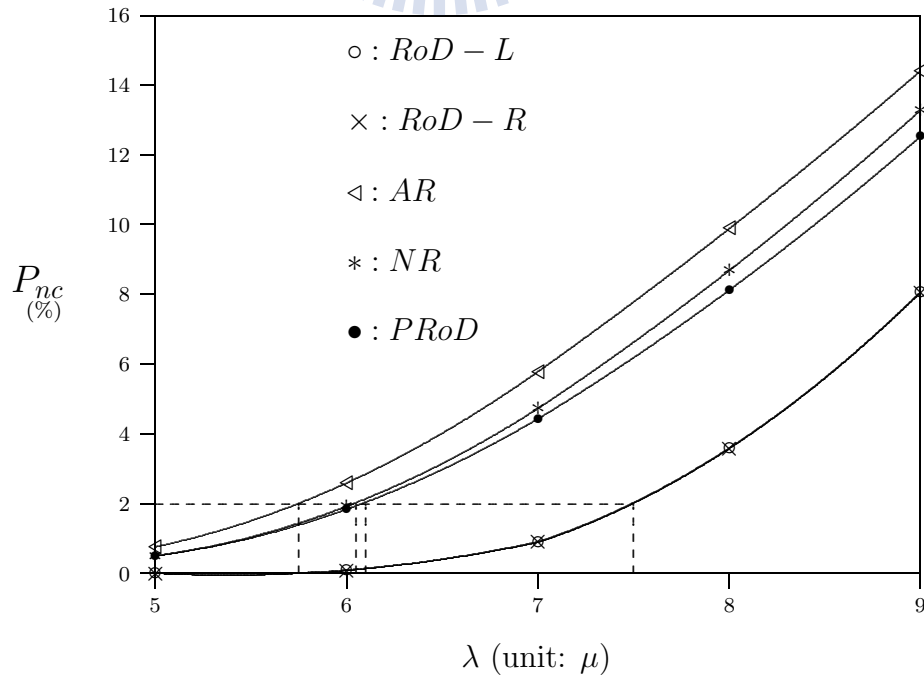


Figure 4.13: Effect of the Arrival Rate  $\lambda$  on Incomplete Probability  $P_{nc}$

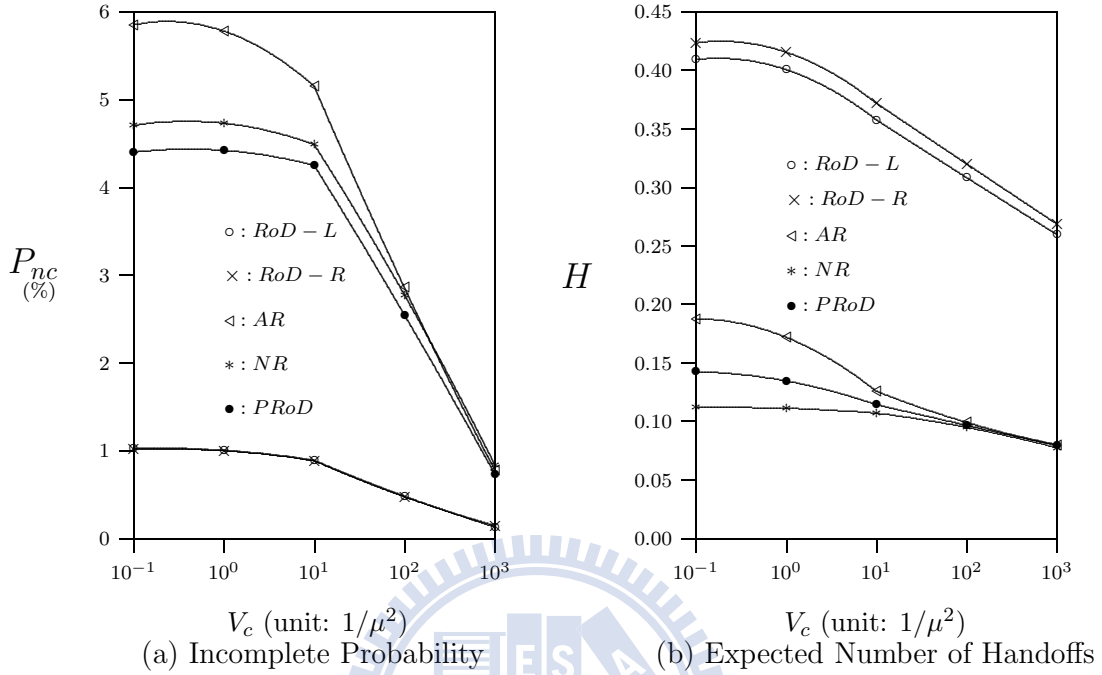


Figure 4.14: Effects of the Variance  $V_c$  for the Call Holding Times

the default values listed above. Figure 4.14 shows that  $P_{nc}$  and  $H$  decrease as  $V_c$  increases. Note that, for the call holding time distributions with the same mean value  $1/\mu$ , the standard deviation  $\sigma = \sqrt{V_c}$ . By the Chebyshev's Inequality, the probability that the call holding times are out of range  $[1/\mu - \frac{5\sqrt{V_c}}{3}, 1/\mu + \frac{5\sqrt{V_c}}{3}]$  is smaller than 36% for all  $V_c$  values. For example, if  $V_c = 100/\mu^2$ , then  $\frac{5\sqrt{V_c}}{3} = 50/3\mu$  and the probability that the call holding time exceeds  $53/3\mu$  is smaller than 36%. As  $V_c$  increases, more long and short call holding times are observed. More short call holding times implies that more calls are completed before next new call attempts arrive or next handoff attempts are exercised. Thus the numbers of blocked calls, force-terminated calls and handoffs decrease.

**Effect of the Variances for the Microcell Residence Times.** Figure 4.15 plots  $P_{nc}$  and  $H$  as functions of variances (i.e.,  $V_{m,s}$  for slow MSs and  $V_{m,f} = \frac{V_{m,s}}{25}$  for fast MSs) for the microcell residence times, where the values for the input parameters except  $V_{m,s}$  and  $V_{m,f}$  follow the default values listed above. Figure 4.15 shows that

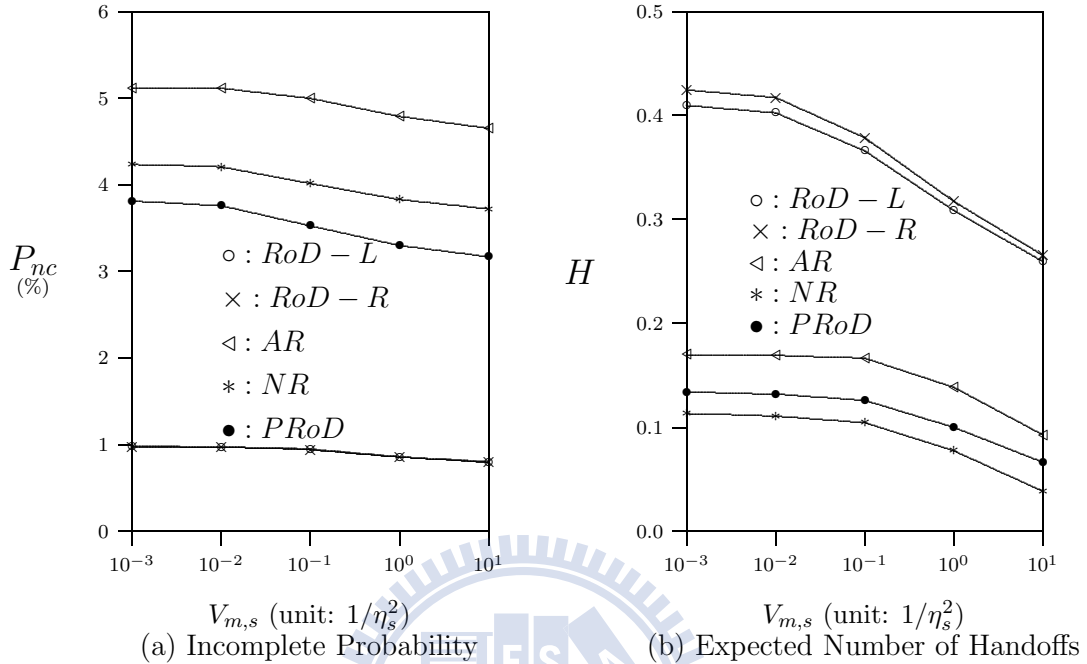


Figure 4.15: Effects of Variance  $V_{m,s}$  for Microcell Residence Times

$P_{nc}$  and  $H$  decrease as  $V_{m,s}$  increases. From the residual life theorem [42], the mean value of the first microcell residence time increases as  $V_{m,s}$  increases, which implies that more calls will complete in the first microcell before they are handed off to the next cells. Therefore, both  $P_{nc}$  and  $H$  drop as  $V_{m,s}$  increases.

## 4.5 Summary

By considering the moving speeds of MSs, this study proposed the repacking on demand (RoD) approach for channel assignment in the WiMAX systems with the hierarchical cell structure (i.e., the *Hierarchical WiMAX Network*; HWN). We developed simulation models to investigate the RoD performance on the blocking probability  $P_b$ , the force-termination probability  $P_f$ , the incomplete probability  $P_{nc}$  and the expected number of handoffs  $H$  during a call (for both slow and fast calls). We compared RoD with other repacking channel assignment approaches including No Repacking (NR), Always Repacking (AR) and Partial RoD (PRoD). Our study indicated that

- If the requests for the macrocell channels can not be satisfied (e.g., when the number of the macrocell channel is small, the call arrival rate and MS mobility are high, and so on), macrocell channels are the bottleneck resources. In this case, RoD significantly reduces  $P_b$ ,  $P_f$ , and  $P_{nc}$  as compared with other approaches.
- The  $P_b$ ,  $P_f$ , and  $P_{nc}$  performance for RoD is not sensitive to the proportion of fast call arrivals as compared with other approaches. That is, the increase of fast calls does not affect RoD as much as other approaches.
- With the same  $P_{nc}$  performance, RoD can support much faster MSs and/or more call arrivals than other approaches.
- In RoD, Random RoD (RoD-R) and Load Balancing RoD (RoD-L) have the same  $P_b$ ,  $P_f$ , and  $P_{nc}$  performance. Note that in repacking, macrocell is a resource pool used to adjust traffic load of each microcell. That is, repacking already conducts the load balancing function to effectively balance the system workload, and the load-balancing improvement by RoD-L becomes insignificant. Therefore, the performance resulted from random selection for repacking candidates (i.e., RoD-R) is similar to that for RoD-L. This result is very important for network operators because RoD-R is much easier to implement than RoD-L.

# Chapter 5

## Conclusions and Future Work

This dissertation investigated the mobility management issue for WiMAX in two aspects: *location management* and *handoff management*. For location management issue, we investigated the performance for the WiMAX location tracking mechanisms with overlapping *Location Area* (LA) configuration. For handoff management, we studied the efficient channel assignment schemes for the *Hierarchical WiMAX Networks* (HWNs) to support higher MS mobility. This chapter concludes our work in Section 5.1, and briefly discusses future direction of our study in Section 5.2.

### 5.1 Concluding Remarks

Chapters 2 and 3 investigated the performance of location tracking mechanisms for mobile networks. In Chapter 2, we studied the *Location Update* (LU) performance with overlapping *Location Area* (LA) configuration to reduce the LU traffic caused by the ping-pong effect. In the overlapping LA configuration, an LA selection policy is required to select the new LA at an LU when the MS enters a new cell covered by multiple LAs. We described four LA selection policies and proposed an analytic model to study the performance of these LA selection policies. Our study provides guidelines to determine appropriate degree of overlapping among the LAs.

In Chapter 3, we investigated the performance of the WiMAX LU procedure. In WiMAX systems, an *Anchor Paging Controller* (APC) is assigned to an MS to handle



location tracking for the MS. During LU procedure, the WiMAX network may or may not relocate the APC for MS mobility. We proposed an analytic model to study the performance of the LU procedure with/without APC relocation. The analytic results provide guidelines to activate the APC relocation mechanism for MSs with various moving behaviors.

In Chapter 4, we proposed *Repacking on Demand* (RoD) for the *Hierarchical WiMAX Networks* (HWNs) by considering the moving speeds of *Mobile Stations* (MSs) to improve system performance. A simulation model was proposed to investigate the system performance on the blocking probability, the force-termination probability, the incomplete probability and the expected number of handoffs during a call (for both slow and fast calls). We compared RoD with other repacking approaches including *No Repacking* (NR), *Always Repacking* (AR) and *Partial RoD* (PRoD). Our study quantitatively shows that RoD is less sensitive to MS moving speeds and significantly outperforms these previous proposed approaches.

## 5.2 Future Work

Based on our study in this dissertation, the following mobility management issues can be further investigated.

**Location Management:** We will further study the performance for mobility management issue in two aspects.

- (1) We will extend our analytic models for two-dimensional network topology. In this dissertation, we have proposed an analytic model to investigate the LU performance for one-dimensional overlapping LA configuration. For the two-dimensional overlapping LA configuration, most entrance cells are covered by multiple LAs, and the utilization of the LA selection policies dominates the LU performance. We will extend our study to investigate the performance for

these selection policies for two-dimensional configuration.

Similarly, we will extend our analytic model to study the LU performance with/without APC relocation in WiMAX systems for two-dimensional network topology. Besides the LU cost, we can also take the costs for the other WiMAX idle mode procedures (i.e., *paging* procedure, LU procedure with *Foreign Agent relocation* and *idle mode exit* procedure) into our consideration.

- (2) There exist several design alternatives for *Tracking Area* (TA) deployment in *Long Term Evolution* (LTE), including *overlapping TAs*, *hierarchical TAs*, *dynamically defined user-specific TAs*, etc. We can propose analytic models to investigate the performance for these TA deployment designs. Besides, we may propose some adaptive algorithms for these designs, such as to dynamically define the user-specific TAs, to decide the levels for hierarchical TAs, or to switch the registration level between hierarchical TAs, etc. Moreover, an LTE MS can be assigned to multiple TAs. Based on the feature, we can further study some algorithms such as how to adjust the number of registered TAs, how to select a group of TAs to register, which previously registered TA should be replaced, and so on.

**Handoff Management:** The RoD scheme will be extended for the packet data transmission. In this dissertation, we have studied the RoD performance for the normal call service. For the data services, the *Quality of Service* (QoS) should be taken into consideration, where the higher QoS levels trivially represent the higher serving priorities. Moreover, an MS can access multiple data services at the same time, and multiple channels can even be assigned for an MS or for a service. These features might imply the different channel allocation and handoff behaviors. The RoD channel assignment procedure will be modified to accommodate the packet data services.

# Appendix A

## An OSA Application Server for Mobile Services

*Open Service Access* (OSA) is a flexible and efficient approach for mobile service deployment. In OSA, network functionality offered to *Application Servers* (AS) is defined by a set of *Service Capability Features* (SCF). The AS implements services by accessing the *Service Capability* (SC) through the standardized OSA *Application Programming Interface* (API). Before accessing an SC, and the applications should be authenticated and authorized by the *Framework* (FW). With this environment, the service developers are not required to access the details of the underlying mobile network, and thus the service deployment can be sped up. This chapter proposes an AS common architecture. We show how the AS provides services by integrating the services supported by the SCFs. Then we use the *Push to Talk over Cellular* (PoC) service to illustrate the interaction among the AS modules and how the AS interacts with the SCFs.

### A.1 Open Service Access (OSA)

Traditional telecommunication services built by *Intelligent Network* (IN) technology are considered as a part of network operation's domain. As Internet and mobility are introduced to the telecommunications environment, it is essential to provide more flexible and efficient approaches for mobile service development and deployment. To meet these

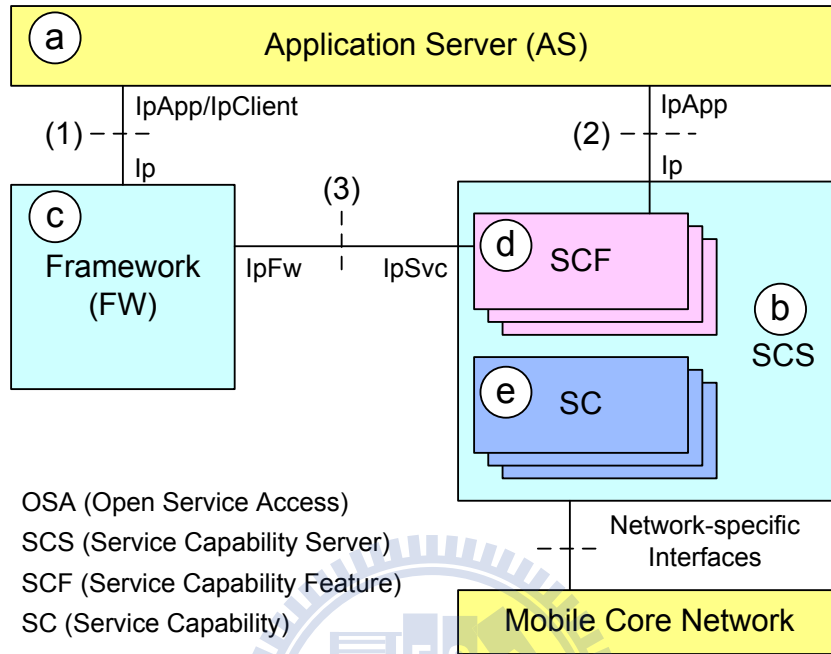


Figure A.1: OSA Architecture

goals, *Open Service Access* (OSA) has been defined by the standardization bodies such as 3GPP CN5, ETSI SPAN12, ITU-T SG11 and the Parlay Group [52]. OSA provides service creation and execution environment independent from the underlying mobile network technologies through the standardized *Application Programming Interfaces* (APIs). With this environment, the service developers are not required to access the details of the underlying mobile network, and thus the service deployment can be sped up.

The OSA architecture consists of three parts: *Application Server* (AS; Figure A.1(a)), *Service Capability Servers* (SCS; Figure A.1 (b)) and *Framework* (FW; Figure A.1 (c)). Through the AS, an application provides services by invoking SCS. Before accessing an SCS, the application should be authorized by the FW. The SCS contains two components: *Service Capability Feature* (SCF; Figure A.1 (d)) and *Service Capability* (SC; Figure A.1 (e)). An SCF, specified in terms of interface classes and their methods (i.e., OSA API), are offered by an SC. The SC realizes the service and potentially interacts with the mobile core network.

The FW is considered as one of the SCSs, and is always present, one per network. The FW provides access control functions to authorize the access to SCFs invoked by an application. Before any application can interact with a network SCF, mutual authentication would be performed between the application and the FW. Then the application can be authorized by the FW to access a specific SCF. Finally, the application can use FW *discovery* function to obtain information on authorized network SCFs. Note that SCFs offered by an SCS are typically registered at the FW, and their information is retrieved when the application invokes the discovery function. The FW allows OSA to go beyond traditional IN technology through openness, discovery, and integration of new features.

Three classes of OSA APIs are defined among the AS, the FW, and the SCFs.

- Interfaces between the AS and the FW (Figure A.1 (1)) provide authentication, network functionality discovery, and service agreement establishment mechanisms that enable the AS to access the SCSs. The FW-side interfaces to be invoked by the AS are prefixed with “Ip”. The AS-side interfaces to be called back by the FW are prefixed with “IpApp” or “IpClient”.
- Interfaces between the AS and the SCFs (Figure A.1 (2)) allow the AS to invoke network functionality for services. The SCF-side interfaces to be invoked by the AS are prefixed with “Ip”. The AS-side interfaces to be called back by the SCFs are prefixed with “IpApp”.
- Interfaces between the FW and the SCFs (Figure A.1 (3)) provide the mechanisms for SCF registration. The FW-side interfaces to be invoked by the SCFs are prefixed with “IpFw”. The SCF-side interfaces to be called by the FW are prefixed with “IpSvc”.

As mentioned above, the OSA APIs are separated into two parts. The SCSs (and the FW) implement the OSA server side of the APIs and the applications implement the OSA client side of the APIs. An application should communicate with an SCS through

standard IT middleware infrastructure such as *Common Object Request Broker Architecture* (CORBA) [60]. Our previous study [17] designs and develops a CORBA-based OSA platform, through which we also show how OSA API interfaces and functions can be implemented by CORBA. The readers can refer it for more details.

The SCS provides two methods for processing requests: synchronous and asynchronous methods. If the AS invokes a synchronous function (e.g., **createCall** that creates a call object in the SCS), the results are returned through this function call. If the AS invokes an asynchronous function (e.g., **createMediaNotification** that asks for notifications when specific events occur), the SCS needs to interact with the core network, and therefore can not produce the results immediately. In this case, the SCS returns an acknowledgement to the AS. This acknowledgement indicates that the requested action is being processed by the SCS. When the results are available, the core network issues an event to the SCS. Then the SCS invokes the corresponding callback function to pass the results to the AS.

This chapter proposes an AS architecture and uses the *Push to Talk over Cellular* (PoC) service as an example to illustrate how the AS interacts with the SCFs. The PoC service is a walkie-talkie like service defined by the OMA PoC working group [58]. A PoC session consists of connections among the participants defined in a PoC group. The session is half duplex; that is, at any time, only one participant can speak and all other participants can only listen. When two or more participants attempt to speak, they are arbitrated by a centralized floor control mechanism to select a speaker. In current OMA PoC v2.0 release specification [57], *Session Initiation Protocol* (SIP) is used for session management [63] and both *Real-Time Transport Protocol* (RTP) and *Real-Time Transport Control Protocol* (RTCP) are used for media streams transport and control [65].

A PoC group is a predefined set of participative members. The addresses of these members are maintained in the group member list. The attributes of a PoC group include the display name (the nickname for the group), PoC address (the identifier of the PoC group), etc. There are two alternatives to specify a PoC address: a *Telephone*

*Uniform Resource Identifier* (TEL URI; e.g., **tel:+886-3-5131350**) or a *SIP URI* (e.g., **sip:poc\_Lab117@pcs1.csie.nctu.edu.tw**). The group member list and the group attributes are maintained in the *Group and List Management Server* (GLMS) [56]. Note that, in OMA PoC v2.0 release specification [57], the GLMS server has been replaced by two components: *shared XML Document Management Servers* (XDMSs) and *aggregation proxy*. The shared XDMSs manage user information (e.g., phone book), the group member list and the group attributes. The aggregation proxy is the contact point for the PoC participants to access the XDMSs, and the PoC participants should be authenticated by the aggregation proxy.

In this chapter, we first propose the AS common architecture in Section A.2. Then based on the AS architecture, we describe the PoC session establishment and termination in Section A.3.

## A.2 Application Server Architecture

This section describes the proposed AS architecture with six modules (see Figure A.2).

- An appService module (Figure A.2 (a)) implements services by accessing SCF through the “**Ip**” interfaces. Furthermore, it generates the interface objects in the corresponding appService callback module (to be elaborated at Steps 2, 8, 9 and 22 in Figure A.4, Section A.3) and passes the references of these objects as the callback references to the SCFs.
- The appService callback module (Figure A.2 (b)) provides the “**IpApp**” and “**Ip-Client**” callback interfaces to the SCFs/FW. Through these interfaces, the AS can receive specific events from the SCFs/FW. Upon receipt of the events, the appService callback module stores them in the AS database and may inform the appService module to handle the events. For each SCF, there exists one appService module and one appService callback module in our AS design.

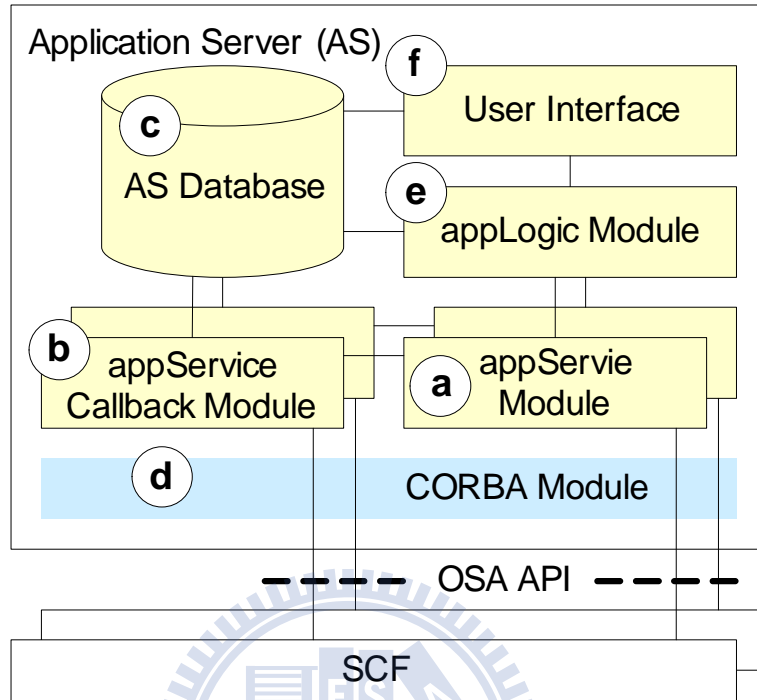


Figure A.2: Application Server Architecture

- The AS database (Figure A.2 (c)) stores the event information to be accessed by other modules. The information includes the list of the authorized SCFs, the events received from the SCFs, the log file of the AS, etc.
- The CORBA module (Figure A.2 (d)) is an emerging open distributed object computing infrastructure. It provides the higher layers (i.e., other AS modules) a uniform view of underlying heterogeneous network [60, 17].
- The appLogic module (Figure A.2 (e)) implements the logic of an AS application. It integrates services supported by different SCFs and the FW through appService modules without directly accessing the CORBA module and OSA interfaces.
- The user interface module (Figure A.2 (f)) provides interfaces to monitor the AS operations, obtain the records stored in the AS database, and invoke the services offered by the SCFs.



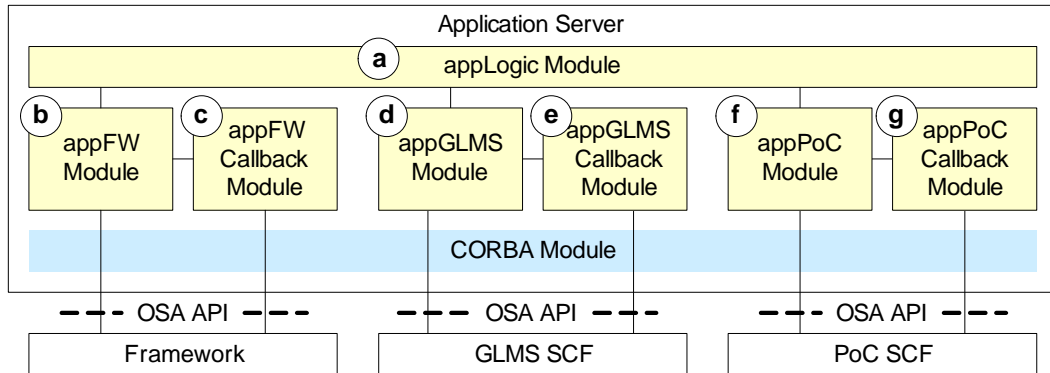


Figure A.3: Application Server Architecture for PoC Service

To offer the PoC service, the AS first accesses the FW, and then communicates with two SCFs: PoC SCF and GLMS SCF. The PoC SCF provides methods to create and control PoC sessions. The GLMS SCF supports methods to retrieve and manage user and group information stored in the GLMS server. The relationship among the FW, SCFs and the AS modules is illustrated in Figure A.3.

- The appLogic module (Figure A.3 (a)) implements the PoC service by integrating the services supported by the FW, the PoC SCF, and the GLMS SCF.
- The appFW module (Figure A.3 (b)) accesses the FW to execute the authentication, service discovery, and service agreement establishment procedures.
- The appFW callback module (Figure A.3 (c)) provides interfaces to be called back by the FW. Details of these callback interfaces can be found in [3].
- The appGLMS module (Figure A.3 (d)) accesses the GLMS server through the GLMS SCF.
- The appGLMS callback module (Figure A.3 (e)) provides callback interfaces to the GLMS SCF. Through these interfaces, the GLMS SCF can pass the results to the AS after accessing the GLMS server.

- The appPoC module (Figure A.3 (f)) manages and establishes the PoC sessions by accessing the PoC SCF.
- The appPoC callback module (Figure A.3 (g)) provides callback interfaces. The PoC SCF uses these interfaces to report specific events to the AS. In our implementation, three callback interfaces are provided. The **IpAppPoCCallControlManager** interface provides the management functions for PoC service (see Steps 6, 19, and 30 in Figure A.4). The **IpAppPoCCall** interface provides the PoC SCF with the control management functions for PoC sessions (see Step 4 in Figure A.5). The **IpAppPoCCallLeg** interface is used to receive specific events of group members from the PoC SCF (see Step 26 in Figure A.4 and Step 1 in Figure A.5).

PoC session establishment consists of four stages:

**Stage 1.** The appLogic module accesses the FW to perform mutual authentication, service discovery, and service agreement establishment through appFw and appFw callback modules. The readers can refer to our studies [17, 31] for more details about the OSA mutual authentication. After this stage, the AS obtains the object references for the PoC SCF and the GLMS SCF.

**Stage 2.** The appLogic module requests the appPoC callback module to provide the callback interface **IpAppPoCCallControlManager** through the appPoC module. With this callback interface, the PoC SCF notifies the appLogic module when a PoC session request occurs. The details are described in Section A.3.

**Stage 3.** When receiving a request, the appLogic module retrieves the group member list by accessing the GLMS SCF through the appGLMS and the appGLMS callback modules or by accessing the AS database.

**Stage 4.** After the group member list is obtained, the appLogic module establishes the PoC session for members in the list through the appPoC and the appPoC callback

modules. The details are described in Section A.3.

### A.3 PoC Session Establishment

In our OSA-based PoC design, the AS first sets up the callback interface **IpAppPoCCallControlManager** (see Steps 1 - 3 in Figure A.4) and subscribes notifications for specific PoC-related events from the PoC SCF (see Steps 4 and 5 in Figure A.4). With this subscription, when a PoC event (e.g., PoC session establishment request) occurs at the SCS, a notification will be sent to the AS. When receiving an event notification from the PoC SCF (see Step 6 in Figure A.4), the AS starts to initiate a PoC session. In the following example, a PoC session for PoC group with the display name “**Lab117**” is requested to be established. This group is identified by the SIP URI “**sip:poc\_Lab117@pcs1.csie.nctu.edu.tw**”, which contains two members: party A and party B. The PoC session establishment procedure is described in the following steps (see Figure A.4).

**Step 1.** The AS control logic **appLogic** invokes **appPoC** function **setCallbackForIpAppPoCCallControlManager**. This function instructs **appPoC** to generate the **IpAppPoCCallControlManager** interface object and to pass the object reference to the PoC SCF. The **IpAppPoCCallControlManager** interface provides management functions for PoC service (e.g., function **reportMediaNotificationWithGroupID** invoked at Step 6, function **initiatePoCCallWithMediaRes** invoked at Step 19, and function **addMemberRes** invoked at Step 30).

**Step 2.** **appPoC** creates the **IpAppPoCCallControlManager** object to provide the callback functions to be called by the PoC SCF.

**Step 3.** **appPoC** invokes function **setCallback** to pass the reference of **IpAppPoCCallControlManager** to the PoC SCF. Through this reference, the PoC SCF invokes the callback functions at Steps 6, 19, and 30.

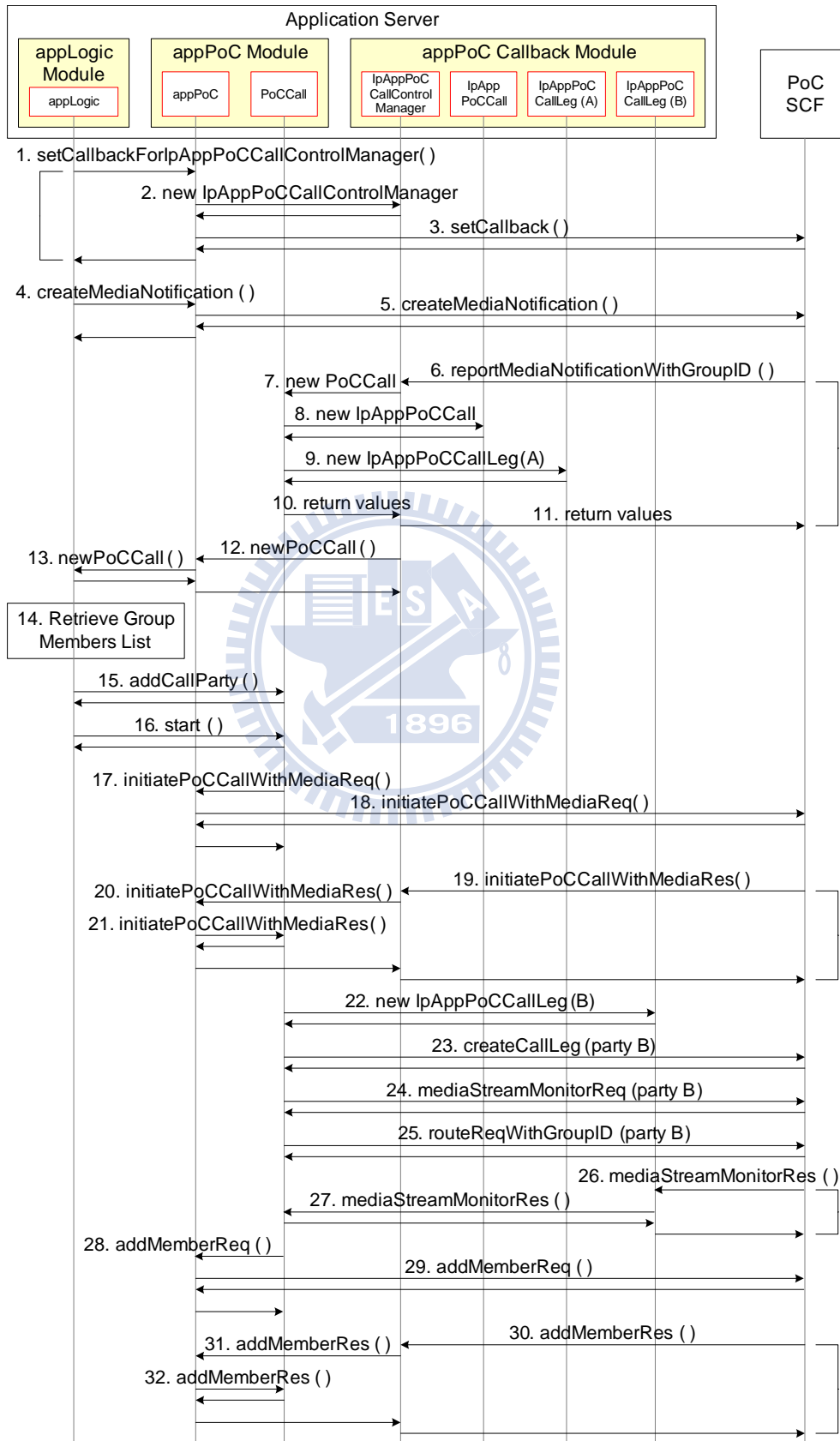


Figure A.4: Message Flow for PoC Session Establishment

**Steps 4 and 5.** **appLogic** invokes the PoC SCF function **createMediaNotification** through **appPoC** to request notifications for specific PoC-related events (e.g., the PoC SCF receives a session request for a PoC group).

**Step 6.** Suppose that PoC party A attempts to establish a PoC session with group **Lab117** that has the SIP URI “**sip:poc\_Lab117@pcs1.csie.nctu.edu.tw**”. The PoC SCF invokes the callback function **reportMediaNotificationWithGroupID** to notify the AS of this PoC session request. This notification includes the media stream information for party A (e.g., codec, the algorithm for compressing and decompressing voice information, such as G.711, G.723, etc) and the SIP URIs of both party A and group **Lab117**.

**Step 7.** **IpAppPoCCallControlManager** creates the **PoCCall** object to store information associated with this new PoC session (e.g., SIP URIs of the PoC group and group members, media stream information, the interface object references related to this session in both the PoC SCF and the AS, etc).

**Steps 8 and 9.** **PoCCall** generates the **IpAppPoCCall** object and the **IpAppPoCCallLeg** object for party A (i.e., **IpAppPoCCallLeg (A)** in Figures A.4 and A.5). **IpAppPoCCall** provides the PoC SCF with the session control management functions (e.g., function **callEnded** invoked at Step 4 in Figure A.5). **IpAppPoCCallLeg (A)** is used to receive specific events of party A from the PoC SCF.

**Steps 10 and 11.** Both interface object references generated at Steps 8 and 9 are stored in **PoCCall** and passed back to the PoC SCF as the return values of function **reportMediaNotificationWithGroupID** invoked at Step 6.

**Steps 12 and 13.** **IpAppPoCCallControlManager** invokes function **newPoCCall** through **appPoC** to notify **appLogic** of the PoC session request.

**Step 14.** **appLogic** retrieves the group member list of the requested group **Lab117**.

The list can be obtained from the GLMS server through the GLMS SCF or from the AS database.

**Step 15.** After the group member list (i.e., SIP URIs of party A and party B) is obtained, **appLogic** stores it in **PoCCall** through function **addCallParty**.

**Step 16.** **appLogic** invokes the **PoCCall** function **start** to establish the PoC session.

**Steps 17 and 18.** **PoCCall** invokes the PoC SCF function **initiatePoCCallWithMediaReq** through **appPoC**. This function asks the PoC SCF to reserve resources for the PoC session and party A; e.g., reserve a RTP port to transmit media streams to party A.

**Steps 19 - 21.** When the resources for the PoC session and party A are reserved, PoC SCF invokes the callback function **initiatePoCCallWithMediaRes** through the **IpAppPoCCallControlManager** and **appPoC** to inform **PoCCall** that the resources are reserved successfully.

**Step 22.** **PoCCall** generates the **IpAppPoCCallLeg** object for party B (i.e., **IpAppPoCCallLeg (B)** in Figures A.4 and A.5). This object is used to receive party B related events from the PoC SCF (e.g., function **callLegEnded** invoked at Step 1 in Figure A.5 ).

**Step 23.** **PoCCall** invokes function **createCallLeg** and passes the callback reference of **IpAppPoCCallLeg (B)** to the PoC SCF.

**Step 24.** **PoCCall** invokes the PoC SCF function **mediaStreamMonitorReq**. This function requests the PoC SCF to report the media stream information of party B to the AS when party B joins in the PoC session (see Steps 26 and 27).

**Step 25.** To invite party B to join in the session, **PoCCall** invokes the PoC SCF function **routeReqWithGroupID**. This function requests the PoC SCF to deliver the invite

message to party B.

**Steps 26 and 27.** When party B joins in the session, the media stream information of party B is passed to the PoC SCF. The PoC SCF invokes the callback function **mediaStreamMonitorRes** through **IpAppPoCCallLeg (B)** to notify **PoCCall** about the media stream information for party B.

**Steps 28 and 29.** **PoCCall** invokes the PoC SCF function **addMemberReq** through **appPoC** to reserve resources for party B; e.g., a RTP port to transmit media streams to party B.

**Steps 30 - 32.** The PoC SCF invokes the callback function **addMemberRes** through **IpAppPoCCallControlManager** and **appPoC** to inform **PoCCall** that the resources have been reserved for party B.

At this moment, the PoC session is successfully established for parties A and B. To end a PoC session, the PoC session termination procedure is executed (Figure A.5). The details are given below.

**Steps 1 and 2.** When party B leaves the PoC session, the PoC SCF invokes callback function **callLegEnded** through **IpAppPoCCallLeg (B)** to notify **PoCCall** that party B has left.

**Step 3.** **PoCCall** invokes the function **destroy** of **IpAppPoCCallLeg (B)** to destroy this object.

**Steps 4 and 5.** When the last party leaves the session (i.e., party A in this example), the PoC SCF invokes the callback function **callEnded** through **IpAppPoCCall** to notify **PoCCall** of the leaving for the last party.

**Steps 6 and 7.** Since all call parties have left, **PoCCall** invokes functions **destroy** of both **IpAppPoCCallLeg (A)** and **IpAppPoCCall** to destroy these objects.

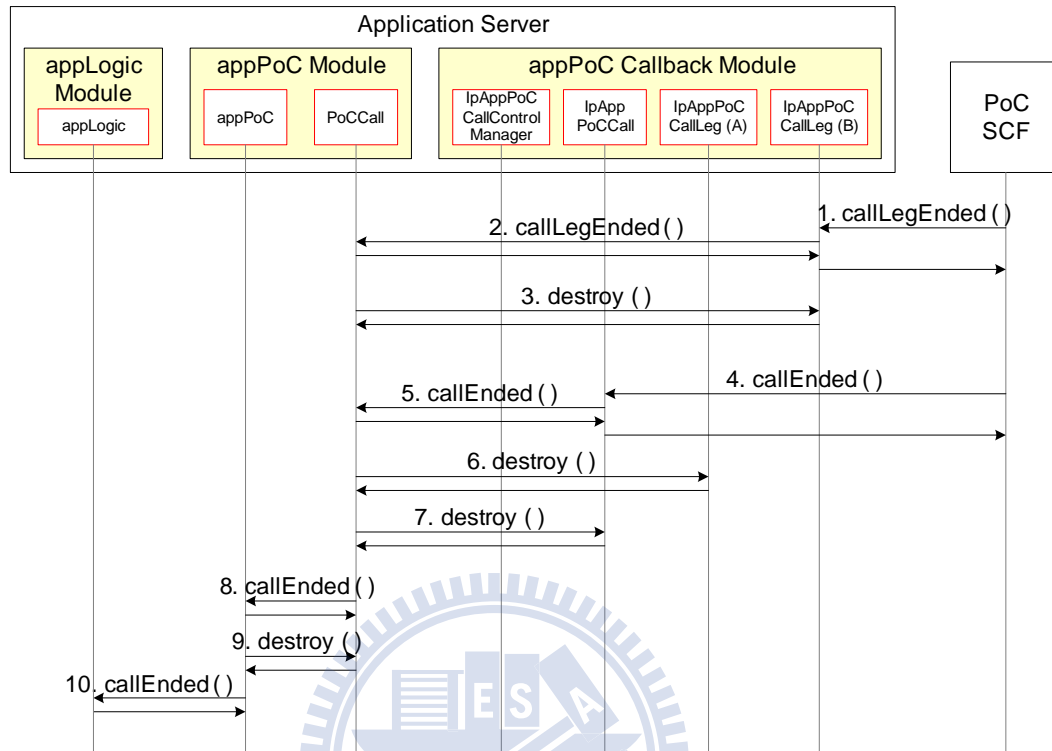


Figure A.5: Message Flow for PoC Session Termination

**Step 8.** **PoCCall** invokes the **appPoC** function **callEnded** to notify the end of the PoC session.

**Step 9.** **appPoC** invokes the **PoCCall** function **destroy** to delete this **PoCCall** object.

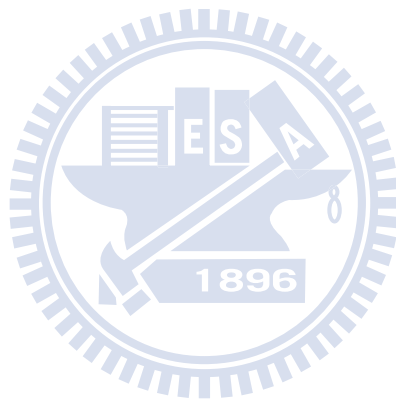
**Step 10.** **appPoC** invokes the **appLogic** function **callEnded** to notify the end of the PoC session.

## A.4 Summary

This chapter proposed an OSA Application Server (AS) architecture. Based on this architecture, a new application is created by implementing the appLogic module that invokes the SCFs through the appService modules and appService callback modules. To interact with an SCF, the AS implements one appService module and one appService callback module for that SCF. When the existing SCFs are reused for new services, the



corresponding appService and appService callback modules for accessing these SCFs can also be reused. Through this modularized AS design, the service deployment can be sped up. We used the PoC service to illustrate the interaction within the AS modules and how the AS interacts with the service SCF.



# Appendix B

## Simulation Model For Speed-Sensitive RoD-R

This appendix describes the discrete event simulation model for RoD-R. In this model, three types of events are defined to represent call arrival, call completion, and MS movement. The following attributes are defined for an event  $e$ :

- The **type** attribute indicates the event type. An **Arrival** event represents a new call arrival. A **Move** event represents an MS movement from one cell to another. A **Complete** event represents a call completion.
- The **ts** attribute indicates the time when the event occurs.
- The **tc** attribute indicates the time when the call corresponding to  $e$  will complete. Note that  $tc \geq ts$ .
- The **mc** attribute indicates the microcell where the MS (corresponding to this event) resides.
- The **ma** attribute indicates the macrocell where the MS (corresponding to this event) resides.
- The **speed** attribute indicates the moving speed (i.e., *Slow* or *Fast*) of the MS (corresponding to this event).

- The **is\_macro** attribute indicates whether the call corresponding to this event occupies a macrocell channel. If a macrocell channel is occupied, **is\_macro** = 1. Otherwise, **is\_macro** = 0.

In the simulation model, an array  $mc\_ch[i]$  is used to represent the number of the idle channels of microcell  $i$ . Another array  $ma\_ch[j]$  is used to represent the number of the idle channels of macrocell  $j$ . Two variables  $new\_mc$  and  $new\_ma$  are used to indicate the target micro and macro cells where the call (corresponding to current event) is newly generated from or handed off to. The output measures of the simulation are the number  $N$  of total call arrivals during the simulation, the number  $N_b$  of blocked calls, the number  $N_f$  of force-terminated calls, the number  $N_R$  of repackings, the number  $N_h$  of handoffs, the number  $N_{sf}$  of successfully connected fast calls, and the number  $N_{ff}$  of force-terminated fast calls. From the above output measures, we can compute

$$\begin{aligned}
 P_b &= \frac{N_b}{N}, & P_f &= \frac{N_f}{N - N_b}, & P_{nc} &= \frac{N_b + N_f}{N}, \\
 P_{ff} &= \frac{N_{ff}}{N_{sf}}, & H_R &= \frac{N_R}{N - N_b} & \text{and} & H &= \frac{N_h}{N - N_b}.
 \end{aligned} \tag{B.1}$$

A simulation clock is maintained to indicate the simulation progress, which is the timestamp of the event being processed. All events are inserted into the event list, and are deleted/processed from the event list in the non-decreasing timestamp order. Figures B.1 and B.2 show the simulation flow chart for RoD-R. In this flow chart, Step 1.1 initializes the input parameters. Step 1.2 generates the first **Arrival** events for each microcell and inserts these events into the event list. In Steps 1.3 and 1.4, the next event  $\mathbf{e}$  in the event list is processed based on its type. There are three cases:

**Case I.  $\mathbf{e.type=Arrival}$ :** At Step 1.5, if  $N - N_b > N^*$  (in our simulation,  $N^* = 6 \times 10^5 \times 64$ ), then Step 1.6 computes the output measures using (B.1), and the simulation terminates. Otherwise, Step 1.7 generates the next **Arrival** event  $\mathbf{e}_1$  for the same microcell (i.e.,  $\mathbf{e}_1.mc=\mathbf{e}.mc$ ,  $\mathbf{e}_1.ma=\mathbf{e}.ma$ ,  $\mathbf{e}_1.speed=\mathbf{e}.speed$  and  $\mathbf{e}_1.is\_macro=0$ ),

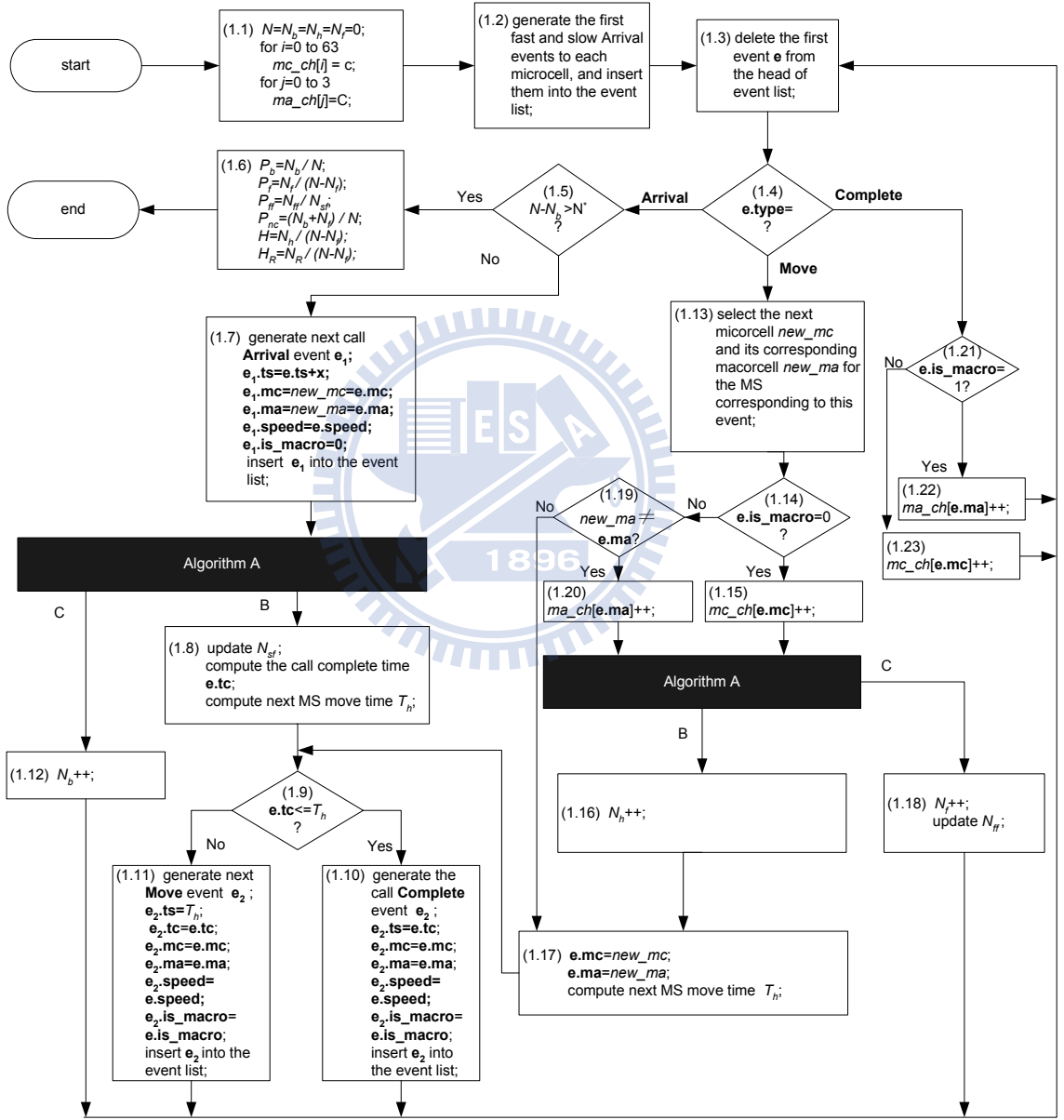


Figure B.1: Simulation Flow Chart for RoD-R

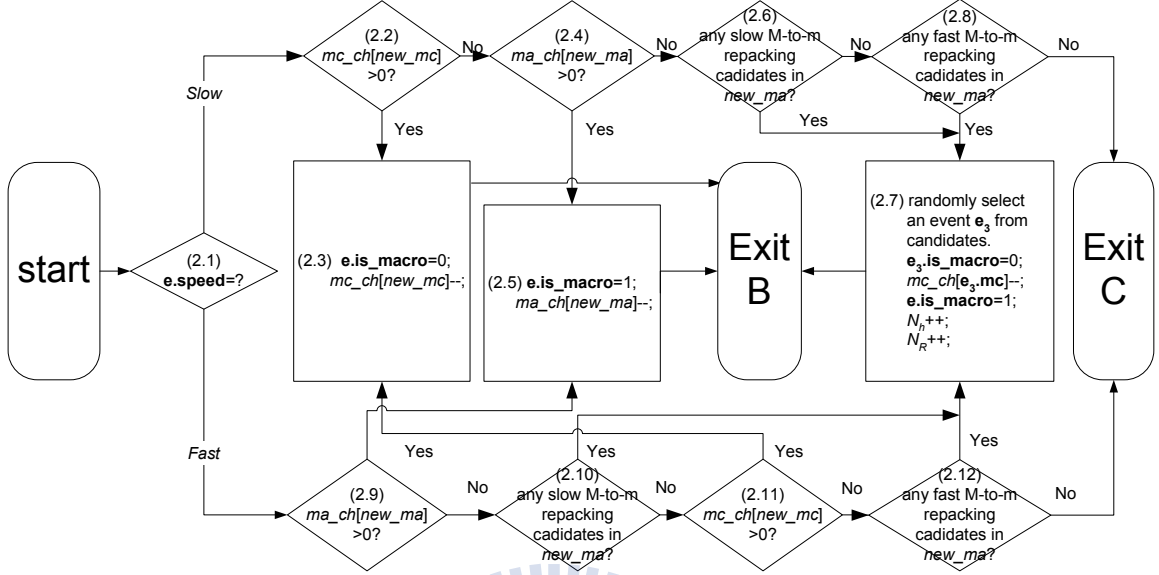


Figure B.2: Flow Chart of Algorithm A

and sets the target cell where the incoming call arrives ( $new\_mc = \mathbf{e.mc}$  and  $new\_ma = \mathbf{e.ma}$ ). The timestamp of  $\mathbf{e}_1$  equals  $\mathbf{e.ts}$  plus the inter call arrival time generated by a random number generator. Then  $\mathbf{e}_1$  is inserted into the event list, and the simulation proceeds to execute *Algorithm A* in Figure B.2.

In *Algorithm A* (see Figure B.2), the HCN tries to allocate a channel for the call. The steps are described as follows. If  $\mathbf{e.speed} = Slow$  at Step 2.1, Step 2.2 checks if microcell  $new\_mc$  has idle channels (i.e.,  $mc\_ch[new\_mc] > 0$ ). If so, a channel is assigned to the incoming call. Then  $mc\_ch[new\_mc]$  is decremented by 1 at Step 2.3 and this algorithm terminates at exit B (i.e., the call is assigned a channel). At Step 2.2, if microcell  $new\_mc$  has no idle channel (i.e.,  $mc\_ch[new\_mc] = 0$ ), the call attempt overflows to macrocell  $new\_ma$ . Then Step 2.4 checks if macrocell  $new\_ma$  has idle channels (i.e.,  $ma\_ch[new\_ma] > 0$ ). If so, a macrocell channel is assigned to the call at Step 2.5. In this case,  $ma\_ch[new\_ma]$  is decremented by 1, and  $\mathbf{e.is\_macro}$  is set to 1. Then this algorithm terminates at exit B. If macrocell  $new\_ma$  has no idle channel (i.e.,  $ma\_ch[new\_ma] = 0$ ) at Step 2.4, then Step 2.6 checks if there is any slow M-to-m repacking candidate in macrocell  $new\_ma$ .

If so, Step 2.7 randomly selects a slow M-to-m repacking candidate (i.e., a call corresponding to a **Complete** or **Move** event  $\mathbf{e}_3$ ) to be handed off from macrocell  $new\_ma$  to microcell  $\mathbf{e}_3.\mathbf{mc}$  (i.e.,  $\mathbf{e}_3.\mathbf{is\_macro}$  is set to 0), and the reclaimed macrocell channel is assigned to the incoming call (i.e.,  $\mathbf{e}.\mathbf{is\_macro}$  is set to 1). Step 2.7 also decrements  $mc\_ch[\mathbf{e}_3.\mathbf{mc}]$  by 1, and increments both  $N_R$  and  $N_h$  by 1. Then this algorithm terminates at exit B. If no slow M-to-m repacking candidate is found at Step 2.6, Step 2.8 checks if there is any fast M-to-m repacking candidate in macrocell  $new\_ma$ . If so, Step 2.7 is executed to randomly select a fast M-to-m repacking candidate, and this algorithm terminates at exit B. Otherwise, if no fast M-to-m repacking candidate is found at Step 2.8, the incoming call is not assigned any idle channel. In this case, this algorithm terminates at exit C (i.e., no channel is assigned to the call).

For the case of  $\mathbf{e}.\mathbf{speed} = Fast$  at Step 2.1, Step 2.9 checks if macrocell  $new\_ma$  has idle channels (i.e.,  $ma\_ch[new\_ma] > 0$ ). If so, Step 2.5 is executed, and the algorithm terminates at exit B. Otherwise, Step 2.10 checks if there is any slow M-to-m repacking candidate in macrocell  $new\_ma$ . If so, Step 2.7 is executed, and this algorithm terminates at exit B. If no slow M-to-m repacking candidates are found in macrocell  $new\_ma$ , then Step 2.11 checks if microcell  $new\_mc$  has idle channels (i.e.,  $mc\_ch[new\_mc] > 0$ ). If so, Step 2.3 is executed, and this algorithm terminates at exit B. If microcell  $new\_mc$  has no idle channel at Step 2.11, Step 2.12 checks if there is any fast M-to-m repacking candidate in macrocell  $new\_ma$ . If so, Step 2.7 is executed, and this algorithm terminates at exit B. Otherwise, the incoming call is not assigned any idle channel, and the this algorithm terminates at exit C.

If any channel is assigned to the incoming call in Figure B.2 (i.e., *Algorithm A* exits from B), Step 1.8 updates the  $N_{sf}$  value (i.e., if this is a fast call, increment  $N_{sf}$  by 1). Step 1.8 then computes the call completion time  $\mathbf{e}.\mathbf{tc}$  as  $\mathbf{e}.\mathbf{ts}$  plus the call

holding time. Step 1.8 also determines the MS move time  $T_h$  when the MS moves out of the microcell.  $T_h$  equals  $\mathbf{e.ts}$  plus the cell residence time. Then Step 1.9 determines the next event (i.e., a **Move** event or **Complete** event) for the call corresponding to  $\mathbf{e}$ . If the MS will move to another cell after call completion (i.e.,  $\mathbf{e.tc} \leq T_h$ ), then Step 1.10 is executed to generate a **Complete** event  $\mathbf{e}_2$  where  $\mathbf{e}_2.ts = \mathbf{e.tc}$ ,  $\mathbf{e}_2.mc = \mathbf{e.mc}$ ,  $\mathbf{e}_2.ma = \mathbf{e.ma}$ ,  $\mathbf{e}_2.speed = \mathbf{e.speed}$  and  $\mathbf{e}_2.is\_macro = \mathbf{e.is\_macro}$ . Event  $\mathbf{e}_2$  is inserted into the event list. Otherwise, if the MS moves to another cell before the call completion (i.e.,  $\mathbf{e.tc} > T_h$ ) at Step 1.9, then Step 1.11 is executed to generate the next **Move** event  $\mathbf{e}_2$  with the timestamp  $T_h$  for this call (i.e.,  $\mathbf{e}_2.ts = T_h$ ,  $\mathbf{e}_2.tc = \mathbf{e.tc}$ ,  $\mathbf{e}_2.mc = \mathbf{e.mc}$ ,  $\mathbf{e}_2.ma = \mathbf{e.ma}$ ,  $\mathbf{e}_2.speed = \mathbf{e.speed}$  and  $\mathbf{e}_2.is\_macro = \mathbf{e.is\_macro}$ ). Event  $\mathbf{e}_2$  is inserted into the event list. On the other hand, if HCN has no idle channel for the incoming call (i.e., *Algorithm A* exits from C), the incoming call is blocked and  $N_b$  is incremented by 1 at Step 1.12.

**Case II.  $\mathbf{e.type}=\text{Move}$ :** Step 1.13 selects the next microcell  $new\_mc$  and its macrocell  $new\_ma$  for the MS corresponding to event  $\mathbf{e}$ . At Step 1.14, if the call of the MS occupies a microcell channel (i.e.,  $\mathbf{e.is\_macro} = 0$ ), the occupied channel of microcell  $\mathbf{e.mc}$  is released ( $mc\_ch[\mathbf{e.mc}]$  is incremented by 1 at Step 1.15). Then the HCN tries to allocate a channel for the call, and the simulation proceeds to execute *Algorithm A* in Figure B.2 as described in **Arrival** event. If the handoff call is assigned a channel (i.e., *Algorithm A* exits from B),  $N_h$  is incremented by 1 at Step 1.16. Step 1.17 updates the current cell for the call (i.e.,  $\mathbf{e.mc} = new\_mc$  and  $\mathbf{e.ma} = new\_ma$ ) and computes the next MS move time  $T_h$  for the call. Then the simulation proceeds to execute Steps 1.9 and 1.10 (or 1.11). On the other hand, if HCN has no idle channel for the call (i.e., *Algorithm A* exits from C), the call is forced to terminate. Then Step 1.18 is executed to increment  $N_f$  by 1 and update the  $N_{ff}$  value (i.e., if this is a fast call, increment  $N_{ff}$  by 1).

If the call occupies a macrocell channel at Step 1.14, then Step 1.19 checks if the MS is moving out of its macrocell  $\mathbf{e.ma}$ . If so (i.e.,  $new\_ma \neq \mathbf{e.ma}$ ), the call is handed off to the new cell. Step 1.20 increments  $ma\_ch[\mathbf{e.ma}]$  by 1; i.e., the occupied channel of  $\mathbf{e.ma}$  is released. Then the simulation proceeds to execute *Algorithm A*. If the handoff call is assigned a channel (i.e., *Algorithm A* exits from B), Steps 1.16, 1.17, 1.9 and 1.10 (or 1.11) are then executed. Otherwise, if HCN has no idle channel for the call (i.e., *Algorithm A* exits from C), Step 1.18 is then executed. If the MS does not move out of its macrocell (i.e.,  $\mathbf{e.ma} = new\_ma$ ) at Step 1.19, the simulation proceeds to execute Step 1.17 and then Steps 1.9 and 1.10 (or 1.11).

**Case III.  $\mathbf{e.type=Complete}$ :** At Step 1.21, if the call occupies a macrocell channel (i.e.,  $\mathbf{e.is\_macro} = 1$ ), then Step 1.22 is executed to increment  $ma\_ch[\mathbf{e.ma}]$  by 1. Otherwise, Step 1.23 is executed to increment  $mc\_ch[\mathbf{e.mc}]$  by 1.

To accommodate RoD-L, we only need to modify Step 2.7 of the flowchart in Figure B.2. In our simulation experiments, the confidence intervals of the 99% confidence levels are within 3% of the mean values in most cases. The simulation models are partially validated by the analytic model in [33] for the no mobility case. The details are omitted.



# Bibliography

- [1] 3GPP. 3rd Generation Partnership Project; Technical Specification Group Core Network; Open Service Access (OSA); Application Programming Interface (API); Part 1: Overview. *3GPP TS 29.198-01 V6.3.1*, 2004.
- [2] 3GPP. 3rd Generation Partnership Project; Technical Specification Group Services and System Aspects; Virtual Home Environment/OSA Service Access. *3GPP TS 23.127 V6.1.0*, 2004.
- [3] 3GPP. 3rd Generation Partnership Project; Technical Specification Group Core Network; Open Service Access (OSA); Application Programming Interface (API); Part 3: Framework. *3GPP TS 29.198-03 V6.4.0*, 2005.
- [4] 3GPP. 3rd Generation Partnership Project; Technical Specification Group Services and System Aspects; Service Requirement for the OSA Services Access (OSA); Stage 1. *3GPP TS 22.127 V7.0.0*, 2005.
- [5] 3GPP. 3rd Generation Partnership Project; Technical Specification Group Services and System Aspects; Voice Call Continuity (VCC) between Circuit Switched (CS) and IP Multimedia Subsystem (IMS); Stage 2. 2007. Technical Specification 3GPP TS 23.206 version 7.5.0.
- [6] 3GPP. 3rd Generation Partnership Project; Technical Specification Group Services and System Aspects; 3GPP System Architecture Evolution: Report on Technical Options and Conclusions (Release 8). *3GPP TR 23.882 V8.0.0*, 2008.

- [7] 3GPP. 3rd Generation Partnership Project; Technical Specification Group Services and System Aspects; General Packet Radio Service (GPRS); Service description; Stage 2 (Release 8). *3GPP TS 23.060 V8.3.0*, 2008.
- [8] Akyildiz, I.F., Jiang, X. and Mohanty, S. A Survey of Mobility Management in Next-generation All-IP-based Wireless Systems. *IEEE Wireless Communications*, 11.
- [9] Aricent Inc. WiMAX Femtocells - Whitepaper. 2009. see also [http://www.femtoforum.org/femto/Files/File/WiMAX\\_Femtocell\\_whitepaper.pdf](http://www.femtoforum.org/femto/Files/File/WiMAX_Femtocell_whitepaper.pdf).
- [10] Beraldi, R., Marano, S., and Mastroianni, C. A Reversible Heirarchical Scheme for Microcellular Systems with Overlaying Macrocells. *Proc. of IEEE Infocom*, pages 51–58, 1996.
- [11] Buchanan, K., Fudge, R., McFarlane, D., Phillips, T., Sasaki, A. and Xia, H. IMT 2000: Service providers perspective. *IEEE Personal Communications*, 4:8–13, 1997.
- [12] Chandrasekhar, V., Andrews, J. and Gatherer, A. Femtocell networks: a survey. *IEEE Communications Magazine*, 46:59–67, 2008.
- [13] Chang, K.-N., Kim, J.-T., Yim, C.-S. and Kim, S. An efficient borrowing channel assignment scheme for cellularmobile systems. *IEEE Transactions on Vehicular Technology*, 47.
- [14] Chiang, K.-H. and Shenoy, N. Performance of an Overlapped Macro-cell Based Location Area Scheme. *International Conference on Communications (ICC '03)*, 1:475–481, May 2003.
- [15] Chiang, K.-H. and Shenoy, N. A 2-D Random-Walk Mobility Model for Location-Management Studies in Wireless Networks. *IEEE Transactions on Vehicular Technology*, 53(2):413–424, 2004.

- [16] Chlamtac, I., Fang, Y., and Zeng, H. Call Blocking Analysis for PCS Networks under General Cell Residence Time. *IEEE Wireless Communications and Networking Conference (WCNC), New Orleans*, September 1999.
- [17] Chou, C.-M., Hsu, S.-F., Lee, H.-Y., Lin, Y.-C., Lin, Y.-B. and Yang, J.-S. CCL OSA: A CORBA-based Open Service Access System. *International Journal of Wireless and Mobile Computing*, 1(3/4), 2006.
- [18] Cimini, L.J., Foschini, G.J., I, C.-L. and Miljanic, Z. Call Blocking Performance of Distributed Algorithms for Dynamic Channel Allocation in Microcells. *IEEE Tran. on Comm.*, 42(8):2600–2607, August 1994.
- [19] Cognola, G., Goodey, P., Howard, R., Reeder, M. and Wang, W. Mobility Management in Next Generation Wireless Systems. *Proceedings of the IEEE*, 87(8).
- [20] Fan, G. and Zhang, J. A Multi-layer Location Management Scheme that Bridges the Best Static Scheme and the Best Dynamic Scheme. *International Conference on Mobile Data Management (MDM '04)*, pages 125–132, 2004.
- [21] Fan, G., Stojmenovic, I. and Zhang, J. A Triple Layer Location Management Strategy for Wireless Cellular Networks. *Proc. IEEE International Conference on Computer Communication and Networks*, pages 489–492, 2002.
- [22] Fang, Y. and Chlamtac, I. Teletraffic Analysis and Mobility Modeling for PCS Network. *IEEE Trans. on Comm.*, 47(7):1062–1072, 1999.
- [23] Fang, Y., Chlamtac, I., and Fei, H.-B. Analytical Results for Optimal Choice of Location Update Interval for Mobility Database Failure Restoration in PCS Networks. *IEEE Transactions on Parallel and Distributed Systems*, 11(6):615–624, June 2000.
- [24] Femto Forum. Regulatory Aspect of Femtocells. 2008. White Paper.

- [25] Gu, D. and Rappaport, S. S. Mobile User Registration in Cellular System with Overlapping Location Areas. *IEEE Vehicular Technology Conference*, 1:802–806, May 1999.
- [26] Gudmundson, B.O.P. (Sollentuna, SE), Eriksson, H. (Vallentuna, SE), Grumlund, O.E. (Kista, SE) . Method of Effecting Handover in a Mobile Multilayer Cellular Radio System. *U.S. Patent*, 1995.
- [27] Haas, Z. and Lin, Y.-B. Demand Re-registration for PCS Database Restoration. *ACM/Springer Mobile Networks and Applications*, 5(3):191–198, 2000.
- [28] Ho, C.-J., Lea, C.-T. and Stuber, G.L. Call Admission Control in the Micro-cell/Macrocell Overlaying System. *IEEE Tran. on Vehicular Tech.*, 50(4):992–1003, July 2001.
- [29] Holma, H. and Toskala, A. *WCDMA for UMTS*. John Wiley & Sons, 2000.
- [30] Holma, H. and Toskala, A. *WCDMA for UMTS V HSPA Evolution and LTE, 4th Edition*. John Wiley & Sons, 2007.
- [31] Hsu, S.-F., Lin, Y.-C., Lin, Y.-B. and Yang, J.-S. An OSA Application Server for Mobile Services. *International Journal of Pervasive Computing and Communications (JPCC)*, 3(1), 2007.
- [32] Hu, L. and Rappaport, S.S. Personal communication systems using multiple hierarchical cellular overlays. *IEEE Journal on Selected Areas in Communications*, 13(2):406–415, 1995.
- [33] Hung, H.-N., Lin, Y.-B., Peng, N.-F., Tsai, H.-M. Repacking on Demand in Two-tier WLL. *IEEE Transactions on Wireless Communications*, 3(3), 2004.

- [34] I, C.-L., Greenstein, L.J. and Gitlin, R.D. A Microcell/Macrocell Cellular Architecture for Low- and High-mobility Wireless Users. *IEEE JSAC*, 11(6):885–891, August 1993.
- [35] IEEE. IEEE Standard for Local and metropolitan area networks - Part 16: Air Interface for Fixed and Mobile Broadband Wireless Access Systems - Amendment 2: Physical and Medium Access Control Layers for Combined Fixed and Mobile Operation in Licensed Bands and Corrigendum 1. *IEEE Std 802.16e-2005*, 2005.
- [36] IEEE. Family of Standards for Wireless Access in Vehicular Environments (WAVE). *IEEE 1609*, Jan. 2006.
- [37] IEEE. Draft Amendment to Part 11: Wireless Medium Access Control (MAC) and Physical Layer (PHY) specifications: Wireless Access in Vehicular Environments (WAVE). *IEEE Std 802.11p/D2.01*, March 2007.
- [38] Jabbari, B. and Fuhrmann, W. F. Teletraffic Modeling and Analysis of Flexible Hierarchical Cellular Networks with Speed-Sensitive Handover Strategy. *IEEE JSAC*, 15(8):1539–1548, 1997.
- [39] Johnson, D., Perkins, C. and Arkko, J. IP Mobility Support for IPv6. *IETF RFC 3775*, June 2004.
- [40] Kanamori, Y., Kawano, K., Kinoshita, K. and Murakami, K. An Effective Dynamic Spectrum Assignment in WiFi/WiMAX Integrated Networks. *Eighth International Conference on Networks (ICN)*, pages 150–155, 2009.
- [41] Kelly, F. P. *Reversibility and Stochastic Networks*. John Wiley & Sons Ltd., 1979.
- [42] Kleinrock, L. *Queueing Systems; Volume I: Theory*. Wiley, 1975.
- [43] Lagrange, X. Multitier Cell Design. *IEEE Communications Magazine*, 35(8):60–64, August 1997.

- [44] Lin, Y.-B. M-Taiwan: A WiMAX Experience, Keynote speech. *The International Conference on Mobile Technology, Applications and Systems (Mobility Conference)*, 2008. See also <http://www.mobilityconference.org/go/programme/keynote/>.
- [45] Lin, Y.-B. and Chlamtac, I. *Wireless and Mobile Network Architectures*. John Wiley & Sons, 2001.
- [46] Lin, Y.-B. and Mak, V. W. Eliminating the Boundary Effect of a Large-Scale Personal Communication Service Network Simulation. *ACM Tran. on Modeling and Computer Simulation*, 4(2):165–190, 1994.
- [47] Lin, Y.-B. and Pang, A.-C. *Wireless and Mobile All-IP Networks*. Wiley, 2005.
- [48] Lin, Y.-B., Lai, W.-R., and Chen, R.J. Performance Analysis for Dual Band PCS Networks. *IEEE Tran. on Computers*, 49(2):148–159, 2000.
- [49] Lin, Y.-B., Tsai, M.-H., Dai, H.-W. and Chen, Y.-K. Bearer Reservation with Pre-emption for Voice Call Continuity. *IEEE Transactions on Wireless Communications*, 8, 2009.
- [50] Maheshwari, K. and Kumar, A. Performance Analysis of Microcellization for Supporting Two Mobility Classes in Cellular Wireless Networks. *IEEE Tran. on Vehicular Tech.*, 49(2):321–333, March 2000.
- [51] Masini, B. M., Zuliani, L. and Andrisano, O. On the Effectiveness of a GPRS based Intelligent Transportation System in a Realistic Scenario. *IEEE 63rd Vehicular Technology Conference (VTC 2006-Spring)*, May 2006.
- [52] Moerdijk, A.-J., and Klostermann, L. Opening the Networks with Parlay/OSA: Standards and Aspects Behind the APIs. *IEEE Network*, May/June 2003.
- [53] Motorola. TECHNICAL WHITE PAPER: Long Term Evolution (LTE): A Technical Overview. Technical report.

- [54] Niyato, D. and Hossain, E. WIRELESS BROADBAND ACCESS: WIMAX AND BEYOND - Integration of WiMAX and WiFi: Optimal Pricing for Bandwidth Sharing. *IEEE Communications Magazine*, 45(5):140–146, 2007.
- [55] Okasaka, S., Onoe, S., Yasuda, S. and Maebara, A. A new location updating method for digital cellular systems. *41st Annual Conference on Vehicular Technology (VTS)*, pages 345–350, May 1991.
- [56] Open Mobile Alliance. Push to Talk over Cellular Architecture. *OMA-AD-PoC-V1\_0-20040109-D*, 2004. Draft Version.
- [57] Open Mobile Alliance. OMA PoC User Plane Version. *OMA-TS-PoC\_ControlPlane-V2\_0-20080806-C*, 2008. Candidate Version 2.0.
- [58] Open Mobile Alliance. Push to Talk over Cellular Architecture. *OMA-AD-PoC-V2\_0-20080806-C*, 2008. Candidate Version.
- [59] Panken, F., Hoekstra, G., Barankanira, D., Francis, C., Schwendener, R., Grondalen, O. and Jaatun, M.G. Extending 3G/WiMAX Networks and Services through Residential Access Capacity [Wireless Broadband Access]. *IEEE Communications Magazine*, 45:62–69, 2007.
- [60] Pyarali, I., and Schmidt, D.C. An Overview of the CORBA Portable Object Adapter. *CM StandardView Magazine*, 6(1), 1998.
- [61] Ramsdale, P.A. (Walden, GB), Gaskell, P.S. (Shelford, GB). Handover Techniques. *U.S. Patent*, 1994.
- [62] Rappaport, S. S. and Hu, L.-R. Microcellular Communication Systems with Hierarchical Macrocell Overlays: Traffic Performance Models and Analysis. *Proceedings of the IEEE*, 82(9):1383–1397, September 1994.
- [63] Rosenberg, J. et al. SIP: Session Initiation Protocol. *IETF RFC 3344*, 2002.

- [64] Ross, S.M. *Stochastic Processes, 2nd Edition*. John Wiley & Sons, 1996.
- [65] Schulzrinne, H., Casner, S., Frederick, R., and Jacobson, V. RTP: A Transport Protocol for Real-Time Applications. *IETF RFC 3550*, July 2003.
- [66] Steele, R., Nofal, M., and Eldolil S. Adaptive Algorithm for Variable Teletraffic Demand in Highway Microcells. *Electronics Letters*, 26(14):988–990, 1990.
- [67] Thomas, G.B., Finney, R.L. *Calculus and Analytic Geometry, 9th Edition*. Addison Wesley, 1996.
- [68] Tsai, H.-M., Pang, A.-C., Lin, Y.-C., and Lin Y.-B. Repacking on Demand for Hierarchical Cellular Networks. *ACM Wireless Networks*, 11(6), 2005.
- [69] Tsai, H.-M., Pang, A.-C., Lin, Y.-C., and Lin Y.-B. Repacking on Demand for Speed-Sensitive Channel Assignment. *ACM Computer Networks*, 47(1), 2005.
- [70] Tsai, M.-H. and Lin, Y.-B. Eavesdropping through Mobile Phone. *IEEE Transactions on Vehicular Technology*, 56(6):3596–3600, 2007.
- [71] Valois, F. and Veque, V. Preemption Policy for Hierarchical Cellular Network. *5th IEEE Workshop on Mobile Multimedia Communication*, pages 75–81, 1998.
- [72] Valois, F. and Veque, V. QoS-oriented Channel Assignment Strategy for Hierarchical Cellular Networks. *IEEE PIMRC*, 2:1599–1603, 2000.
- [73] Wang, L.-C., Stuber, G.L. and Lea, C.-T. Architecture Design, Frequency Planning, and Performance Analysis for a Microcel/Macrocell Overlaying System. *IEEE Tran. on Vehicular Tech.*, 46(4):836–848, November 1997.
- [74] Whiting, P. A. and McMillan, D. W. Modeling for Repacking in Cellular Radio. *7th U.K. Teletraffic Symp.*, 1990.



- [75] WiMAX Forum. WiMAX End-to-End Network Systems Architecture (Stage 2: Architecture Tenets, Reference Model and Reference Points). *NWG Stage 2 - Release 1.1.0*, July 2007.
- [76] WiMAX Forum. WiMAX Forum Network Architecture (Stage 3: Detailed Protocols and Procedures). *NWG Stage 3 - Release 1.0.0*, March 2007.
- [77] WiMAX Forum. WiMAX Forum Network Architecture (Stage 3: Detailed Protocols and Procedures). *NWG Stage 3 - Release 1.1.0*, July 2007.
- [78] Yahiya, T.A., Beylot, A.-L. and Pujolle, G. . Policy-Based Threshold for Bandwidth Reservation in WiMax and WiFi Wireless Networks. *Third International Conference on Wireless and Mobile Communications (ICWMC)*.
- [79] Yang, S.-R. Dynamic power saving mechanism for 3G UMTS system. *ACM/Springer Mobile Networks and Applications (MONET)*, 12(1):5–14, 2007.
- [80] Yang, S.-R., Lin, Y.-C. and Lin, Y.-B. Performance of Mobile Telecommunications Network with Overlapping Location Area Configuration. *IEEE Transactions on Vehicular Technology*, 57(2), 2008.
- [81] Yeh, S.-P., Talwar, S., Lee, S.-C. and Kim, H.-C. WiMAX Femtocells: a Perspective on Network Architecture, Capacity, and Coverage. *IEEE Communications Magazine*, 46:58–65, 2008.
- [82] Zang, Y.-P., Weiss, E., Stibor, L., Chen, Hui and Cheng, Xi. Opportunistic Wireless Internet Access in Vehicular Environments Using Enhanced WAVE Devices. *International Conference on Future Generation Communication and Networking (FGCN)*, 1:447–452, December 2007.
- [83] Zhang, Y., Luo, J. and Hu, H. *Wireless mesh networking*. Wiley, 2006.